Development of Polymer-based Pressure Sensors for Electronic Devices

Vera Filipa Barbosa das Neves Gonçalves

Dissertation presented to obtain the degree of
Doctor in Chemical and Biological Engineering
by the
University of Porto

Supervisor:

Adélio Miguel Magalhães Mendes, Associated Professor

Co-Supervisors:

Lúcia Raquel Brandão, Post-Doc Researcher

Sérgio Reis Cunha, Assistant Professor

Paulo Ferreira dos Santos, Coordinator at Kinematix

LEPABE - Faculty of Engineering
University of Porto

———

Kinematix – Making Sense of Body Dynamics
Porto, 2014

“Valeu a pena? Tudo vale a pena se a alma não é pequena.”
Fernando Pessoa

Acknowledgments

I would like to acknowledge financial support of the Portuguese Foundation for Science and Technology (FCT) and Kinematix (former Tomorrow Options) for my PhD grant (Ref. SFRH/BDE/33880/2009). I would also like to thank LEPABE, DEQ and FEUP for giving me the conditions to accomplish my work.

My thankful words go to my supervisors Professor Adélio Mendes, Dr. Lúcia Brandão and Professor Sérgio Cunha for all the helpful weekly discussions. I would like to thank Prof. Adélio for always finding time for me, supervision and support, to Dr. Lúcia Brandão for her patience during discussions and to Prof. Sérgio Cunha for his vision. I would like to also acknowledge Professor Fernão Magalhães for helpful discussions.

I would like to express my gratitude to Dr. Paulo Ferreira dos Santos for the opportunity of working in business environment and for helpful discussions. I want to thank to Eng. João Neiva for guidance and fundamental support in the development of my work.

Many thanks to my labmates, for their friendship and support: Margarida Catarino, Alfredo Tanaka, Paula Oliveira, Yoann Leydet, Isabel Mesquita, Ana Catarina Duarte, Paula Dias, Diana Dias, Sandra Rodrigues, Sofia Félix, Daniel Ferreira and Cecilia Pedrero. I want to thank with a special word to my friend Joana Ângelo for the affection and for listen to me. My recognition to D. Fátima Faustino through her help with bureaucratic questions.

To all my friends, thank you for your support and advice. A special thanks to Sara Ascenção and Sílvia Coelho for the fundamental support in my life.

I want to thank my family, my parents Alcindo e Teresa for all the love, support, advices and for always being there for me, a special word to my brother Daniel for being an inspiration for me, a special thanks to my sister-in-law Sandra and finally a

special gratitude to my beautiful niece Beatriz. Thank you to all for never letting me feel alone.

My last gratitude goes to António for the patience, comprehension and love. Thank you for all your love and for making me truly happy.

Preface

The present work was developed in a cooperation protocol between FEUP (Faculty of Engineering of University of Porto) and Kinematix (former Tomorrow Options-Microelectronics S.A.) and the PhD grant (Ref. SFRH/BDE/33880/2009) in industrial environment supported by the Portuguese Foundation for Science and Technology (FCT) and Kinematix.

Kinematix is a start-up specialised in designing innovative electronic devices with a main focus on medical applications. The company's first product was Walkinsense, a medical device designed to monitor and assess lower human limb movement. Nowadays, this company designs, develops and markets electronics portable systems to monitor the movements of people or their body parts during activities in all environments. There are different types of commercial pressure sensors, but from all off-the-shelf models tested by Kinematix, only one brand has demonstrated adequate strength, with the remaining showing significant degradation of their parameters over use. The dependence of this situation led Kinematix to promote the development of pressure sensors for medical applications, mainly in order to produce a simple, robust and low cost solution. Therefore, the objective of the present work is the development and manufacture of a new pressure sensor (lightweight, highly flexible, cheap, robust and elastic) based on electrically conductive polymer composites (ECPCs).

This thesis comprises different papers, which were submitted for publication during the development of the PhD research work.

Abstract

The present work targets the development of a simple, robust and low cost piezoresistive pressure sensor, with minimum hysteresis and drift, to respond between 0 to 50 $N \cdot cm^{-2}$; the electrodes should preferentially be made of the same material of the sensor and have an electrical conductivity 100 to 1000 times higher than the sensor (negligible electrical resistance).

Electrically Conductive Polymer Composites (ECPCs) assembled with polymeric electrodes to form a pressure sensor were developed and studied. The ECPCs prepared were based on dense and on porous polymer matrices of polydimethylsiloxane (PDMS) and polyetherblockamide (PEBA) incorporating conductive particles. The influence of the way the electrodes were bonded to the ECPC, casted or glued at the edges, on the electrical resistance measurements was addressed. The author concluded that the type of electrodes used to measure the piezoresistive response largely influences the electrical response of the ECPCs. Different types of electrodes originated different electrical responses to the pressure. The electrical resistance of the ECPCs changes with the type of the electrodes mainly due to the roughness present on the ECPC surface where among the materials tested only polymeric electrodes casted on the ECPC provide an effective electrical contact.

Pressure sensors based on dense polymer matrices incorporating carbon black assembled with polymeric electrodes casted on the ECPC presented no piezoresistive response despite their good adhesion and strength.

Porous ECPCs were also developed once the porosity of the ECPC is directly related to the performance of the pressure sensor. Porous PDMS matrices were prepared by the foaming and emulsion methods while porous PEBA matrices were prepared by the phase inversion method. The phase inversion method allowed the

preparation of porous PEBA films with a nodular structure, highly porous and with a symmetric morphology that showed to be very promising for preparing porous ECPCs. Different conductive particles were incorporated on the porous polymeric matrix. When using carbon black, the matrix obtained was dense due to the addition of hydrophobic particles. Silver, spherical and lamellar zinc presenting hydrophilic characteristics were also incorporated and in this case the PEBA polymer matrix remained porous. A piezoresistive response was observed for the porous PEBA ECPCs assembled with casted polymeric electrodes incorporating silver and lamellar zinc although with poor mechanical properties due to the high concentration of metals incorporated (approximately 50 vol.%).

Graphene platelets were also incorporated on porous PEBA matrix due to the similar morphology with the lamellar zinc but with a significantly smaller density. PEBA 4033 polymer was mixed with five different graphene platelets: grade H5, grade MX (M5, M15 and M25) and grade C–750. A porous morphology was obtained for the ECPCs prepared with the graphene platelets grade MX and H5 while for the grade C–750 only a dense ECPC was obtained. The ECPC incorporating 15 vol.% of graphene M5 assembled with casted polymeric electrodes exhibited a piezoresistive response more linear in a log-log plot than the other grades of graphene platelets. The results confirmed the potential of a porous PEBA 4033 matrix with the incorporation of graphene as pressure sensor but some limitations were detected as hysteresis and drift response after compression. Crosslinked PEBA 4033 and the incorporation of carbon black were considered to improve the mechanical properties but significantly worse piezoresistive responses were observed.

The influence of the polymeric electrodes on the piezoresistive response was tested after being casted or glued to different ECPCs. The ECPCs pressure sensors assembled with glued polymeric electrodes exhibited a linear piezoresistive response in a log-log plot while the others prepared with casted polymeric electrodes exhibited a nearly flat profile. Results indicated that the glued polymeric electrodes influence

the electrical resistance response due to a change in the interface contact with the ECPC while the casted polymeric electrodes induced a negligible pieozoresistive effect due to the formation of a very good electrical contact with the ECPC. Moreover, the dense ECPCs assembled with polymeric electrodes glued at the edges to the ECPC exhibited both low hysteresis and drift.

Resumo

O presente trabalho visa o desenvolvimento de um sensor de pressão piezoresistivo simples, robusto e de baixo custo, com o mínimo de histerese e de acondicionamento, com uma resposta de 0 a 50 $N \cdot cm^{-2}$; os elétrodos devem ser feitos preferencialmente do mesmo material do sensor e devem ter uma condutividade elétrica de 100 a 1000 vezes mais elevada do que o sensor (resistência elétrica desprezável).

Sensores de pressão baseados em compósitos poliméricos eletricamente condutores (ECPCs) ligados com elétrodos poliméricos foram desenvolvidos e estudados. Os ECPCs baseiam-se em matrizes poliméricas densas ou porosas de polidimetilsiloxano (PDMS) e poliéter-bloco-amida (PEBA) com a incorporação de partículas condutoras. A influência da forma como os elétrodos foram ligados ao ECPC, fundido ou colado nas bordas, nas medições de resistência elétrica foi abordada. Concluiu-se que o tipo de elétrodos utilizados para medir a resposta piezoresistiva influencia em grande parte a resposta elétrica dos ECPCs. Diferentes tipos de elétrodos originaram respostas elétricas à pressão diferentes. A resistência elétrica dos ECPCs alterou com o tipo de elétrodos, principalmente devido à rugosidade presente na superfície do ECPC onde entre os materiais testados apenas os elétrodos poliméricos fundidos no ECPC proporcionam um contato elétrico eficaz.

Os sensores de pressão baseados em matrizes poliméricas densas incorporando negro de fumo com elétrodos poliméricos fundidos no ECPC não apresentaram resposta piezoresistiva apesar de sua boa aderência e robustez.

ECPCs porosos também foram desenvolvidos uma vez que a porosidade do ECPC está diretamente relacionada com o desempenho do sensor de pressão. Foram preparadas matrizes porosas de PDMS utilizando o método de formação de espuma e

o método de emulsão enquanto que as matrizes porosas de PEBA foram preparadas utilizando o método de inversão de fase. Este método permitiu a preparação de filmes porosos de PEBA com uma estrutura nodular, altamente porosa e com uma morfologia simétrica que se mostrou muito promissora para a preparação de ECPCs porosos. Várias partículas condutoras foram incorporadas na matriz polimérica porosa. No entanto, utilizando o negro de fumo, a matriz obtida não é porosa devido à adição das partículas hidrofóbicas. Por sua vez, prata, zinco esférico e zinco lamelar que apresentam características hidrófilas permitiram a obtenção da matriz de polímero PEBA porosa. Uma resposta piezoresistiva foi observada para os ECPCs baseados na matriz polimérica porosa PEBA com os elétrodos poliméricos fundidos incorporando prata e zinco lamelar embora com propriedades mecânicas fracas devido à elevada concentração de metais incorporados (cerca de 50 % vol.).

Plaquetas de grafeno foram também incorporadas na matriz polimérica porosa de PEBA devido à morfologia semelhante com o zinco lamelar mas que apresenta uma densidade bastante inferior à do zinco. PEBA 4033 foi misturada com cinco plaquetas de grafeno diferentes: H5, MX (M5, M15 e M25) e C - 750. Uma morfologia porosa foi obtida para os ECPCs preparados com as plaquetas de grafeno MX e H5 enquanto para a classe C - 750 apenas ECPCs densos foram obtidos. O ECPC incorporando 15 vol.% de grafeno M5 com elétrodos poliméricos fundidos exibiram uma resposta piezoresistiva mais linear (escala log – log) do que os outros tipos de plaquetas de grafeno. Os resultados confirmam o potencial de uma matriz porosa de PEBA 4033 com a incorporação de grafeno como sensor de pressão, mas foram detetadas algumas limitações como histerese e acondicionamento na resposta do sensor após a compressão. A reticulação da matriz PEBA 4033 e a incorporação de negro de fumo foram consideradas para melhorar as propriedades mecânicas mas foram observadas respostas piezoresistivas significativamente piores.

A influência dos elétrodos poliméricos na resposta piezoresistiva foi testada depois destes serem fundidos ou colados aos diferentes ECPCs. Os sensores de

pressão com elétrodos poliméricos colados exibiram uma resposta piezoresistiva linear (escala log - log) enquanto que os ECPCs preparados com elétrodos poliméricos fundidos exibiram um perfil quase plano. Os resultados indicaram que os elétrodos poliméricos colados influenciam a resposta de resistência elétrica devido a uma alteração no contacto com a interface do ECPC enquanto os elétrodos poliméricos fundidos apresentam uma resposta pieozoresistiva insignificante devido à formação de um bom contacto elétrico com o ECPC. Além disso, os ECPCs densos com elétrodos poliméricos colados nas bordas do ECPC exibiram uma baixa histerese e boa repetibilidade.

Contents

CHAPTER III

Figure Captions

Table Captions

CHAPTER I

1 Introduction

The diabetic foot is a disease that affects the hind limbs of patients suffering from diabetes mellitus (DM). These patients often suffer biomechanical changes that lead to overpressure areas of the lower limbs and due to the also typical loss of sensation (the pain is an alarm) tend to develop pressure ulcers. The treatment of these ulcers is long lasting due to circulatory problems and frequently lead to the need of limbs amputation [1-3]. More than 371 million of people have diabetes. International Diabetes Federation indicates that half of people who die from diabetes are under the age of 60. In 2012, 471 000 million USD were spent due to this type of pathology [4].

The clinical treatment of the pressure ulcers is done by the use of footwear adapted to the conditions of each patient. For this it is important to measure the plantar pressure distribution and even to develop tools of feedback to alert the patient to dangerous levels of pressure. There are some technologies that allow measuring the plantar pressure distribution such as: force/ pressure plates and in-shoe systems [5]. Force plates measure the patient barefoot and therefore only have relevance for morphological analysis, not taking into account the effect of the interaction between the foot and shoe, which is the source of development of ulcers. On the other hand, in-shoe systems measure the pressure inside the shoe, but most systems are mainly targeted for use in laboratory or research and not adequate for the current demands of clinical work: simplicity and speed of use, providing enough relevant information dynamically as it is during the walk that the effects of pressure causing damage.

The WALKiNSENSE developed by Kinematix, former Tomorrow Options (Figure 1.1) is a device, targeted specifically for the use of clinicians that deal with lower limbs

biomechanical or postural disorders, composed by a unit that monitors simultaneously the human lower limb movement together with the plantar pressure in 8 spots of the foot insole. The device measures the walking speed and the consequent effect from it is variation on the plantar pressure measurements, which is essential to evaluate, for example, the effect of customised footwear or orthotics on the patients' plantar pressure distribution, allowing a reliable and fast analysis of patients without a serious conditioning of his walking patterns. To analyse and compare the plantar pressure effects of footwear through in-shoe and dynamic assessment, it is necessary to use a similar walking speed, eliminating it is effect [6].

WALKiNSENSE allows gathering the clinical site information necessary to design, for example, customised footwear (shoe, insole, or both) to minimise the conditions that lead to the onset of ulcers, in foot of diabetic patients. On the other hand, it allows the immediate evaluation of the effects of the developed footwear, assessing if the mechanical behaviour is or is not the pretended. Often clinicians don't count with results that dynamics provoke on forces intensity and directions, neither with the reactions of patients' bodies when their plantar pressure is changed. So, eventually some corrections or adjustments are needed to get an optimal result, and if not done immediately it can lead to harmful effects [6].

Besides, WALKiNSENSE can be used for orthopaedics, neurology, cardiology and podiatry activities, when assessing or changing patients biomechanics is relevant [6].

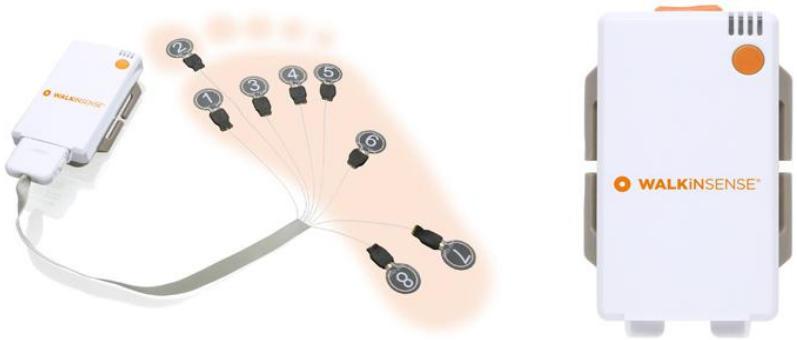

Figure 1.1 - WALKiNSENSE device [6].

There are different types of commercial pressure sensors and 3 main manufacturers worldwide that produce them (IEE (Luxembourg), Interlink (USA) and Tekscan (USA)), but from all models tested by Kinematix, only one brand has demonstrated adequate strength, with the remaining showing significant degradation of their parameters over use. The dependence of Kinematix on a single producer led this company to search for support at FEUP for developing their own pressure sensor solution.

The aim of the present work is then the development and characterization of a new pressure sensitive device based on a non-conductive polymer matrix containing conductive particles or a conductive polymer. The sensor should be lightweight, highly flexible, cheap and elastic and should be very resistant to compression (low hysteresis and drift effect) but mainly to the shear forces observed in the insole of shoes. The electrodes (electrical contacts) should be made with the same material to avoid stress and delamination of the contact area (mechanically robust). The electrodes should have an electrical conductivity 100 to 1000 times higher than the sensor (negligible electrical resistance) and should exhibit a very good adhesion to the sensor. On the

other hand, this sensor can not be influenced by temperature and humidity due to the ambient conditions in shoe.

1.1 Pressure Sensors

Polymer films play an essential and growing role in sensors. Recent advances in polymer science and film preparation have made polymer films useful, practical and economical in a wide range of sensor designs and applications. Further, the continuing miniaturization of microelectronics favors the use of thin polymeric films in sensors [7]. Pressure sensors are devices that show a variation in electrical conductivity when a force is applied. Polymer-based pressure sensors can be made of a non-conductive polymer matrix containing conductive particles or one blend of a conductive polymer [7-8].

When pressure is applied to the polymer-based sensor, the conducting particles or conductive polymer come in contact with each other and a conducting path is formed. Figure 1.2 sketches the formation of conductive paths in a composite polymer film when applying pressure.

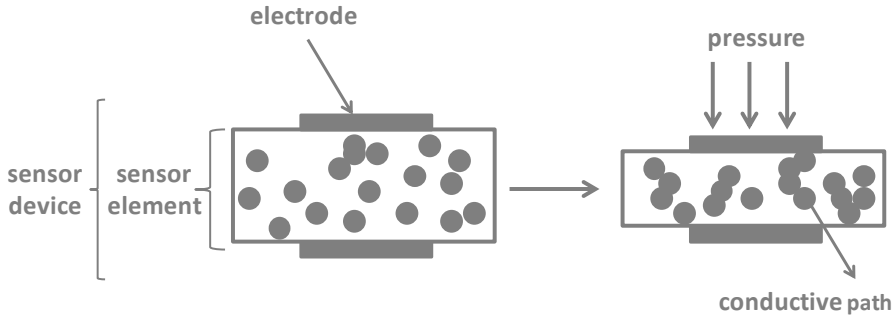

Figure 1.2 - Formation of conductive paths in polymer by applying pressure (adapted from [9]).

1.2 Sensors Types

Nowadays, sensors are also involved in a myriad of applications fostered by developments in digital electronics and involving the measurement of several physical and chemical quantities in automobiles, medical products, personal computers and pollution control [10].

Pressure sensors are widely used in automotive, sport, and physiological monitoring applications. In recent years, the global market for electronic products has grown rapidly with products such as phones and automotive electronics. The common requirements for these electronics are ultra-low cost, lightweight, portability, small size, multi-functionality, and high performance. In sports, pressure sensors are also useful for example to assisting in teaching how to play golf, namely in what concerns the correct feet placement. Covering different foot regions with pressure sensors provides a simple way to monitor and assess weight transfer during the golf swing, which is an important factor influencing the quality of the swing [5]. For health applications, as mentioned previously, pressure sensors are used for measuring the plantar pressure distribution during walking. These sensors allow the evaluation of the foot disorders caused by e.g. diabetes [5].

The best-known brand of pressure and force measurement system is TEKSCAN® (Tekscan Inc, USA), which comprehends simple sensors up to a highly complex array of 100,000 sensors. Tekscan sensors are made of a conductive ink deposited on a flexible polyester substrate [5, 11]. The F-Scan® sensor consists of insoles for the evaluation of pressure during walk over the entire area of the foot [5]. FlexiForce® sensors, produced by Tekscan, are made of two layers of flexible polyester substrate. A silver layer is applied to the substrates, followed by a layer of pressure sensitive ink – see Figure 1.3. An adhesive is then used to laminate the two layers of substrate

together to form the force sensor. The electric contact is defined by the silver track on top of the pressure sensitive ink [5].

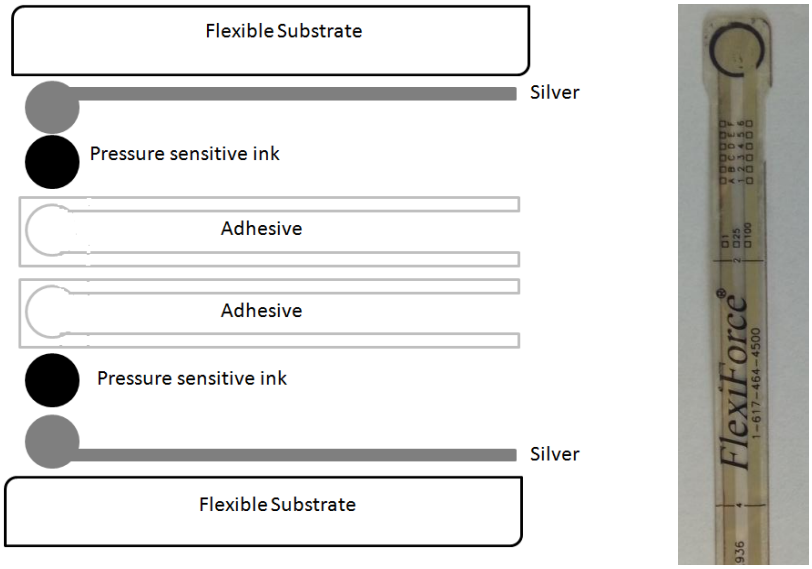

Figure 1.3 – FlexiForce® Sensor construction (adapted from [5]).

Peratech® sensors are ultra-thin pressure sensing technology. The sensor, Figure 1.4, is made of two layers of carbon ink electrodes (top and bottom substrate) with a silver track print. In the middle there is an adhesive layer to form the pressure sensor [12].

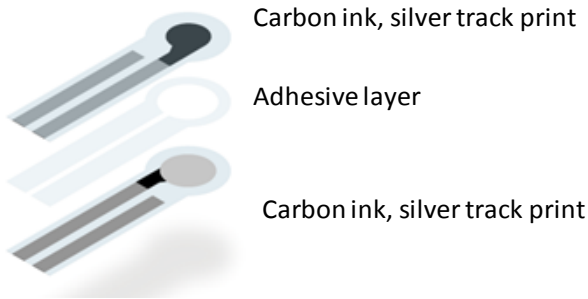

Figure 1.4 - Peratech® pressure sensor (adapted from [12]).

FlexiForce® and Peratech® pressure sensors are interface sensors because the electric resistance changes with the contact area within the sensor element.

1.3 Polymer Matrix

As mentioned before, polymer-based pressure sensors can be made of a non-conductive polymer matrix containing conductive particles or one blend of a conductive polymer. Different preparation processes and materials preparations have been studied. The polymer matrix should resist to the shear and compression forces as those observed in the insole of shoes.

Polymer matrix films can be classified, according to their morphology, as porous or dense. Dense polymer sensors are based on an interface sensor (electrical resistance dependent on the contact area), as the majority of commercial sensors [11, 13-15]. Recently, few studies report the development of porous polymer-based pressure sensors prepared by different methods without the influence of the contact area [16-19]. The effect of porosity on the sensor is directly related to the sensor's response.

1.3.1 Dense Polymer Matrix

Dense films can be prepared by solution deposition (casting method) and extrusion. In the casting method, a polymer is dissolved in a solvent and the solution deposited on a support; the solvent evaporating leads to the formation of a dense film. In the case of the extrusion method, the thermoplastic polymers are melted and extruded, solidifying and forming dense films when cooled [20-21].

1.3.2 Porous Polymer Matrix

Porous films comprise a polymer matrix with pores. Hentze and Antonietti [22] review the most used methods for the synthesis of porous films. This review presents some examples of polymers matrices to obtain different pores sizes accordingly to the porogene used. Table 1.1 shows different techniques that have been studied for synthesis of porous polymer films.

Table 1.1 – Some techniques for synthesis of porous polymer films (adapted from [22]).

Method	Porogene
Foaming	Gases Solids Solvents Supercritical CO_2
High internal phase emulsion	Emulsions
Phase separation Thermally induced phase separation (TIPS) Air casting of a polymer solution Precipitation from the vapour phase Immersion precipitation	Solvents
Other techniques	
Mechanical stretching	Mechanical deformation
Interparticular crosslinking	Solvent

Foaming methods

Porous polymer films obtained by **foaming methods** use gases, solvents, solids or supercritical CO_2 ($scCO_2$) as porogenes. The porous structure in the polymeric films can be induced by evaporation of solvents triggered by pressure drop or temperature

increase. Gases, volatile liquids and $scCO_2$ can be removed from the matrix after obtaining the desired matrix morphology. $ScCO_2$ can be used as a foaming agent to generate pores in polymeric matrices [23-24].

Some solids are used as porogenes to create pores in the polymer matrix: sugar particles, ammonium hydrogen carbonate, sodium bicarbonate, among others. Sugar particles are incorporated into a polymeric matrix and after polymer curing can be dissolved and removed to induce the formation of pores in the polymer matrix [25]. Ammonium hydrogen carbonate is used as a gas foaming agent; the polymer matrix loaded with ammonium hydrogen carbonate is heated to induce matrix solidification and the formation of ammonia and carbon dioxide that originates the formation of pores [26-27]. On the other hand, the chemical reaction between sodium bicarbonate and citric acid, results in the generation of carbon dioxide that induces porosity formation in the polymer matrix. At 120 °C, sodium bicarbonate starts to decompose and more CO_2 is produced due to the chemical reaction between the citric acid and the sodium bicarbonate [28].

Emulsions methods

Emulsions methods (high internal phase emulsions) are dispersions of water in oil phase (Figure 1.5). The water is added very slowly with the help of a solution of a surfactant in the oil phase [29]. These surfactants are adsorbed on the surface of water droplets and create a physical barrier (interfacial film with viscoelastic properties), which prevents the coalescence of emulsion droplets. The emulsifier molecules are oriented in the interface of the active surface such that the polar hydrophilic groups are directed to the water while the hydrophobic non polar hydrocarbon chains are directed to the continuous phase (oil) [30-32].

The properties of the surfactant (e.g., fluidity, cohesiveness, etc.) often affect the overall characteristics of the emulsion (e.g., stability, droplet size, etc.). Surfactants are classified as anionic, cationic, non-ionic and amphoteric according to the ionic characteristics of the head, see Table 1.2.

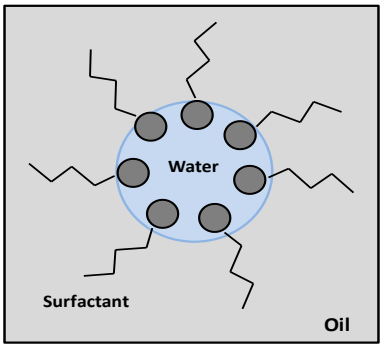

Figure 1.5 – Water in oil emulsion.

Table 1.2 – Surfactants classification (adapted from [33]).

Hydrophilic	Hydrophobic	Classification
		Non ionic
–		Anionic
+		Cationic
–	+	Amphoteric

Ionic surfactants interact more strongly than non-ionic surfactants with non-ionic polymers. In fact, anionic surfactants have a higher affinity for non-ionic polymers than cationic surfactants. The interaction between non-ionic polymers and all types of surfactants is usually controlled by hydrophobic interactions [33].

One of the most important non-ionic surfactant used are Pluronic triblock copolymers (BASF) based on poly (ethylene oxide) (PEO) and poly (propylene oxide) (PPO). Due to the amphiphilic character (hydrophilic character of PEO and hydrophobic character of PPO), Pluronics show good behaviour as surfactant because they have compatibility and stability in the polymer matrix [34-35]. One of the most used is Pluronic P-123 (molecular weight of around 5800 au) that has the following general chemical formula, Figure 1.6:

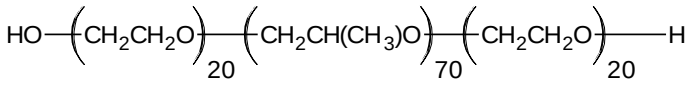

Figure 1.6 – Structural representation of P-123.

In the case of anionic surfactant [29], one of the most usual for water in oil dispersion is sodium dodecyl sulphate (SDS) with the following general chemical formula, Figure 1.7:

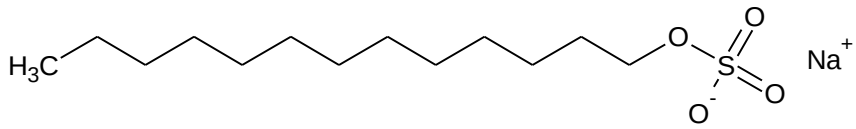

Figure 1.7 – Structural representation of SDS.

Anionic surfactants (SDS, for example) have good solubility in water and in organic solvents. The non-ionic surfactants (P-123, for example) have surface activity due to their polar structure. The hydrophilic properties are the result of the hydrogen bond between the oxygen atoms of the alcohol chain and the hydrogen atoms in the water molecules.

The ionic surfactants present at the interface of the droplets induce the appearance of electrical charges in the region and near the interface accumulate opposite charges. This mechanism is responsible for the electrostatic repulsion [33].

The most important factor to take into account to achieve good emulsion stability is the particle size obtained during the process of emulsion. The most important factors for process control are: emulsion method, amount of energy used to form droplets and surfactant efficiency. The surfactant has the function of reducing the interfacial tension between water and oil. The emulsion stability is also dependent on the physical characteristics of the interfacial film formed [30, 32-33].

As described above, water is used to create porosity in the polymer matrix. During the polymer cure, the porosity is obtained heating the sample loaded with water above the water boiling temperature; pores are formed due to water evaporation [29, 36-37]**.**

Phase inversion method

On the other hand, porous films can be prepared by **phase inversion method**. Porous films obtained by phase inversion may be prepared by essentially four techniques: thermally induced phase separation (TIPS), air casting of a polymer solution, precipitation from the vapour phase and immersion precipitation [20, 38-40]. **TIPS** is a method where the polymer matrix is dissolved in a solvent and where the solvent is vacuum evaporated at low temperature. At the end, the solvent is removed by extraction, freeze drying or evaporation. In the **air casting of a polymer solution**, the polymer matrix is dissolved in a mixture of a volatile solvent and a less volatile non-solvent (typically water or alcohol). When the solvent evaporates, the solubility of the polymer decreases and phase separation begins. The non-solvent

must be completely incompatible with the polymer matrix because if compatible non-solvents are used, the precipitating polymer phase will contain residual solvent to allow polymer to flow and collapse as solvent and non-solvent evaporate. **Precipitation from the vapor phase** refers to the phase separation induced by the penetration of non-solvent vapour in the solution. **Immersion precipitation** method considers the induction of phase separation in a homogeneous polymer solution by immersing the solution in a non-solvent bath or exposing it to a non-solvent atmosphere (Figure 1.8). The polymer solution is immersed in a non-solvent bath and a solvent/non-solvent exchange leads to phase separation [20, 38, 40-41].

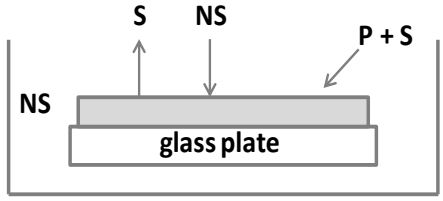

Figure 1.8 - Schematic of the immersion precipitation process (P: polymer, S: Solvent, NS: non-solvent), (adapted from[20] [38]).

In the immersion precipitation, the polymeric solution is precipitated into two phases: a liquid phase (low concentrated polymer) that forms the film pores and a solid phase (polymer rich) that forms the matrix film. The parameters that allow controlling the porosity of the films are: polymer concentration, nature of the solvent, casting temperature and time, coagulation time and temperature and time between casting and coagulation bath [38, 42]. It is very important that non-solvent be completely incompatible with the polymer matrix. The concentration of the polymer solution changes by solvent/non-solvent exchange, the mobility of the system decreases because the solvent concentration decreases. If the system gels and solidifies demixing the phase separation step a porous structure will be obtained. A

phase diagram for mixtures of a polymer, a solvent and a non- solvent system is shown in Figure 1.9. The ternary phase diagram is divided into a homogeneous region, liquid-liquid demixing and gelation. The location of the demixing gap is determined by the interaction between polymer, solvent and non-solvent [20, 38, 41].

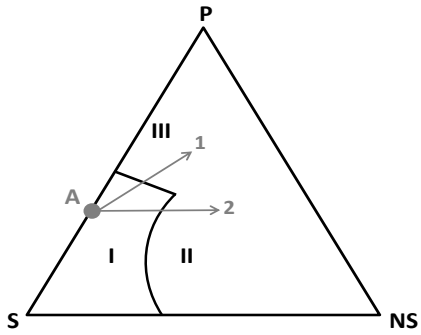

Figure 1.9 – Schematic representation of a ternary phase diagram (I- homogeneous solution, II- liquid-liquid demixing, III-gelation, 1 and 2 are possible coagulation phases)(adapted from [20]).

Lines 1 and 2 represent the change in composition for the skin layer (direct contact with non-solvent) and sub-layer if a film with composition A is immersed in a non-solvent bath. Liquid-liquid demixing can be divided into: i) nucleation and growth of a rich in polymer phase, ii) nucleation and iii) spinodal composition [20, 38].

The choice of polymer is important due to the influence of the range of the solvents and non-solvents that can be used. Another parameter that should be controlled is the choice of pair solvent/non-solvent. The solvent must be completely miscible in the non-solvent. Water can often be used as non-solvent but other non-solvent can be used as well. A very large number of combinations of solvents and non-solvents are possible; Table 1.3 shows several possible pairs of solvent/non-solvent.

Table 1.3 – Combination of solvent/non-solvent pairs (adapted from [20]).

Type of film	Solvent	Non-solvent
Porous	N-Methyl-2-Pyrrolidone (NMP)	Water
Porous	Dimethylacetamide (DMAc)	Water
Porous	Dimethyl sulfoxide (DMSO)	Water
Porous	Dimethylformamide (DMF)	Water

The concentration of the polymer defines the final porosity obtained. When the volume fraction of solvent increases, the porosity of the film increases. On the other hand, if solvent is added to the coagulation bath, the morphology of the film can change to dense. Different morphological structures can be obtained by immersion methods: macrovoids, cellular structures, nodules and bi-continuous structures [38]. Macrovoids are big porous and result of the rapid penetration of non-solvent (instantaneous precipitation) in the film. For the cellular structures, the delay time for demixing is important for the morphology definition. Nodules are spherical beads with diameter of 25-200 nm. Bi-continuous structures contain a layer with interconnected pore.

A large number of studies can be found in the literature regarding the development of porous films by phase inversion with control of different parameters such as: solvent/non-solvent combinations, polymer concentration, casting and coagulation temperature and evaporation time. These parameters influence the morphology of the film [43-46]. The authors reported that higher polymer concentrations and a longer time between casting and coagulation tends to reduce the porosity and induce the formation of a denser film [47].

Some studies use polyethylene glycol (PEG) as additive and study the effect of the molecular weight of PEG on the porosity (size, distribution). They concluded that the porosity increases in films with PEG with higher molecular weight due to the decrease in miscibility of the casting solution with water [45-46, 48-49]. Idris et al. [49], for example, found that the addition of PEG 200 in the casting solution decreases the size of macrovoids while PEG 400 and PEG 600 increases the number and size of macrovoids. With the increase of PEG concentration, the viscosity of casting solution increases because the concentration of solvent decreases and the performance of the film changes.

Zhao et al. [50] studied the blend of different amphiphilic polymers with the polymer matrix to prepare porous films via the immersion precipitation method. The effects of structural variation of the amphiphilic polymers on the morphology of the films were investigated.

1.4 Electrically Conductive Polymer Composites Sensors

Sensors based on Electrically Conductive Polymer Composites (ECPCs) are composed by an insulating polymer matrix loaded with conductive particles or conducting polymers [8]. The most often used particles materials are metals, carbon black and semiconducting metal-oxides. Composite sensors made from conductive carbon black dispersed in various polymers have been developed and studied extensively by Lewis and co-workers [51-53]. With increasing concentration of the conductive particles, the polymer matrix becomes conductive. This process can be described by percolation theory [8].

1.4.1 Percolation Theory

Percolation models are used to describe the relationship between electrical resistance and the concentration of conductive particles in a matrix. When the

concentration of conductive particles is very low, there is no extensive connected pathways for electrical conduction that penetrate or percolate through the composite, and the resistivity of the composites remains very high. When the concentration of conductive particles is very high, the conductive particles pack very close in the composite and form conductive pathways, which impart a low resistance response of the sensor. The relationships among composite resistance, conductive particles concentration, resistivity and polymer swelling are not well known [54-56]. Most studies on ECPCs have sought to lower the percolation threshold because a high filler concentration raises the product cost and changes the mechanical properties of the polymer matrix; for example the viscosity increases with the increase of filler concentration. The volume fraction of fillers is an important parameter to study the electrical properties of these composites at the percolation threshold [8-9, 54-55]. Particle size and morphology, polymer matrix viscosity, particle - matrix interaction influences the percolation threshold of ECPCs. For instance, a poor dispersion of the conductive particles in the polymer matrix increases the percolation threshold [57].

1.4.2 Piezoresistive Effect

The sensitivity to pressure of ECPCs is known as piezoresistive effect [57-58]. This effect is the change in electrical resistance of the polymer matrix when a stress is applied. The maximum sensitivity of ECPCs sensors may be expected at the percolation threshold [59]. When pressure is applied to compress the polymer matrix, the overall volume reduces and increases the contact area between the conductive particles [60]. Sensitivity of the piezoresistive materials can be characterized by gauge factor (GF). The GF is the change in electrical resistance per unit of deformation. This parameter can be calculated as follows:

$$GF = \frac{\frac{\Delta R}{R_0}}{\frac{\Delta L}{L_0}} \quad (1.1)$$

where R_0 is the electrical resistance of the material before deformation, ΔR is the variation of electrical resistance caused by the deformation, L_0 is the dimension of the sensor, ΔL is the deformation applied.

The piezoresistivity of ECPCs, as well as their mechanical flexibility and ease of processing, make these composites promising candidates for use in cheap, flexible and large area pressure sensors.

A large number of studies can be found in the literature regarding the development of dense polymer-based pressure sensors. The most common are the polymer films containing carbon black particles [8-9, 16-17, 54-55, 59, 61-62]. The sensor's response depends on a number of different parameters, including: geometry and concentration of the conductive component dispersed in the polymer matrix, conductive particle (size and morphology), solvent nature and thickness of the film [54-55].

On the other hand, few studies report the development of porous polymer-based pressure sensors prepared by different methods [17-19, 56, 62]. King et al. [17] studied a porous polymer matrix containing carbon black particles. To introduce porosity into the polymer matrix they used sugar particles. The sensor obtained showed an electrical resistance change from 20 kΩ to 100 Ω for an applied 95 % compressive strain. Li et al. [62] described a conductive porous nanocomposite based on polypropylene (PP) and polystyrene (PS) and carbon black as conductive particles; these authors concluded that when increasing the porosity, the percolation threshold

decreases. Ravati et al. [18] studied a porous polymeric pressure sensor by the deposition of polyaniline (Pani) on a matrix blend composed by (poly(methyl methacrylate) (PMMA), high-density Polyethylene (HDPE) and polystyrene (PS)). The conductive polymer is sensitive to pressure providing that the void volume percentage and the applied load is sufficiently high. Danesh et al. [16] developed a porous conductive composite by phase separation. The matrix used by these authors was poly (methyl methacrylate) (PMMA), the solvent was ethyl acetate (EA), the non-solvent (less volatile) was 2-methyl-2, 4 -pentanediol (MPD) and conductive particles were of carbon black. After complete evaporation of the solvent, the film was immersed in aqueous methanol solution to remove the non-solvent. The maximum sensitivity to pressure was obtained by introducing porosity in the film. Brady et al. [19] reported smart textiles based on conducting polymers deposited on a foam (polyurethane). However, this pressure sensor presents some limitations, such as: drift in conductivity of the conducting foam and hysteresis after compression.

According to Danesh et al. [16], King et al. [17] and Ravati et al. [18] the effect of porosity on the sensor is directly related to the sensor's response. In other words, when the porosity increases, the sensitivity to pressure of the ECPCs increases; when the sensor is compressed, the conductive particles come into contact and the sensor becomes conductive. The pores are the limiting links in the percolation threshold [17].

1.5 Motivation and thesis outline

The present work was developed under the framework of the cooperation protocol between FEUP (Faculty of Engineering of University of Porto) and Kinematix (former Tomorrow Options-Microelectronics S.A.). Kinematix targets the development of a simple, robust and low cost piezoresistive sensor, with minimum hysteresis and drift, to respond between 0 to 50 $N \cdot cm^{-2}$. Moreover, the production

process should be reproducible. Therefore, the aim of the present work is the development of a robust and low cost pressure sensitive device based in conducting polymer films. The sensor should be lightweight, highly flexible, cheap and elastic and should be very resistant to compression but mainly to the shear forces observed in the insole of shoes. For that, the electrodes should preferentially be made with the same material to avoid stress and delamination of the contact area. The electrodes should have an electrical conductivity 100 to 1000 times higher than the sensor (negligible electrical resistance) and should exhibit a very good adhesion to the sensor. So, this pressure sensitive device (sensor element) was envisioned as a pressure sensitive layer sandwiched between two electrical conductive layers.

This work is divided in seven Chapters. Chapter I is a literature survey over the main topics related to this thesis. This Chapter presents an overview concerning pressure sensors. Chapter II presents the experimental methods and some materials used to prepare and characterize polymer films based on ECPCs. Chapter III describes the development of sensor elements based on dense ECPCs, the development of electrodes based on the similar composite material and the influence of electrode type, conductive component type, mechanical properties and film morphology. In Chapter IV a study of different methods to create porosity in the polymer matrix, PDMS and PEBA, was evaluated. This Chapter addresses the effect of film morphology of the polymeric matrix on the response of the sensor towards pressure. In Chapter V of this Chapter, a study of the development of porous PDMS and PEBA based ECPCs was addressed. The influence of the type of conductive particles and the combination of solvent/ non-solvent on the porous morphology was studied; the effect of the conductive particles on the piezoresistive effect was also evaluated. Chapter VI describes the preparation of PEBA 4033 based on ECPCs by the immersion precipitation method and graphene nanoplatelets used as conductive particles. The influence of the type of graphene nanoplatelets and the combination of solvent/non-

solvent on the porous morphology was studied. The piezoresistive response and mechanical properties were also evaluated. In Chapter VII a study of the way the electrodes are bonded to the ECPC, casted or glued by the edges, on the electrical resistance measurements (piezoresistive response) is addressed and hysteresis and drift response are evaluated. A commercial pressure sensor was compared to the ECPCs prepared. The last Chapter, Chapter VIII, presents the main conclusions of this work and gives suggestions for future work.

1.6 References

1. http://www.min-saude.pt/portal/conteudos/a+saude+em+portugal/noticias/arquivo/2010/3/pe+diabetico.htm. [cited 2013 april].
2. http://www.mdsaude.com/2012/08/pe-diabetico.html. [cited 2013 april].
3. http://diabeticfootonline.blogspot.pt/. [cited 2013 april].
4. http://www.idf.org/. [cited 2013 may].
5. http://www.tekscan.com/. [cited 2013 january].
6. www.tomorrow-options.com. [cited 2013 january].
7. Harsányi, G., *Polymeric sensing films: new horizons in sensorics?* Materials Chemistry and Physics, 1996. **43**(3): p. 199-203.
8. Knite, M., Teteris, V., Polyakov, B., Erts, D., *Electric and elastic properties of conductive polymeric nanocomposites on macro- and nanoscales.* Materials Science and Engineering: C, 2002. **19**(1-2): p. 15-19.
9. Hussain, M., Choa, Y.-H., Niihara, K., *Fabrication process and electrical behavior of novel pressure-sensitive composites.* Composites Part A: Applied Science and Manufacturing, 2001. **32**(12): p. 1689-1696.
10. Pallàs-Areny, R., Webster, J.G., *Sensors and Signal Conditioning*, I. John Wiley & Sons, Editor. 2000, Wiley-Interscience.
11. Podoloff, R., Benjamin, M., *Flexible, tactile sensor for measuring pressure distributions and for gaskets*, WO 91/09289, June 27, 1991.

12. http://www.peratech.com/qtc-material-inspirations.html. [cited 2013 january].

13. Lussey, D., Jones, D., Leftly, S., *Flexible Switching Devices*., WO 01/88935 A1, November 22, 2011.

14. Lussey, D., Laughlin, P., Bloor, D., Hilsum, C., *Polymer composition with electrically-conductive filler*, U.K. Patent GB 2465077 A, May 12, 2010.

15. Lussey, D., *Conductive Strutures*, WO 00/79546 A1, December 28, 2000.

16. Danesh, E., Ghaffarian, S.R., Molla-Abbasi, P., *Non-solvent induced phase separation as a method for making high-performance chemiresistors based on conductive polymer nanocomposites.* Sensors and Actuators B: Chemical, 2011. **155**(2): p. 562-567.

17. King, M.G., Baragwanath, A.J., Rosamond, M.C., Wood, D., Gallant, A.J., *Porous PDMS force sensitive resistors.* Procedia Chemistry, 2009. **1**(1): p. 568-571.

18. Ravati, S., Favis, B.D., *3D porous polymeric conductive material prepared using LbL deposition.* Polymer, 2011. **52**(3): p. 718-731.

19. Brady, S., Diamond, D., Lau, K.-T., *Inherently conducting polymer modified polyurethane smart foam for pressure sensing.* Sensors and Actuators A: Physical, 2005. **119**(2): p. 398-404.

20. Mulder, M., *Basic Principles of Membrane Technology*. 2 nd ed. 2000: Klumer Academic Publishers.

21. Kesting, R.E., Fritzsche, A.K., *Polymeric Gas Separation Membranes*. 1993: John Wiley & Sons, Inc.

22. Hentze, H.P., Antonietti, M., *Porous polymers and resins for biotechnological and biomedical applications.* Reviews in Molecular Biotechnology, 2002. **90**(1): p. 27-53.

23. Huang, S., Wu, G., Chen, S., *Preparation of open cellular PMMA microspheres by supercritical carbon dioxide foaming.* The Journal of Supercritical Fluids, 2007. **40**(2): p. 323-329.

24. Siripurapu, S., Gay, Y.J., Royer, J.R., DeSimone, J.M., Spontak, R.J., Khan, S.A., *Generation of microcellular foams of PVDF and its blends using supercritical carbon dioxide in a continuous process.* Polymer, 2002. **43**(20): p. 5511-5520.

25. Yuen, P.K., Su, H., Goral, V.N., Fink, K.A. (2011) *Three-dimensional interconnected microporous poly(dimethylsiloxane) microfluidic devices*. **11**, 1541-1544 DOI: 10.1039/c01c00660b.

26. Wang, Y.-Q., Tao, J., Zhang, J.-L., Wang, T., *Effects of addition of NH4HCO3 on pore characteristics and compressive properties of porous Ti-10%Mg composites.* Transactions of Nonferrous Metals Society of China, 2011. **21**(5): p. 1074-1079.

27. Muehling, J.K., Arnold, Heather R., House Jr, J. E., *Effects of particle size on the decomposition of ammonium carbonate.* Thermochimica Acta, 1995. **255**(0): p. 347-353.

28. Zhang, P., Yang, L. C., Li, L., Qu, Q. T., Wu, Y. P., Shimizu, M., *Effects of preparation conditions on porous polymer membranes by microwave assisted effervescent disintegrable reaction and their electrochemical properties.* Journal of Membrane Science, 2010. **362**(1–2): p. 113-118.

29. Chen, J., Zhang, R., Wang W. (2012) *Fabricating microporous PDMS using a water-in-PDMS emulsion*.

30. Becher, P., *Encyclopedia of Emulsion Technology*. Vol. 4. 1996: Marcel Dekker, Inc. 359.

31. Gilbert, R.G., *Emulsion Polymerization : A Mechanistic Approach*. 1995: Academic Press.

32. Schramm, L.L., *Emulsion, Foam and Suspensions : Fundamentals and Applications*. 2005: Wiley-VCH.

33. Hartmann, D., *Resinas Alquídicas Base Água Emulsionadas Por Inversão de Fase*, in *Departamento de Química*. 2011, Universidade Federal de Rio Grande do Sul: Porto Alegre. p. 104.

34. Foster, B., Cosgrove, T., Hammouda, B., *Pluronic Triblock Copolymer Systems and Their Interactions with Ibruprofen.* 2009: p. 6760-6766.

35. Ulrich, K., Galvosas, P., Karger, J., Grinberg, F., *"Pore-Like" Effects of Super-Molecular Self-Assembly on Molecular Diffusion of Poly(Ethylene Oxide) - Poly(Propylene Oxide) - Poly(Ethylene Oxide) in Water.* Materials, 2012. **5**: p. 966-984.

36. Juchniewicz, M., Stadnik, D., Biesiada, K., Olszyna, A., Chudy, M., Brzózka, Z., Dybko, A., *Porous crosslinked PDMS-microchannels coatings.* Sensors and Actuators B: Chemical, 2007. **126**(1): p. 68-72.

37. Zhang, S., Zhu, Y., Hua, Y., Jegat, C., Chen, J., Taha, M., *Stability of surfactant-free high internal phase emulsions and its tailoring morphology of porous polymers based on the emulsions.* Polymer, 2011. **52**(21): p. 4881-4890.

38. Van de Witte, P., Dijkstra, P.J., Van den Berg, J.W.A., Feijen, J., *Phase separation processes in polymer solutions in relation to membrane formation.* Journal of Membrane Science, 1996. **117**(1–2): p. 1-31.

39. Baker, R.W., Cussler, E.L., Eykamp, W., Koros, W.J., Riley, R.L., Strathmann, H., *Membrane Separation Systems : Recent Developments and Future Directions*. 1991, United States: Noyes Data Corporation.

40. Nunes, S.P., Peinemann, K.-V., *Membrane Technology*. Second ed. 2006, Germany: Wiley-VCH.

41. Sperling, L.H., ed. *Introduction to physical polymer science*. 2006, John Wiley & Sons: New Jersey.

42. Seixas de Melo, J.S., Moreno, M.J., Burrows, H.D., Gil, M.H., *Química de Polímeros*. 2004, Coimbra.

43. Gugliuzza, A., Ricca, F., Drioli, E., *Controlled pore size, thickness and surface free energy of super-hydrophobic PVDF® and Hyflon®AD membranes.* Desalination, 2006. **200**(1–3): p. 26-28.

44. Gugliuzza, A., Drioli,E., *New performance of hydrophobic fluorinated porous membranes exhibiting particulate-like morphology.* Desalination, 2009. **240**(1–3): p. 14-20.

45. Chakrabarty, B., Ghoshal, A.K., Purkait, M.K., *Effect of molecular weight of PEG on membrane morphology and transport properties.* Journal of Membrane Science, 2008. **309**(1–2): p. 209-221.

46. Ma, Y., Shi, F., Ma, J., Wu, M., Zhang, J., Gao, C., *Effect of PEG additive on the morphology and performance of polysulfone ultrafiltration membranes.* Desalination, 2011. **272**(1–3): p. 51-58.

47. Jansen, J.C., Buonomenna, M.G., Figoli, A., Drioli, E., *Ultra-thin asymmetric gas separation membranes of modified PEEK prepared by the dry–wet phase inversion technique.* Desalination, 2006. **193**(1–3): p. 58-65.

48. Kim, J.-H., Lee, K.-H., *Effect of PEG additive on membrane formation by phase inversion.* Journal of Membrane Science, 1998. **138**(2): p. 153-163.

49. Idris, A., Norashikin M.Z., Noordin, M.Y., *Synthesis, characterization and performance of asymmetric polyethersulfone (PES) ultrafiltration membranes with polyethylene glycol of different molecular weights as additives.* Desalination, 2007. **207**(1–3): p. 324-339.

50. Zhao, Y.-H., Qian, Y.-L., Zhu, B.-K., Xu, Y.-Y., *Modification of porous poly(vinylidene fluoride) membrane using amphiphilic polymers with different*

structures in phase inversion process. Journal of Membrane Science, 2008. **310**(1–2): p. 567-576.

51. Albert, K.J., Lewis, N.S., Schaner, C.L., Sotzing, G.A., Stitzel, S.E., Vaid, T.P., *Cross-Reactive chemical sensor arrays.* Chem. Rev, 2000. **100**: p. 2595-2626.

52. Freund, M.S., Lewis, N.S., *A chemically diverse conduction polymer-based "electronic nose".* 1995. **92**: p. 2652-2656.

53. Lonergan, M.C., Severin, E.J., Doleman, B.J., Beaber, S.A., Grubbs, R.H., Lewis, N.S., *Array-based vapor sensing using chemically sensitive, carbon black-polymer resistors.* Chem. Mater., 1996. **8**: p. 2298-2312.

54. Lei, H., Pitt, W. G., McGrath, L.K., Ho, C.K., *Resistivity measurements of carbon-polymer composites in chemical sensors: impact of carbon concentration and geometry.* Sensors and Actuators B: Chemical, 2004. **101**(1-2): p. 122-132.

55. Lei, H., Pitt, W.G., McGrath, L.K., Ho, C.K., *Modeling carbon black/polymer composite sensors.* Sensors and Actuators B: Chemical, 2007. **125**(2): p. 396-407.

56. Bendo, L., Soldi, V., Domenech, S.C., *Compósitos elastoméricos condutores a base de terpolímero de etileno-co-propileno-5-etilideno-2-norborneno e negro de fumo modificado com polímeros condutores intrínsecos utilizados na construção de um protótipo de sensor de dígito-pressão*, in *Departamento de Química*. 2006, Universidade Federal de Santa Catarina: Florianópolis. p. 57.

57. Hwang, J., Jaeyoung, J., Hong, K., Kim, K.N., Han, J.H., Shin, K. , Park, C.E., *Poly(3-hexylthiophene) wrapped carbon nanotube/poly(dimethylsiloxane) composites for use in finger-sensing piezoresistive pressure sensors.* Carbon, 2011. **49**(1): p. 106-110.

58. Cochrane, C., Koncar, V., Lewandowski, M., Dufour, C., *Design and development of a flexible strain sensor for textile structures based on a conductive polymer composite.* Sensors, 2007. **7**(4): p. 473-492.

59. Knite, M., Teteris, V., Kiploka, A., Kaupuzs, J., *Polyisoprene-carbon black nanocomposites as tensile strain and pressure sensor materials.* Sensors and Actuators A: Physical, 2004. **110**(1-3): p. 142-149.

60. Brady, S., Lau, K.T., Megill, W., Wallace, G.G., Diamond, D., *The Development and Characterisation of Conducting Polymeric-based Sensing Devices.* Synthetic Metals, 2005. **154**(1-3): p. 25-28.

61. Wang, S.L., Wang, P., Ding, T.H., *Development of wireless compressive/relaxation-stress measurement system integrated with pressure-*

sensitive carbon black-filled silicone rubber-based sensors. Sensors and Actuators A: Physical, 2010. **157**(1): p. 36-41.

62. Li, M., Zhang, W., Wang, C., Wang, H., *In situ formation of 2D conductive porous material with ultra low percolation threshold.* Materials Letters, 2012. **82**(0): p. 109-111.

CHAPTER II

2 Electrically Conductive Polymer Composites - Experimental

2.1 Introduction

Various techniques have been developed to prepare conducting polymer films. The casting method was used for preparing thin films where the thickness of the film is determined by the amount of polymer solution deposited on the cast. This is a process by which the polymeric solution is introduced into a mould and allowed to solidify into a specific shape. This method is practical, cheap and convenient [1-5].

The author selected and studied various combinations of polymers with electrical conductive particles and the operating conditions for their synthesis. It was found that at least the following materials exhibited good characteristics: a) matrix polymers: poly (dimethylsiloxane) (PDMS), polyetherblockamide (PEBA), b) fillers: zinc, graphite, carbon black and graphene, c) conducting polymers: polyaniline (PANi) and polyvinylpyrrolidone (PVP). These materials have been studied systematically as well as other meanwhile selected.

One of the factors taken into account in the choice of materials is related to biocompatibility. It can never be forgotten that the materials when used as components of a device for health applications must be biocompatible. Below are described the main characteristics of some of the polymers chosen for this application.

The present Chapter describes the preparation of polymer matrices with and without conducting fillers and/or conducting polymers and the methods used for their characterization.

2.2 Experimental

2.2.1 Materials and Methods

a) Preparation of PEBA films

PEBAX polymer grades were supplied by Atofina Chemicals with 2533 grade specified to have a polyether content of 80%, 3533 grade about 70% and 4033 grade about 47 %. Atochem uses nylon 12 and polytetramethylene oxide (PTMO) in its PEBAX XX33 series, where XX represents the shore D hardness of the material. Poly (ether-block-amide) (PEBA) is used as an insulating matrix [6-7].

PEBA is a thermoplastic elastomer comprising hard polyamide and soft polyether, Figure 2.1. The copolymer consists of a linear chain of polyamide segments interspaced with polyether segments, having the following general chemical formula:

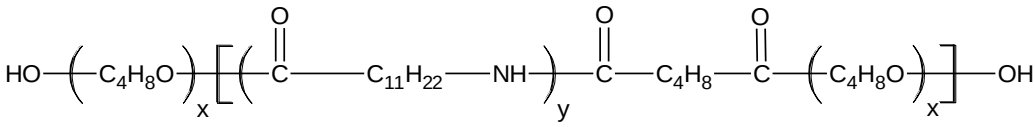

where x: composition of polyether segment

and y: composition of the aliphatic polyamide segment

Figure 2.1 - Structural representation of PEBAX (adapted from [6]).

Different grades of PEBA polymers have excellent mechanical strength and good chemical resistance. Table 2.1 shows the chemical and physical properties of some grades of PEBA copolymers. Its solubility properties strongly depend on the amount of PE component in block copolymer and the polarity of the PE and PA backbone elements.

PEBA membranes were prepared by the dissolution of the copolymer in the solvent or a mixture of the solvents. In polyamides (one of the copolymer parts), high

intermolecular forces and strong hydrogen bonding forces make solubility difficult. Therefore, only polar solvents that interacted strongly with the polymer to break down the hydrogen bonds could be used [8].

Table 2.1 – The most important properties of PEBA (adapted from [6]).

Grade	PA[a]	PE[b]	PE content (wt%)	Density (g/cm^3)	T_g (°C)	T_m (°C)
2533	PA12	PTMO	80, 78.4	1.01	-77, -76	126, 137
3533	PA12	PTMO	70, 72.9	1.01	-72	155, 142
4033	PA12	PTMO	47,44	1.01	-78	180,159

a. PA12 is polyamide (nylon) 12

b. PTMO is poly (tetramethylene oxide)

Different polymer grades (trademark: PEBAX) were used for preparing sensors. A predetermined amount of PEBA (2533, 3533 or 4033) was dissolved in a solvent to form a polymer solution. The polymer solution was stirred vigorously at 110 °C under reflux and kept at 90 °C. PEBA (2533, 3533 and 4033) solutions were mixed with the conducting particles suspensions previously dispersed in the same solvent. Dense films were poured on a glass plate thermostated at 60 °C. After one hour, the heating was switched off and the membrane was kept at room temperature overnight [6-8].

Porous PEBA films were prepared by phase inversion method, exposed to ambient before immersion into water bath at room temperature. The films were washed under running water and then kept overnight in a water bath. The films were air dried at room temperature for 2 days [9-17].

b) Preparation of PDMS films (Dehesive ®920)

Polydimethylsiloxane (**PDMS**) polymers can be used in various applications. The development and application of this material have been significantly influenced by advances in medicine, biotechnology and materials science.

The cross-linkable polydimethylsiloxane (PDMS) Dehesive® 920 was purchased from Wacker Silicon Corporation. Silicone rubber has the combined properties of resilience, high temperature stability and general inertness, unavailable in any other elastomers. Tetrahydrofuran (THF) was used as the solvent for preparing PDMS solutions.

PDMS (Figure 2.2) is used as an insulating matrix.

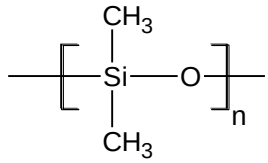

Figure 2.2 – Chemical structure of polydimethylsiloxane (PDMS).

Table 2.2 shows the most important properties of Dehesive® 920, Crosslinker V24 and Catalyst OL.

Table 2.2 – Properties of PDMS Dehesive ° 920 (adapted from [18]).

Product name		**Dehesive® 920**	**Crosslinker V24**	**Catalyst OL**
Content of active agent	(%)	100	100	1.0
Viscosity at 25 °C	(mPa·s)	500	22	350
Appearance		Colorless	Colorless, clear	Colorless, slightly brown
Specific gravity at 25 °C	(g/cm^3)	0.97	1.0	0.98
Flash point	(°C)	173	113	110
Storage stability at 20 °C	months	12	12	6

Polydimethylsiloxane (PDMS) from Wacker Silicon Corporation (Dehesive® 920) was mixed with suspensions of conducting particles in tetrahydrofuran (THF). The required amount of crosslinker was added to the PDMS solution. Stirring was maintained until a homogeneous mixture was obtained. After that, the crosslinking catalyst (platinum complex with 1,1,3,3-tetramethyle-1,3-divinyledisiloxane) was added to the mixture. Directly after mixing, the solution was poured on a Teflon coated glass plate. The solvent was evaporated at 90 °C for 30 minutes, followed by drying at room temperature overnight and dense films were formed [18].

Porous PDMS (Dehesive® 920) were prepared by the same method but with addition of Pluronic P-123. During the dissolution step to place the polymer films immersed in an ethanol solution on an ultrasonic bath for 3 hours at high

temperature to extract 80 % of the non-conductive phase. After extraction, the films were placed in an oven at 80 °C for 12 hours and then more catalyst was added to the final crosslinking. Finally, they were put back in the oven to finish the curing process.

c) Preparation of PDMS films (Sylgard 184)

The Sylgard 184 was purchased from Dow Corning Co. Table 2.3 shows the most important properties of Sylgard 184.

Table 2.3 – Properties of Sylgard 184 (adapted from [19]).

Mix ratio	Base: curing agent	10:1
Viscosity at 23 °C	(mPa·s)	4000
Heat cure	(°C)	150 - 10 minutes 125 - 20 minutes 100 - 45 minutes
Room temperature cure	(hours)	48
Specific Gravity at 25°C	(g/cm^3)	1.03
Pot life	(hours)	2
Temperature range	(°C)	- 45 to 200
Hardness	(Shore A)	50

Dense films were obtained with a mixture of PDMS pre polymer (polymer base) with conductive particles and a curing agent in 10:1, weight ratio. Finally, the film was poured on a Teflon coated glass plate at room temperature.

Porous PDMS (Sylgard 184) were prepared by high internal phase emulsions method. Water was added to dodecyl sulphate sodium salt (SDS) or to P-123 to stabilize the emulsion. The process consisted in addition of conductive particles to the PDMS and mixed. After a homogeneous mixture was added the curing agent of 10:1. The water (SDS or P-123 inside) was added step by step to facilitate the blending. The mixture is heated at 80 °C under highly humid environment during two hours for pre-polymer cures with droplets and then placed at 120 °C to evaporate water and form porosity in the PDMS [20-21].

d) Carbon black

Carbon black (Vulcan® XC72R) was selected as conductive particles in the polymeric films. Before the incorporation in the polymeric solution, carbon black aggregates needs to be dispersed to obtain a homogenized composite.

e) Graphite

Graphite was supplied by American elements® and was used as conductive particles.

f) Metals

Different metallic particles: zinc (spherical and lamellar) was supplied by Umicore® and silver nanopowder was purchased from Sigma Aldrich and was dispersed in polymer matrix.

g) Graphene (xGNP)

Graphene nanoplatelets (GNP) grade C-750, M5, M15, M25 and H5, were purchased from XG Sciences with following characteristics given by the producer: M - maximum length 5 µm, 15 µm or 25 µm (M5, M15, M25, respectively), average thickness of 6 nm-8 nm and surface area between 120 $m^2 \cdot g^{-1}$ and 150 $m^2 \cdot g^{-1}$, H5 - maximum length 5 µm, average thickness of 15 nm and surface area between 50 $m^2 \cdot g^{-}$

[1] and 80 $m^2 \cdot g^{-1}$ and C-750 - maximum length 1 µm -2 µm, average thickness of 2 nm and average surface area of 750 $m^2 \cdot g^{-1}$.

h) Conductive polymers

Polyaniline (emeraldine salt) and Polyvinylpyrrolidone (PVP) were purchased from Sigma Aldrich and were selected as conducting polymer for preparing conductive films.

2.3 Characterization

2.3.1 Electrical Resistance

The electrical resistance of the prepared dense films was measured using a multimeter (Fluke 11) in an in-house made mechanical press at a pressure of 0 to 50 $N \cdot cm^{-2}$. The effective area of the electrode was 1 cm^2. The electrical contact between the ECPC film and the multimeter was obtained using a copper layer applied over a polymeric film (FlexPCB). Since the copper coated FlexPCB originates a poor electrode with the ECPC surface two layers of a polymeric film with similar composition of the ECPC film were applied in each side of the ECPC film having an electric conductivity two orders of magnitude higher than the ECPC film to be characterized. The high electrical conductivity of the electrode was obtained by adding a higher concentration of conductive particles. The experimental set-up for the measurement of the electrical resistance is shown in Figure 2.3.

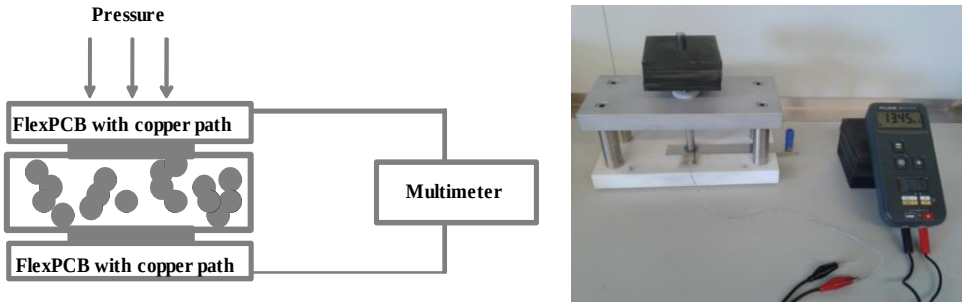

Figure 2.3 - Experimental set-up for measurement of electrical resistance of the ECPCs.

2.3.2 Mechanical Resistance

Mechanical testing of materials is performed for a variety of reasons such as a criteria in quality control, for comparing materials and establishing a basis for material selection in product development, to provide data for design purposes and as a starting basis for the formulation of theories in materials science [22-24]. In this case, the synthesized sensors should resist to the shear and compression forces as those observed in the insole of shoes.

Stress strain information provides an understanding of the mechanical behaviour of polymers and examines the influence of molecular structure on the ultimate properties of polymers. The most frequently applied stress strain measurement is made in tension. A tensile stress can thus be defined by

$$\sigma_1 = \frac{F_1}{A_0} \tag{2.1}$$

where σ_1 is the tensile stress, F_1 the tensile force, and A_0 the cross-sectional area of the specimen.

If the specimen is stretched by the tensile stress to a length l_1, the tensile strain is

$$\varepsilon_1 = \frac{l1 - l_0}{l_0} = \frac{kt}{l_o} \quad (2.2)$$

where κ is the rate of extension and t is the time.

Continuing the stressing test to the ultimate, that is, measuring the force at which the material breaks, results in a tensile strength known as the ultimate tensile stress:

$$\sigma = \frac{F}{A} \quad (2.3)$$

where F is the force at failure and A is the area of cross section at failure.

Elongation at break is usually expressed as a percentage of the original sample length:

$$\varepsilon = \frac{l - l_0}{l_0} \times 100 \ \% \quad (2.4)$$

Where l is the length at failure and l_0 is the original length.

The tensile modulus of elasticity, E, is defined as the ratio of stress to strain and is determined from the initial slope of the stress strain curve:

$$E = \frac{\sigma}{\gamma} = \frac{F l_0}{A\,(l - l_0)} \quad (2.5)$$

where γ is the strain rate[22, 24].

To select a portion in which failure is to occur and thus obtain a breaking load on a cross-sectional area that is unaffected by the gripping mechanisms, a “dumbbell” specimen is employed. The basic types of dumbbell configurations and dimensions recommended are presented in ISO 37 [22].

One of the most commonly used mechanical tests in industry is tensile testing, in which the stress exerted by the material is measured at a constant strain rate. In addition to providing direct measurements of relevant properties, the stress-strain curves constitute fingerprints of a material's mechanical performance and are often used for quality control of either raw materials or products.

The equipment used, Figure 2.4, was Mecmesin Multitest – 1d. Loadings were recorded with Mecmesin basic force gauge (BFG) 200 N digital dynamometer, at a strain rate of 50 mm/min [22-25]. Before performing the stress-strain tests, the thickness of the film needs to be measured, using a digital micrometer. This information is used to compute the initial cross sectional area of the specimen, on which the loading stress will be based.

Figure 2.4 - Experimental set-up for measurement of mechanical resistance.

2.3.3 Dynamic Mechanical Analysis (DMA)

Dynamic Mechanical Analysis (DMA) can be described as applying an oscillating force to a sample and analyzing the material's response to that force. DMA measures

the response of the material as a function of the temperature. An elastic modulus (E') and a loss modulus (E'') are calculated from the material response to the sine wave. Damping is the ability of the material to return energy (E'), to lose energy (E'') and the ratio of these effects (tan delta).

DMA experiments, Figure 2.5, were realized using a DMA 242 E from Netzsch in film compression mode at a fixed frequency of 1 and 10 Hz. Nitrogen gas was used at a flowing rate of 80 ml/min. The sample was tested with a temperature ranging from -20 °C to 100 °C and heating rate of 2 °C/min.

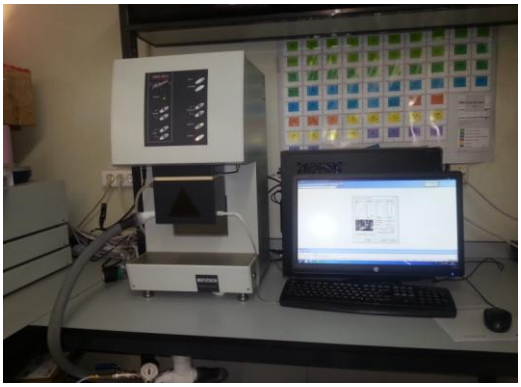

Figure 2.5 - Experimental set-up for measurement of dynamic mechanical properties – DMA.

2.4 Conclusions

This Chapter summarizes a set of experimental techniques that were used in the present work. The methods used were: preparation of the composite sensor and electrodes, determination of the electrical and mechanical resistance of the film.

The electrical resistance of the composite sensor as well as the electrical resistance of the outer conductive layers in the assembled sensor were measured using a press to measure the variation in electrical resistivity as a function of applied

pressure. The mechanical resistance of the composite sensors provides an indication of the resistance behaviour of the polymer sensor when embedded in the shoe insole. This property was evaluated by stress strain curves obtained by tensile forces applied to the film probes.

2.5 References

1. Panek, D., Konieczny, K., *Preparation and applying the membranes with carbon black to pervaporation of toluene from the diluted aqueous solutions.* Separation and Purification Technology, 2007. **57**(3): p. 507-512.
2. Bengtson, G., Scheel, H., Theis, J., Fritsch, D., *Catalytic membrane reactor to simultaneously concentrate and react organics.* Chemical Engineering Journal, 2002. **85**(2-3): p. 303-311.
3. Bengtson, G., Oehring, M., Fritsch, D., *Improved dense catalytically active polymer membranes of different configuration to separate and react organics simultaneously by pervaporation.* Chemical Engineering and Processing, 2004. **43**(9): p. 1159-1170.
4. Brandão, L., Madeira, L.M., Mendes, A.M., *Mass transport on composite dense PDMS membranes with palladium nanoclusters.* Journal of Membrane Science, 2007. **288**(1-2): p. 112-122.
5. Fritsch, D., Kuhr, K., Mackenzie, K., Kopinke, F.-D., *Hydrodechlorination of chloroorganic compounds in ground water by palladium catalysts: Part 1. Development of polymer-based catalysts and membrane reactor tests.* Catalysis Today, 2003. **82**(1-4): p. 105-118.
6. Liu, L., *Gas Separation by Poly(Ether Block Amide) Membranes*, in *Departement of Chemical Engineering* 2008, University of Waterloo: Canada. p. 213.
7. Sridhar, S., Suryamurali, R., Smitha, B., Aminabhavi, T.M., *Development of crosslinked poly(ether-block-amide) membrane for CO2/CH4 separation.* Colloids and Surfaces A: Physicochemical and Engineering Aspects, 2007. **297**(1-3): p. 267-274.
8. Shirmohammadi, R., *Temperature transients in spherical medium irradiated by laser pulse.* International Communications in Heat and Mass Transfer, 2008. **35**(8): p. 1017-1023.

9. Danesh, E., Ghaffarian, S.R., Molla-Abbasi, P., *Non-solvent induced phase separation as a method for making high-performance chemiresistors based on conductive polymer nanocomposites.* Sensors and Actuators B: Chemical, 2011. **155**(2): p. 562-567.

10. Zhao, Y.-H., Qian, Y.-L., Zhu, B.-K., Xu, Y.-Y., *Modification of porous poly(vinylidene fluoride) membrane using amphiphilic polymers with different structures in phase inversion process.* Journal of Membrane Science, 2008. **310**(1–2): p. 567-576.

11. Gugliuzza, A., Ricca, F., Drioli, E., *Controlled pore size, thickness and surface free energy of super-hydrophobic PVDF® and Hyflon®AD membranes.* Desalination, 2006. **200**(1–3): p. 26-28.

12. Gugliuzza, A., Drioli,E., *New performance of hydrophobic fluorinated porous membranes exhibiting particulate-like morphology.* Desalination, 2009. **240**(1–3): p. 14-20.

13. Jansen, J.C., Buonomenna, M.G., Figoli, A., Drioli, E., *Ultra-thin asymmetric gas separation membranes of modified PEEK prepared by the dry–wet phase inversion technique.* Desalination, 2006. **193**(1–3): p. 58-65.

14. Chakrabarty, B., Ghoshal, A.K., Purkait, M.K., *Effect of molecular weight of PEG on membrane morphology and transport properties.* Journal of Membrane Science, 2008. **309**(1–2): p. 209-221.

15. Kim, J.-H., Lee, K.-H., *Effect of PEG additive on membrane formation by phase inversion.* Journal of Membrane Science, 1998. **138**(2): p. 153-163.

16. Idris, A., Norashikin M.Z., Noordin, M.Y., *Synthesis, characterization and performance of asymmetric polyethersulfone (PES) ultrafiltration membranes with polyethylene glycol of different molecular weights as additives.* Desalination, 2007. **207**(1–3): p. 324-339.

17. Li, M., Zhang, W., Wang, C., Wang, H., *In situ formation of 2D conductive porous material with ultra low percolation threshold.* Materials Letters, 2012. **82**(0): p. 109-111.

18. http://www.wacker.com/cms/en/productsmarkets/products/product.jsp?product=8989. [cited 2013 january].

19. http://www.dowcorning.com/applications/. [cited 2013 may].

20. Chen, J., Zhang, R., Wang, W. (2012) *Fabricating microporous PDMS using a water-in-PDMS emulsion*.

21. Juchniewicz, M., Stadnik, D., Biesiada, K., Olszyna, A., Chudy, M., Brzózka, Z., Dybko, A., *Porous crosslinked PDMS-microchannels coatings.* Sensors and Actuators B: Chemical, 2007. **126**(1): p. 68-72.

22. Brow, R., ed. *Handbook of polymer testing: physical methods*. 1999, Marcel Dekker New York.

23. Féodosiev, V., ed. *Resistência dos materiais*. 1977, Edição Lopes da Silva: Porto.

24. Sperling, L.H., ed. *Introduction to physical polymer science*. 2006, John Wiley & Sons: New Jersey.

25. Pedrosa C., M.J., Magalhães F.D., *Mechanical testing of common use polymeric materials with an in-house built apparatus.*

CHAPTER III

3 Development of pressure sensors based on dense electrically conductive polymer composites[1]

Abstract

Electrically Conductive Polymer Composites (ECPCs) are promising candidates for using in low cost, flexible and large area pressure sensors. Different formulations were screened for preparing dense ECPCs for using in pressure sensors: conductive particles and conductive polymers were incorporated into polydimethylsiloxane (PDMS) and polyetherblockamide (PEBA) matrices. The conductive component type in the ECPC showed a strong influence on the electrical resistance of the prepared films. PEBA 2533 loaded with carbon black particles showed good electrical and mechanical properties suitable for ECPCs to be used as pressure sensors. Carbon black revealed to be a promising filler to incorporate in ECPCs due to the low cost, close density compared to the polymer matrix, high conductivity and small particle size. Electrodes for measurement of the electrical properties of the ECPCs were also developed. These were fabricated in a similar composite material as the ECPC one showing very good adhesion to the ECPC and uniform electrical contact. The developed electrodes demonstrated to be critical for obtaining reproducible responses without an electrical response influenced by the contact area.

[1] Adapted from: Gonçalves, V., Brandão, L., Cunha S., Mendes, A., Development of pressure sensors based on dense electrically conductive polymer composites, *Submitted*.

3.1 Introduction

Electrically Conductive Polymer Composites (ECPCs) have received considerable attention for use in pressure sensor applications owing to their electrical and mechanical properties and easy processing [1]. ECPCs are made of an insulating polymer matrix loaded with particles with high electrical conductivity (carbon black, graphite, metals or semiconducting metal-oxides) or blended with a conductive polymer (polyaniline (PANi) and polyvinylpyrrolidone (PVP)) [2]. Pressure sensors based on ECPCs show an electrical resistivity change with the pressure applied [3] and are known as piezoresistive. When pressure is applied, the conducting particles in the ECPC come in contact with each other and a conducting path is formed – the percolation threshold. As pressure increases more conductive paths are formed and the overall electrical resistance decreases. However, if pressure load continues to increase this conductive path might be destroyed resulting in an overall ECPC resistance increase [2, 4-7].

The maximum sensitivity of a ECPC to pressure is obtained at the percolation threshold [7], when the electrical resistivity begins changing quickly. The percolation threshold of ECPCs can be affected by the polymer matrix, conductive particle (size, concentration and morphology), dispersion of the conductive particles in the polymer matrix and thickness of the film [8]. In this Chapter, dense ECPCs are developed dispersing conductive particles or conducting polymers in an insulating polymer matrix. This work aims at screening the most promising formulations for developing a lightweight, robust and cheap piezoresistive pressure sensor. The most important factors concerning the ECPC performance when inserted in a pressure sensor were studied: conductive component type, mechanical properties and film morphology. The influence of the electrodes type on the electrical resistance measurements was also addressed.

3.2 Materials

The cross-linkable polydimethylsiloxane (PDMS), Dehesive® 920, was purchased from Wacker Silicon Corporation. PEBAX polymer (polyether block amide) was supplied by Atofina Chemicals. Carbon black powder (Vulcan® XC72R) was purchased from Cabot Corporation. Zinc was supplied by Umicore® and graphite was purchased from American elements®. Polyvinylpyrrolidone (PVP), polyaniline (PANi), ethanol, n-butanol, tert-butanol, n-methyl-2-pyrrolidone (NMP) and tetrahydrofuran (THF) were purchased from Sigma Aldrich.

3.3 Preparation of Electrically Conductive Polymer Composites

Various ECPCs formulations were prepared and characterised, see Table 3.1. Polymer matrices PEBA 2533 and PDMS were used for hosting particles of various shapes, sizes and densities. Polymer blends ECPCs were also prepared and characterised; conductive polymers PANi and PVP were selected for that.

Table 3.1 – Different prepared dense ECPCs.

Polymer matrix	Conductive particle	Conductive polymer
PEBA 2533	Spherical zinc	
	Lamellar zinc	
	Graphite	
	Carbon black	
		PANi
		PVP
	Spherical zinc	PANi
	Lamellar zinc	PANi
PDMS	Spherical zinc	
	Lamellar zinc	
	Graphite	
	Carbon black	
	Lamellar zinc	PANi

3.3.1 Dispersion of the conductive fillers

Fillers dispersed in the appropriate solvents were stirred in an ultrasonic bath at room temperature for 2 hours and 30 minutes [9]. For PDMS based films, THF was used for all fillers tested (33 wt.% of PDMS in the solvent). For PEBA based films, NMP was used for spherical and lamellar zinc, PANi, PVP and butanol (80 wt.% n-butanol and 20 wt.% tert-butanol) was used for graphite. For carbon black particles (CB), NMP or ethanol was used. In all PEBA based films, the polymer concentration in the solvent was 10 wt.%.

3.3.2 Preparation of PDMS films

Polydimethylsiloxane (PDMS), Dehesive® 920, was added to the previously prepared fillers suspensions in THF to a final concentration in PDMS of 33 wt.%. The required amount of crosslinker (2.5 wt.% of polymer) was added to the PDMS suspension. Stirring was maintained until a homogeneous mixture was obtained. After that, the cross-linking catalyst (platinum complex with 1,1,3,3-tetramethyle-1,3-divinyledisiloxane) was added to the mixture (3 wt.% of the polymer) and the suspension poured on a Teflon coated glass plate. The solvent was evaporated at room temperature overnight [9-11]. PDMS films' thicknesses of ca. 250 μm were determined with a digital micrometer.

3.3.3 Preparation of PEBA films

PEBA were dissolved in NMP, ethanol or butanol (10 wt.% of polymer) and stirred vigorously up to 110 °C under reflux. PEBA solutions (kept at 90 °C) were added to the fillers suspensions previously dispersed in the same solvent. The hot suspension was poured on a glass plate thermostated at 60 °C. After 1 hour, the heating was switched off and the membrane was kept at room temperature overnight [9, 12-15]. PEBA 2533 films' thicknesses of ca. 150 μm were determined with a digital micrometer.

3.4 Characterization

3.4.1 Measurement of Electrical Resistance

The electrical resistance of the prepared dense films was measured using a multimeter (Fluke 11) in an in-house made mechanical press. The effective area of the electrode was 1 cm^2. The electrical contact between the ECPC film and the multimeter was obtained using a copper layer applied over a polymeric film (FlexPCB). Since the copper coated FlexPCB originates a poor electrode contact with the ECPC surface, a

layer of carbon black powder followed by a carbon paper layer (type *a*) was applied on both ECPC surfaces (Figure 3.1, left image). In another configuration, two layers of a polymeric film with similar composition of the ECPC film (type *b*) were applied in each side of the ECPC film and then the system was sandwiched between the copper/FlexPCB. Type *b* electrodes have an electric conductivity two orders of magnitude higher than the ECPC film to be characterized (Figure 3.1, right). The elevated electrical conductivity of the electrode was obtained by adding a higher concentration of conductive particles (usually 25 vol.% carbon black). Other electrode types were also considered (see description along the text).

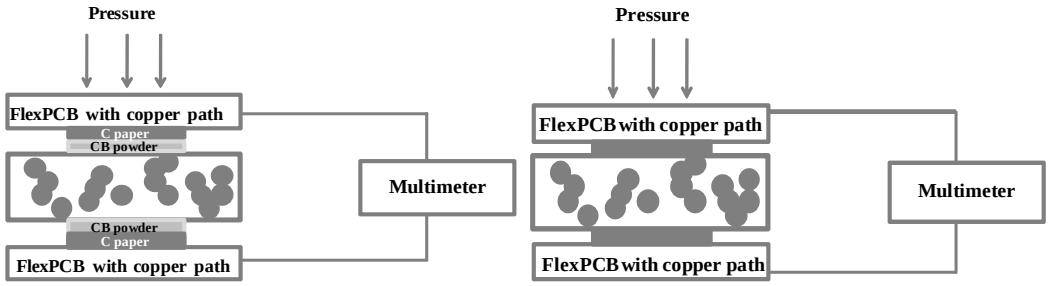

Figure 3.1 – Experimental set-up for measuring the electrical resistance of the ECPC (left – type *a* electrodes, right – type *b* electrodes).

3.4.2 Measurement of Mechanical Resistance

Stress-strain curves were used to evaluate the mechanical resistance to traction of some of the prepared ECPC films. The equipment used was a Mecmesin Multitest – 1d. Loadings were recorded with Mecmesin basic force gauge (BFG) 200 N digital dynamometer, at a strain rate of 50 mm/min [16-19].

3.4.3 Scanning Electron Microscopy (SEM)

The surface and cross-sectional films morphologies were observed by Scanning Electron Microscopy (SEM) using a JEOL JSM-6301F, Oxford INCA Energy 350 equipment. Before being analyzed, the samples were fractured in liquid nitrogen and sputtered with gold/ platinum using a K575X Sputter Coater by Quorum Technologies. This technique was used in order to evaluate if the conductive particles are clustered or not in the synthesized films and to visualise the contact between the ECPC film and the polymeric electrode.

3.5 Results and discussion

3.5.1 Effect of conductive particles on mechanical resistance

For dense ECPCs, the insulating matrix used is very important and elastomers are normally used because of their softness [2]. For use in diabetic foot diagnosis and treatment [20], the pressure sensor is subjected to significant shear forces. For this and other applications, mechanical properties of the insulating elastomer are important. PDMS and PEBA based ECPCs were characterized concerning their mechanical resistance and the corresponding tensile modulus of elasticity. Additionally, the influence of the filler in the elastomeric matrix was also evaluated. Table 3.2 shows the Young's modulus, ultimate tensile strength and ultimate strain of PDMS and PEBA 2533 loaded with different particles.

Table 3.2 - Young's modulus, ultimate tensile strength and ultimate strain for carbon black filled ECPCs and pristine elastomers.

ECPCs	Young's modulus (MPa)	Ultimate tensile strength (MPa)	Ultimate strain (%)
PEBA 2533	0.10	3.83	200
PEBA2533 + 7 vol.% CB	0.14	11.7	823
PEBA 2533 + 25 vol.% CB	0.27	8.26	434
PEBA 2533 + 25 vol.% graphite	0.020	2.53	508
PEBA 2533 + 25 vol.% lamellar zinc	0.010	2.01	327
PDMS	0.080	1.92	29.8
PDMS + 7 vol.% CB	0.057	2.17	40.2

Figure 3.2 shows the typical thermoplastic behaviour observed for PEBA 2533 films. The best mechanical properties were observed for ECPC prepared with carbon black particles. Table 3.2 and Figure 3.2 show that PEBA 2533 loaded with carbon black presents Young's modulus, ultimate strain and ultimate tensile strength greater than the pristine PEBA 2533. On the other hand, Table 3.2 and Figure 3.3 show that there are no significant differences between the pristine PDMS and PDMS loaded with carbon black.

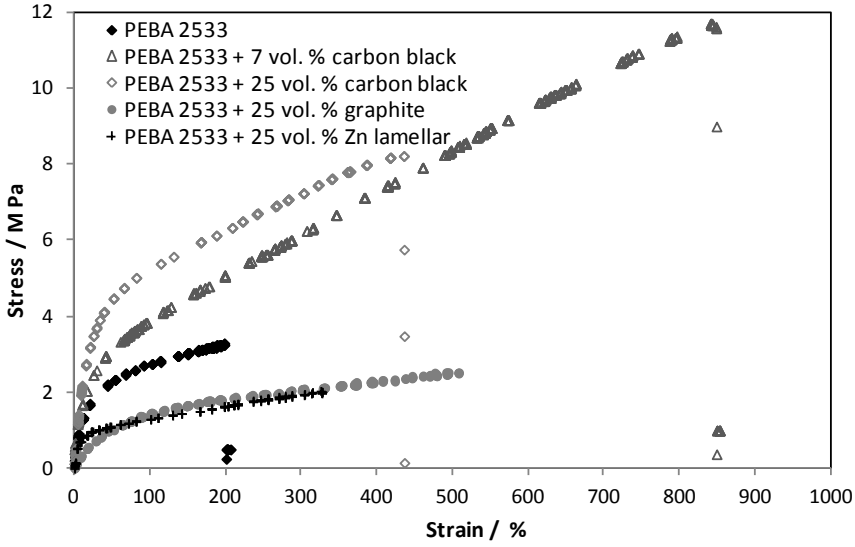

Figure 3.2 - Stress-strain curve of pristine PEBA 2533 film and loaded with different electroconductive particles.

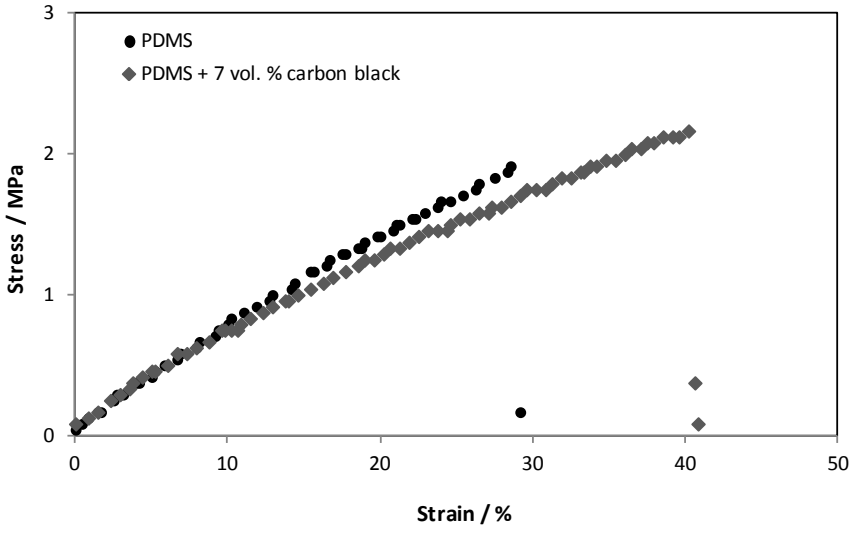

Figure 3.3 - Stress-strain curve of pristine PDMS film and loaded with carbon black.

PEBA 2533 based ECPCs show Young's modulus, ultimate strain and ultimate tensile strength greater than the PDMS ones, indicating a better performance when compared to the PDMS in terms of mechanical properties.

3.5.2 Electrical Resistance

According to the previously mentioned, there are many factors that influence the pressure sensor's response such as the type of the electrode and the type of the conductive component. In turn, these factors influence the percolation and piezoresistive effect.

Conducting Component Type

The influence of different types of electrical conducting components in the elastomeric matrices of PDMS and PEBA 2533 was addressed. The electrical resistivity characterization was performed at a constant pressure of 1.5 $N \cdot cm^{-2}$. Table 3.3 shows the electrical resistivity of the different dense ECPCs prepared with a 7 vol.% concentration of electrical conducting components.

ECPCs prepared with conductive polymers (PVP and PANi) blended in the elastomeric polymer matrix exhibited higher electrical resistance and showed a poor film visual uniformity when compared to ECPCs produced with carbon black. Formulations based on carbon black appear to be the most promising for pressure sensor applications because of the small size of carbon black particles (nanometer scale) and the lower carbon density (~2 $g \cdot cm^{-3}$) given by the producer. On the other hand, carbon black contributes for improving the mechanical properties of the polymeric films (Figure 3.2).

Table 3.3 - Electrical resistivity (ρ) of different films prepared with 7 vol.% filler content assembled with type *b* electrodes (Solvent used for PDMS films: THF, solvent used for PEBA films: NMP or butanol).

	ρ (kΩ·cm)	
Conductive particles / polymers	**PEBA 2533**	**PDMS**
Spherical Zn	Insulating	Insulating
Lamellar Zn	Insulating	Insulating
PANi	Insulating	n.a.
PVP	Insulating	n.a.
Spherical Zn/PANi	Insulating	n.a.
Lamellar Zn/ PANi	Insulating	Insulating
Graphite	Insulating	Insulating
Carbon black	13	100

Note - n.a.: not available.

Percolation Threshold

The electrical resistance as a function of the concentration of carbon black on dense PEBA film was determined. When the conductive particles concentration is low there are almost no electrical pathways linking both surfaces of the ECPC and its resistivity is very high [21]. When conductive particles concentration is very high, the conductive particles pack up very closely in the composite and form conductive pathways, which give a very low resistance response to the sensor [8, 21-22]. A pressure sensitive sensor is only obtained for a concentration of carbon back within a certain range [2, 7]. For this concentration range, as the sensor is compressed an increasing number of conductive electrical pathways is formed and the electrical

resistance decreases responding to the weight load. The percolation threshold concentration is when conductive electrical pathways are formed and the sensor becomes electrically conductive [23].

Figure 3.4 shows the percolation threshold of dense PEBA 2533/CB ECPCs for different concentrations of carbon black for an applied pressure of 1.5 $N \cdot cm^{-2}$ assembled with type *a* electrodes.

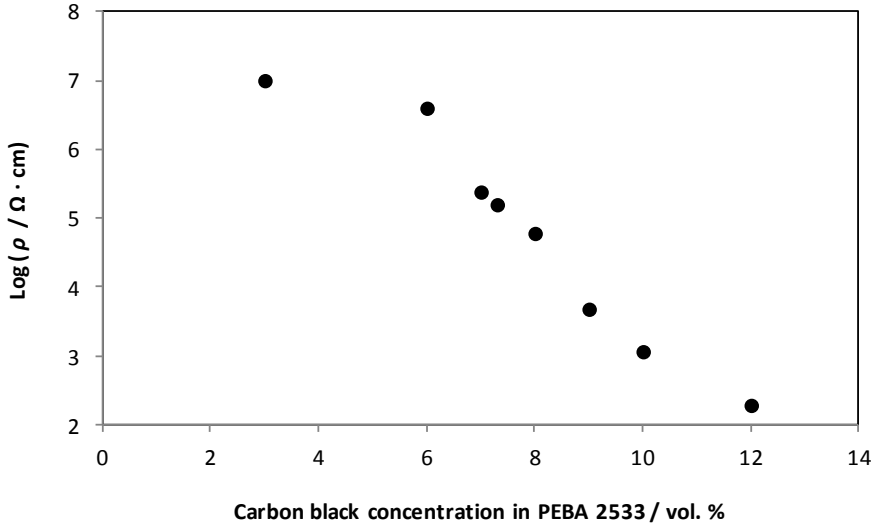

Figure 3.4 – Electrical resistivity (log value) of PEBA 2533/CB ECPCs for different carbon black concentrations assembled with type *a* electrodes.

The electrical resistivity decreases with carbon black concentration due to the increasing number of conductive paths formed. The carbon black concentration expected range for using that ECPCs on a pressure sensor with a probable high sensitivity to pressure (piezoresistive effect) is observed for the ECPCs incorporating ca. 6-10 vol.% of carbon black particles, i.e. in the region of the percolation threshold.

However, these results were determined with type *a* electrodes that as will be shown later strongly influenced the electrical resistivity measurement (see below).

Piezoresistive Effect

The electrical resistance as a function of the applied pressure for the dense PEBA 2533/CB ECPC incorporating 7 vol.% of carbon black and assembled with type *a* electrodes was determined, Figure 3.5. A significant piezoresistive response was observed up to ~ 21 N·cm^{-2} where the electrical resistance changed from 7.5 kΩ to 1 kΩ (approximately). From approximately 21 N·cm^{-2} up to 45 N·cm^{-2}, the ECPCs did not show any pressure sensitivity.

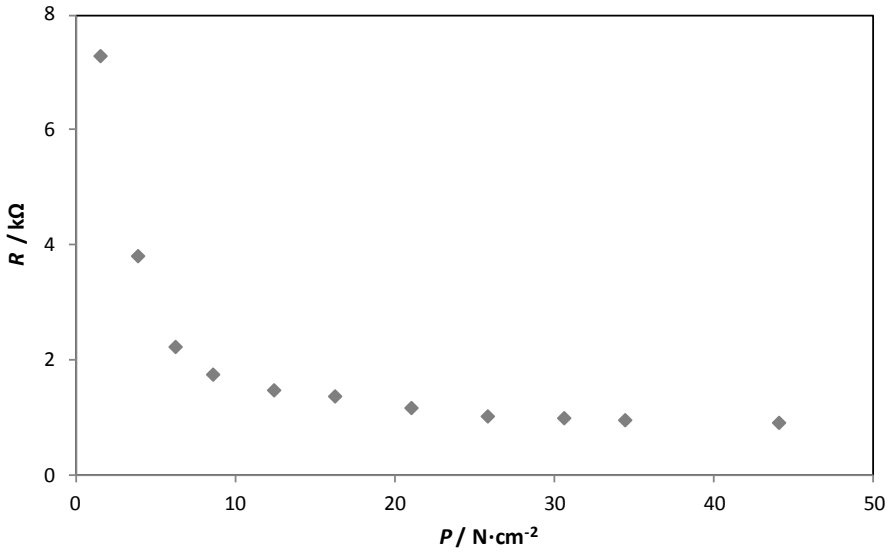

Figure 3.5 - Electrical resistance as a function of the applied pressure of dense ECPC film based on PEBA 2533 incorporating 7 vol.% of carbon black, thickness 150 µm, assembled with type *a* electrodes**.**

Electrical Contact Effect

During the present work it was observed that the type of electrodes used to measure the piezoresistive effect largely influences the electrical response of the ECPCs. Because of that, good adhesion and robust electrodes (stable towards shear forces) were developed with the same material as the dense ECPC material in order to avoid changes in the contact area (type *b* electrodes). A change in contact area would produce a response of the sensor that changes with the time (interface responsive element), originated for example by the walk shear strength. Because of that, interface responsive pressure sensors usually suffer from low robustness.

The polymeric electrodes developed have an electrical conductivity ca. 2 orders of magnitude higher than the ECPCs to be characterized to ensure that a significant additional resistance is not added to the sensor (see Figure 3.6). After realizing the strong influence of the electrodes type on ECPCs characterization, all the electrical results presented in this work were carried on using the developed electrodes (type *b* electrodes). Figure 3.6 evidences the very high electrical conductivity of type *b* electrodes developed in this work. This figure shows the electrical resistance of a sensor element (PEBA 2533 ECPC containing 10 vol.% of carbon black with type *b* electrodes*)* as a function of its thickness for an applied pressure of 1.5 $N \cdot cm^{-2}$. The electrical resistance changes linearly with the thickness of the sensor element showing the negligible influence of the electrodes resistance on the overall resistance, even for a sensor element with a relatively low electrical resistance.

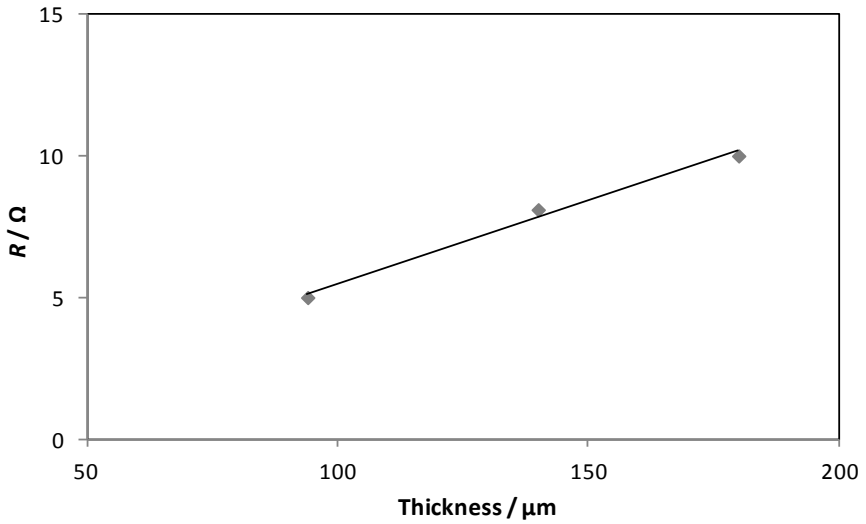

Figure 3.6 - Electrical resistance as a function of the sensor element thickness type *b* electrodes; element sensor of PEBA 2533 containing 10 vol.% of carbon black and 1.5 $N \cdot cm^{-2}$ of applied pressure.

Table 3.4 gives an overview of the strong influence of the type of electrodes used for measuring the electrical resistivity of the ECPCs. This table compares the electrical resistivity of a dense PEBA 2533 composite film incorporating carbon black measured with three electrodes: type 0 – copper/ FlexPCB; type a – FlexPCB followed by a carbon paper layer covered with carbon black powder layer that is in contact with the sensor element (Figure 3.1, left image) and type b – FlexPCB followed by a polymeric film with similar composition of the ECPC film (Figure 3.1, right image). These results show that the electrical resistivity of the ECPC decreases significantly from type 0 to type *b* because the quality of the electrodes improves as well (due to the roughness present on the ECPC surface only type *b* electrodes can provide an effective electrical contact). To further confirm the influence of the electrode type,

other electrode configurations were also studied: type *c* - type 0 + the polymeric electrodes casted on carbon paper where the polymeric electrode face contacts with the ECPC; type *d* – type 0 + the polymeric electrodes casted on FlexPCB where the polymeric electrode face contacts with the ECPC; type *e* – type *d* + type *c* where the polymeric electrode face contacts with the carbon paper of type *c* electrode and this with the ECPC; type *f* – type 0 + carbon black powder. Figure 3.7 shows the electrical resistance of PEBA 2533/ CB ECPCs as a function of the applied pressure characterized with these electrodes. It is clear that for each type of electrodes the electrical resistance is different. Type 0 electrodes have the higher electrical resistance followed by type *c*, *d* and *e*. The trend observed seems to be related to the surface roughness of the sensor and the ability of the electrodes to gain electrical contact with this surface; as the electrodes show improved ability to intimately contact the rough surface of the sensor, the overall electrical resistance decreases - Table 3.4 and Figure 3.7. SEM images shown in Figure 3.8 and Figure 3.9 of a type *b* electrode/ECPC interface illustrate an intimate contact between the electrode and the surface of the sensor. Figure 3.8 shows a SEM image of the cross-section of a dense ECPC based on PEBA 2533, at the interface between the ECPC itself (Z_1) and the polymeric electrode (Z_2). Both composite polymer layers have a good adhesion and carbon black particles look like being well dispersed. On the other hand, Figure 3.9 evidences that the roughness present on the ECPC surface is eliminated due to the polymeric electrodes filling of the “valleys” what consequently reduces the effect of contact area.

Table 3.4 - Electrical resistivity (ρ) of a film PEBA 2533 containing 7 vol.% concentration of the carbon black for an applied pressure of 1.5 N·cm^{-2} assembled with different electrodes configurations.

PEBA 2533 + 7 vol.% carbon black	Electrical resistivity (kΩ·cm)
Type 0	800
Type *a*	500
Type *b*	13

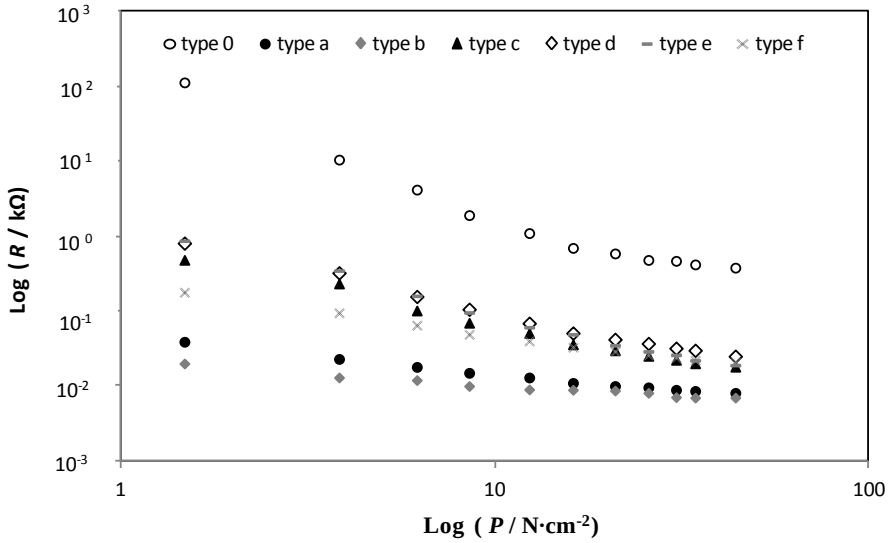

Figure 3.7 - Electrical resistance (log value) of sensor PEBA 2533/CB ECPCs as a function of applied pressure assembled with different electrode configurations: (type 0, type *a*, type *b,* type *c*, type *d*, type *e* and type *f*).

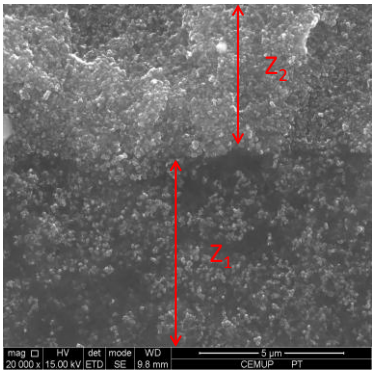

Figure 3.8 - SEM images of the cross-section of PEBA 2533 film (Z_1) containing 7 vol.% of carbon black assembled with type *b* electrodes (PEBA 2533 incorporating 25 vol.% of carbon black(Z_2)).

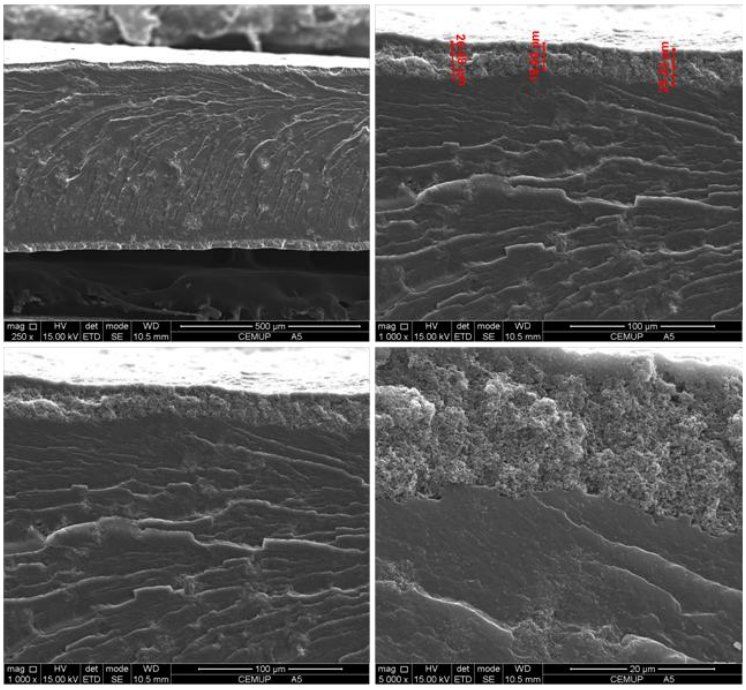

Figure 3.9 – SEM images of the cross-section of PEBA 2533 film incorporating carbon black assembled with type *b* electrodes.

Figure 3.10 compares the electrical resistivity of sensors fabricated with ECPCs loaded with increasing concentration of carbon black and previously characterized with type *a* electrodes (Figure 3.4) but now using the type *b* electrodes. In this case there is no clear region of percolation threshold.

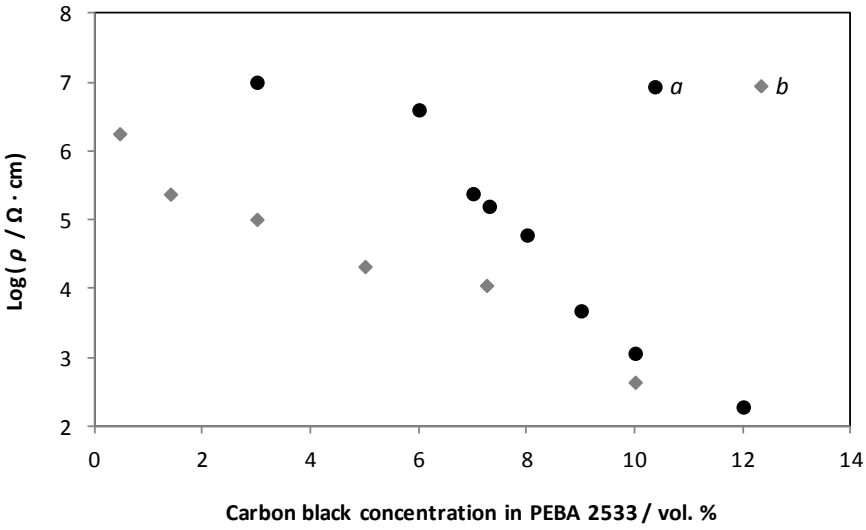

Figure 3.10 - Electrical resistivity (log value) of PEBA 2533/CB ECPCs for different carbon black concentrations assembled with different electrodes: (a: type *a* and *b*: type *b*).

Figure 3.11 compares the electrical resistance as function of the applied pressure of a sensor fabricated with ECPCs and characterized in Figure 3.5 with type *a* electrodes with sensors fabricated with the same ECPCs but now with type 0 and *b* electrodes. A very high sensitive pressure response from the ECPC was obtained for type 0 and *a* electrodes, the response of these pressure sensors seems to be related to the development of a improved electrical contact between the electrode surface and the rough ECPC surface; as pressure builds up, the valleys of the rough ECPC

surface gain contact with the surface of the electrodes. On the other hand, the ECPC characterized with the polymeric electrodes (type *b* configuration) shows the intrinsic electrical resistance behaviour as a function of the pressure very low electrical resistance and very small sensitivity towards the pressure load. Such behaviour was observed for all ECPCs considered in this work (data not shown).

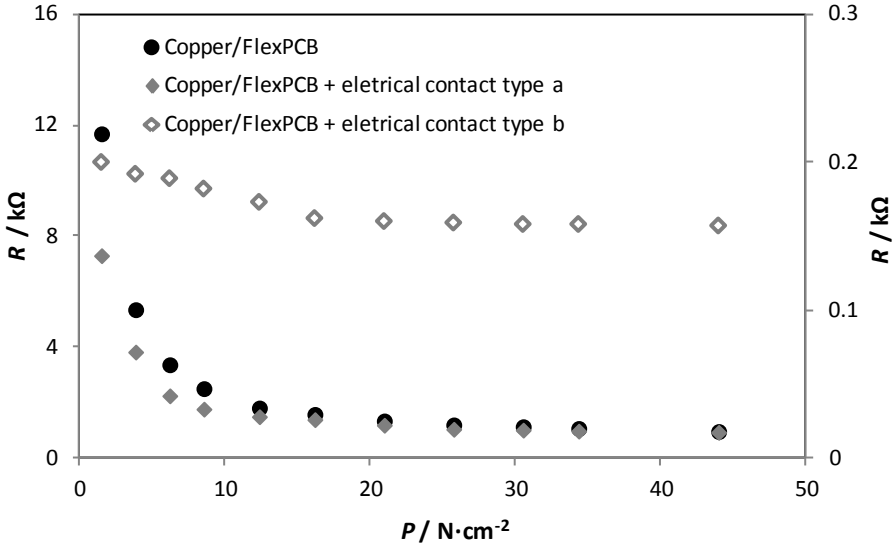

Figure 3.11 - Electrical resistance as a function of the applied pressure of dense ECPC film based on PEBA 2533 incorporating 7 vol.% of carbon black, thickness 150 µm, assembled with different types of electrodes**.**

These results indicate that further work has to be performed for fabricating pressure sensors with an intrinsic response when using polymeric electrodes (type *b*).

Figure 3.12 shows the stress-strain curve of a PEBA 2533 film loaded with carbon black particles with polymeric type *b* electrodes. PEBA 2533 based ECPC with the polymeric electrodes showed a mechanical resistance greater than the pristine PEBA 2533 film and no delamination of the three layers was observed during all the

mechanical tests, indicating that a very good adhesion between the layers exists. This indicates that type *b* electrodes meet the objective of a good mechanical stability since the electrodes are bonded to the ECPC.

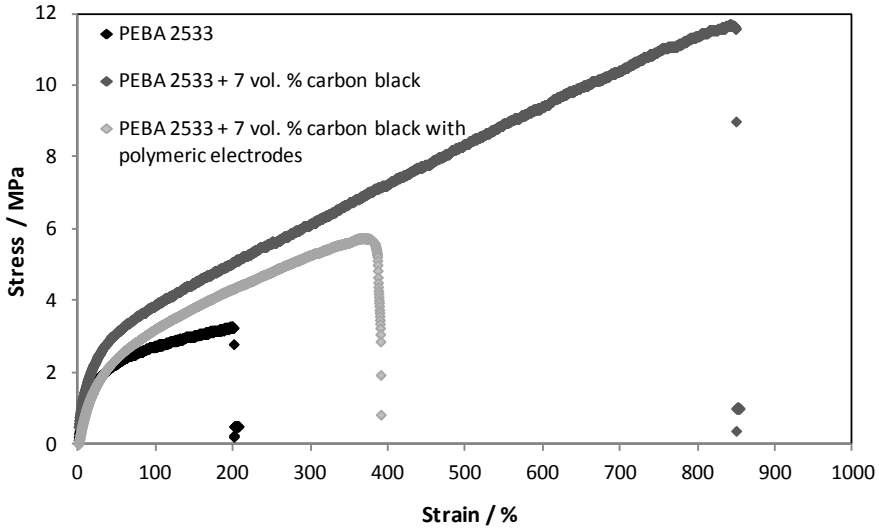

Figure 3.12 – Stress-strain curve of PEBA 2533 films without and with the type *b* electrodes.

3.6 Conclusions

The dense ECPCs prepared in this work showed good mechanical properties for incorporating in insoles. PEBA 2533 based ECPCs showed a Young's modulus, ultimate strain and an ultimate tensile strength greater (0.10 MPa, 3.83 MPa and 200 % respectively) than the PDMS based ones (0.08 MPa, 1.92 MPa and 29.8 % respectively). Moreover, the incorporation of carbon black on PEBA 2533 improved the mechanical properties of these films.

ECPCs produced with conductive polymers (PVP and PANi) blended in the elastomeric polymer matrices exhibited very high electrical resistances and poor film

uniformity. Zinc particles also produced non-homogeneous polymer composite films with a poorly reproducible electrical response. Polymer formulations based on carbon black seem to be the most promising for developing pressure sensors.

The type of electrodes largely influenced the electrical response of the ECPC films due to changes in the contact area established between surfaces. Because of that, electrodes (type *b*) based on the same material as the ECPCs films were developed to improve the adhesion between surfaces and with very good mechanical properties. The type *b* electrodes when were used to characterize the ECPC showed the intrinsic electrical response of the ECPCs prepared: the electrical resistance decreased about 2 orders of magnitude and the pressure sensitivity decreased very significantly in comparison to the type *a* and type 0 electrodes when such electrodes were used. In these cases, a very good pressure sensitive response was obtained only because of the change in contact area between sensor and electrodes.

3.7 References

1. Hwang J., J.J., Hong K., Kim K. N., Han J. H., Shin K. , Park C. E., *Poly(3-hexylthiophene) wrapped carbon nanotube/poly(dimethylsiloxane) composites for use in finger-sensing piezoresistive pressure sensors.* Carbon, 2011. **49**(1): p. 106-110.
2. Knite M., T.V., Polyakov B., Erts D., *Electric and elastic properties of conductive polymeric nanocomposites on macro- and nanoscales.* Materials Science and Engineering: C, 2002. **19**(1-2): p. 15-19.
3. Cochrane C., K.V., Lewandowski M., Dufour C., *Design and development of a flexible strain sensor for textile structures based on a conductive polymer composite.* Sensors, 2007. **7**(4): p. 473-492.
4. Del Castillo-Castro T., C.-O.M.M., Encias J.C., Herrera Franco P.J., Carrillo-Escalante H.J., *Piezo-resistance effect in composite based on cross-linked polydimethylsiloxane and polyaniline:potential pressure sensor application.* 2012. **47**: p. 1794-1802.

5. Luheng W., T.D., Peng W., *Influence of carbon black concentration on piezoresistivity for carbon-black-filled silicone rubber composite.* Carbon, 2009. **47**(14): p. 3151-3157.

6. Lei, H.P., William G.;McGrath, Lucas K.;Ho, Clifford K., *Modeling carbon black/polymer composite sensors.* Sensors and Actuators B: Chemical, 2007. **125**(2): p. 396-407.

7. Knite M., T.V., Kiploka A., Kaupuzs J., *Polyisoprene-carbon black nanocomposites as tensile strain and pressure sensor materials.* Sensors and Actuators A: Physical, 2004. **110**(1-3): p. 142-149.

8. Lei H., P.W.G., McGrath L.K., Ho C.K., *Resistivity measurements of carbon-polymer composites in chemical sensors: impact of carbon concentration and geometry.* Sensors and Actuators B: Chemical, 2004. **101**(1-2): p. 122-132.

9. Panek D., K.K., *Preparation and applying the membranes with carbon black to pervaporation of toluene from the diluted aqueous solutions.* Separation and Purification Technology, 2007. **57**(3): p. 507-512.

10. Luheng W., T.D., Peng W., *Effects of conductive phase content on critical pressure of carbon black filled silicone rubber composite.* Sensors and Actuators A: Physical, 2007. **135**(2): p. 587-592.

11. Brandão L., M.L.M., Mendes A.M., *Mass transport on composite dense PDMS membranes with palladium nanoclusters.* Journal of Membrane Science, 2007. **288**(1-2): p. 112-122.

12. Jiraratananon R., S.P., Uttapap D., Huang R.Y.M., *Pervaporation separation and mass transport of ethylbutanoate solution by polyether block amide (PEBA) membranes.* Journal of Membrane Science, 2002. **210**(2): p. 389-409.

13. Sridhar S., S.R., Smitha B., Aminabhavi T.M., *Development of crosslinked poly(ether-block-amide) membrane for CO2/CH4 separation.* Colloids and Surfaces A: Physicochemical and Engineering Aspects, 2007. **297**(1-3): p. 267-274.

14. Bengtson G., O.M., Fritsch D., *Improved dense catalytically active polymer membranes of different configuration to separate and react organics simultaneously by pervaporation.* Chemical Engineering and Processing, 2004. **43**(9): p. 1159-1170.

15. Bengtson G., S.H., Theis J., Fritsch D., *Catalytic membrane reactor to simultaneously concentrate and react organics.* Chemical Engineering Journal, 2002. **85**(2-3): p. 303-311.

16. Brow, R., ed. *Handbook of polymer testing: physical methods*. 1999, Marcel Dekker New York.

17. Féodosiev, V., ed. *Resistência dos materiais*. 1977, Edição Lopes da Silva: Porto.

18. Pedrosa C., M.J., Magalhães F.D., *Mechanical testing of common use polymeric materials with an in-house built apparatus.*

19. Sperling, L.H., ed. *Introduction to physical polymer science*. 2006, John Wiley & Sons: New Jersey.

20. Brady S., L.K.T., Megill W., Wallace G.G., Diamond D., *The Development and Characterisation of Conducting Polymeric-based Sensing Devices.* Synthetic Metals, 2005. **154**(1-3): p. 25-28.

21. Zavickis J., K.M., Ozols K., Malefan G., *Development of percolative electroconductive structure in piezoresistive polyisoprene-nanostructured carbon composite during vulcanization.* Materials Science and Engineering: C, 2011. **31**(2): p. 472-476.

22. Bendo L., S.V., Domenech S.C., *Compósitos elastoméricos condutores a base de terpolímero de etileno-co-propileno-5-etilideno-2-norborneno e negro de fumo modificado com polímeros condutores intrínsecos utilizados na construção de um protótipo de sensor de dígito-pressão*, in *Departamento de Química*. 2006, Universidade Federal de Santa Catarina: Florianópolis. p. 57.

23. Hussain, M., Choa, Y.-H., Niihara, K., *Fabrication process and electrical behavior of novel pressure-sensitive composites.* Composites Part A: Applied Science and Manufacturing, 2001. **32**(12): p. 1689-1696.

CHAPTER IV

4 Development of dense and porous matrices for polymer-based pressure sensors[1]

Abstract

Aluminium oxide, titanium dioxide, calcium carbonate, glucose, yttria stabilized zirconia and barium sulphate were tested as non-conducting particles on dense electrically conductive polymer composites (ECPCs) made from PEBA and PDMS. Different particle sizes were considered where yttria stabilized zirconia showed the smallest average particle size and the narrowest distribution (~130 nm). These dense ECPCs incorporating non-conductive particles and carbon black with polymeric electrodes showed however very low sensitivity towards pressure. Porous conducting polymer composite films for assembling ECPCs were then considered. Porous PDMS films were prepared by the foaming and emulsion methods while PEBA films were prepared by the phase inversion method. The emulsion method using water and butanol as emulsifiers allowed the preparation of porous PDMS films with a high amount of pores. However, larger and more abundant pores are observed on the top surface morphology in comparison with the cross-section. On the other hand, the phase inversion method allowed the preparation of porous PEBA films with a nodule structure, high porous and symmetric morphology very promising for preparing porous ECPCs.

[1] Adapted from: Gonçalves, V., Brandão, L., Mendes, A., Development of porous polymer-based pressure sensors, *Submitted*.

4.1 Introduction

Polymer-based pressure sensors are made from a polymer matrix containing conductive particles or blended with conductive polymers and different preparation processes and materials can be used [1-5]. A large number of studies can be found in the literature regarding the development of dense polymer-based pressure sensors. The most common are polymeric films containing carbon black particles [1, 3-6]. Hussain et al. [5] reported the preparation of a dense polymer-based pressure sensor by dispersing carbon particles in a silicone rubber matrix. Aluminium oxide (Al_2O_3) was added to improve the sensitivity of the sensor, meaning to obtain a gradual resistance decrease when pressure is applied. Composites with a carbon content of 35 vol.% showed a very good resistance response to the applied pressure.

Other methods for preparing polymer–based pressure sensors were also disclosed in some patents [7-12]. These authors described pressure-sensitive devices composed of metal, metal oxide, semiconductor, conducting polymer or carbon particles dispersed in a dense polymeric insulating matrix. Lussey et al. [8] described a pressure responsive device consisting of two electrodes connected to a pressure sensitive element (polymer film loaded with particles of a metal or a reduced metal oxide). The same authors [7] described the composition of a polymer film incorporating electrical conductive particles to use in the production of pressure sensor elements. These sensor elements consist of an elastomeric dense polymer with conductive particles. The conductive particles may be of one or more types: metals, semiconductors, carbon nanotubes, etc. The viscosity of the polymer solution (in water–based or an organic solvent) should be relatively low. The manufacturing processes include doctor blade, screen-printing and mayer rod technique.

Podoloff et al. [9] reported tactile sensors used for measuring the compression distribution in the foot. They prepared composite pressure sensors made of dense

silicone rubber (SR) and carbon black (CB) with a mass ratio CB / SR between 0.10 and 0.14. They also describe a pressure sensor based on polyamide allowing continuous film production, robust and low cost.

Krivopal [10] studied a pressure sensitive ink that can be used as a component to fabricate a pressure-sensitive device. The ink was made of an polymer binder mixed with well-dispersed semi conductive nanoparticles present in concentrations between 1 wt.% and 7 wt.% based on polymer weight. The thickness of the ink varied between 1.27 µm to 1270 µm. Lima et al. [11] described pressure-sensitive devices based on polymer films and the methods of their manufacture. The pressure-sensitive layer was sandwiched by electrodes layers. The pressure-sensitive layer comprises carbon nanoparticles dispersed in a dense polymeric matrix. Moreover, Lussey et al. [12] investigated a device based on a flexible conductive material. The disclosed materials of the conductive layer are metal, metal oxide, semiconductor, conducting polymer (polyaniline, polypyrrole and polythiophene) and carbon dispersed in a dense polymeric matrix.

On the other hand, few studies report the development of pressure sensors based on a porous polymer composite film [13-17]. The porosity in an ECPC is directly related to the performance of the pressure sensor, e.g., when ECPC porosity increases, sensitivity to pressure increases [13-15]. This happens because upon applying pressure, the conductive particles come into contact but the pores become the limiting link in the percolation threshold [14]. Ravati et al. [13] studied porous polymeric pressure sensors depositing polyaniline (Pani) on a matrix blend composed of poly(methyl methacrylate) (PMMA), high-density polyethylene (HDPE) and polystyrene (PS). The conductive polymer is sensitive to the pressure providing that the void volume percentage and the applied load are sufficiently high. King et al. [14] investigated porous polymers produced by the foaming method using sugar as

porogene agent. The sensor obtained showed an electrical resistance variation from 20 kΩ to 100 Ω. However, the authors showed no results concerning reproducibility, hysteresis or drift. Danesh et al. [15] developed a porous conductive polymer composite film by phase separation; the matrix used was poly (methyl methacrylate) (PMMA), the solvent was ethyl acetate (EA), the non-solvent (less volatile) was 2-methyl-2, 4 -pentanediol (MPD) and the conductive particles were carbon black. After complete evaporation of the solvent, the film was immersed in an aqueous methanol solution to remove the non-solvent. The maximum pressure sensitivity was obtained for the films showing the highest porosity. Li et al.[16] described a conductive porous nanocomposite polymer film based on polypropylene (PP) and polystyrene (PS) and carbon black as conductive particles; these authors concluded that when increasing the porosity, the percolation threshold decreased. The percolation threshold obtained for the dense PP/PS/CBs ECPC was between 5 wt.% and 10 wt.% of carbon black while for porous PP/CBs ECPC was between 0.5 wt.% and 1 wt.%. Brady el al. [17] reported a pressure sensor made from a conducting polymer deposited on porous polyurethane but drift and hysteresis after compression were observed.

The present work addresses the development of dense electrically conductive polymer composites (ECPCs) to be used as pressure sensor elements and the development of porous composite polymeric matrices for preparing ECPCs targeting pressure sensor applications. Dense ECPCs loaded with carbon black particles and non-conductive particles such as titanium dioxide were tested. Different methods were assessed concerning the preparation of porous films (Chapter I) such as: foaming, emulsion and phase inversion methods. This Chapter addresses the effect of film morphology of the polymeric matrix on the response of the sensor towards pressure.

4.2 Experimental

4.2.1 Materials

Dehesive® 920 was purchased from Wacker Silicon Corporation and Sylgard® 184 Silicone Elastomer was supplied by Dow Corning Corporation. PEBAX polymer was supplied by Atofina Chemicals. Carbon black powder (Vulcan® XC72R) was purchased from Cabot Corporation. Titanium dioxide, Ti-Pure ® R-706 (TiO_2), was supplied by DuPont ™ and titanium dioxide, Aeroxide® TiO_2 P25 (80 wt.% anatase, 20 wt.% rutile) was supplied by Evonik®. The tri-block copolymer of polyethylene glycol / polypropylene glycol/poly ethylene glycol (P-123), sodium dodecyl sulphate (SDS), ammonium carbonate ($(NH_4)_2CO_3$), aluminium oxide (Al_2O_3), calcium carbonate ($CaCO_3$), barium sulphate ($BaSO_4$) , ethanol, butanol, n-methyl-2-pyrrolidone (NMP) and tetrahydrofuran (THF) were purchased from Sigma Aldrich. Glucose was supplied by Merck. Yttria stabilized zirconia (YSZ) sol was prepared by the sol-gel method [18]. Distilled water was used as a porogene agent.

4.2.2 Preparation of dense PDMS based ECPCs incorporating non-conductive particles

PDMS (Dehesive 920) was added to the previously prepared filler (non-conductive particles and 6.6 vol.% of carbon black) suspensions in THF. Different non-conductive particles such as Al_2O_3, titanium dioxides (Ti-Pure ® R-706 (TiO_2) and Aeroxide® TiO_2 P25), $CaCO_3$, glucose, YSZ and $BaSO_4$ were used in the range of 1 wt.% to 10 wt.% of carbon black. Ultrasonic bath was used for particle dispersion for two hours. After that, the crosslinker and cross-linking catalyst were added to the mixture. The solution was then poured on a Teflon coated glass plate at room temperature and left overnight. During this period of time, the solvent evaporation occurred along with crosslinking.

4.2.3 Preparation of porous PDMS films

Table 4.1 summarizes the different methods used to prepare dense and porous PDMS films. Method "***a***" was used to prepare the dense PDMS films while the others methods were used to prepare porous films.

Table 4.1 – Different methods used to prepare PDMS films.

Method		Polymer matrix	Solvent	Porogene agent
a	-	PDMS	THF	-
b	Foaming		THF	pluronic P_{123}
c	Foaming		-	$(NH4)_2CO_3$
d	Emulsion		-	water (P_{123})
e	Emulsion		-	water (SDS)
f	Emulsion		-	water (butanol)

For preparing the dense PDMS film (method *a*), the procedure described in Chapter II and Chapter III was followed [1, 3, 5, 19-21].

4.2.4 Preparation of porous PDMS films (Foaming method "*b*")

Polydimethylsiloxane (PDMS), (Dehesive® 920), and Pluronic 123 (porogene agent) were added to THF. Stirring was maintained until a homogeneous mixture was obtained. At this instant the required amount of crosslinker (2.5 wt.% of polymer) was added. For casting the PDMS film, the procedure described in Chapter II was followed. Briefly, the catalyst was added to the mixture and the suspension poured on a Teflon coated glass plate. The solvent was evaporated at room temperature overnight. For porogene agent extraction, PDMS films were sonicated for 3 hours ca. 80 °C in an

ethanol solution; ca. 80 % of the initially loaded P-123 was extracted. Afterwards, films were placed in an oven at 80 °C for 12 hours. More catalyst was then added and the films were put back in the oven to finish the curing process. Table 4.2 presents the different compositions of porogene agent P-123 used to prepared porous films by the foaming method "**b**".

Table 4.2 – Composition of the PDMS films prepared by the foaming method "***b***" (P-123).

Polymer matrix	Pluronic P-123 (wt.% of polymer)
PDMS	5
	7.5
	10
	15

4.2.5 Preparation of porous PDMS films using porogene agent ammonium carbonate (Foaming method "*c*")

Ammonium carbonate ($(NH_4)_2CO_3$) particles were homogeneously dispersed in the pre-polymer PDMS (Sylgard 184) followed by the addition of the curing agent, mass ratio pre-polymer: curing agent of 10:1. The mixture was heated for two hours for curing the pre-polymer and then placed at 120 °C to induce the formation of ammonia and carbon dioxide within the solidified polymer matrix [22-24]. Table 4.3 shows the initial ammonium carbonate loaded of the PDMS films prepared by the foaming method "**c**" and pre-polymer cure temperature.

Table 4.3 – Composition and pre-polymer cure temperature of the PDMS films prepared by the foaming method "***c***".

Polymer matrix	Ammonium carbonate (wt. % of polymer)	Temperature for pre-polymer cure (°C)
PDMS	1	25
	3	25
	5	25
	3	50
	3	65
	3	80

4.2.6 Preparation of porous PDMS films by the emulsion methods

For the preparation of porous PDMS film by the emulsion method, water containing either surfactant SDS (method "**d**"), surfactant P-123 (method "**e**") or butanol (method "**f**") was added to the PDMS pre-polymer (Sylgard 184) using a homogenizer (Ultrasound UIP1000hd Hielscher - 1000 watts, 20 kHz). After a homogeneous mixture was achieved the curing agent in the proportion of 10:1 was added (mass based). The mixture was heated at 80 °C and 100 % relative humidity for two hours for pre-polymer cure and then placed at 120 °C to evaporate the trapped water and to form a porous PDMS film. Different water/polymer volume ratios were considered to evaluate the quantity of pores formed [25-26]. Table 4.4 shows the composition of the porous PDMS films prepared by the emulsion methods studied and the ultrasound powder used for homogenization.

Table 4.4 – Composition of the PDMS films prepared by the emulsion methods "***d***", "***e***" and "***f***".

Method	Water (wt.% based on the polymer)	Type of Emulsifier	Emulsifier (wt.% based on the water)	Sonication power (%)
d	5	SDS	1	50
				70
				90
			2	90
			4	
e	5	P-123	1	90
			2	
			4	
f	5	Butanol	1	90
			2	
			4	
	10		4	
	30			
	50			

4.2.7 Preparation of dense PEBA films

For the preparation of the PEBA based ECPCs, the procedure described in Chapter II and Chapter III was followed [19, 27-30]. Briefly, ECPCs were prepared by the casting method of a polymer solution.

4.2.8 Preparation of dense PEBA ECPCs incorporating non-conductive particles

PEBA 2533 was added to previously prepared fillers (non-conductive and 6.6 vol. % of carbon black) suspensions in NMP. Different non-conductive particles such as Al_2O_3, titanium dioxides (Ti-Pure ® R-706 (TiO_2) and Aeroxide® TiO_2 P25), $CaCO_3$, glucose, YSZ and $BaSO_4$ were used in the range of 1 wt.% to 10 wt.% based on the carbon black load. Ultrasonic bath was used for particle dispersion for two hours. For the preparation of the PEBA based ECPCs, the procedure described in Chapter II was followed.

4.2.9 Preparation of porous PEBA films by the immersion precipitation method

PEBA (2533 and 4033) porous films were prepared by the immersion precipitation method. PEBA 2533 or 4033 were dissolved in NMP or ethanol to form a polymer solution. The polymer solution was stirred vigorously at 110 °C under reflux and kept at 90 °C or 25 °C (films ***a*** and ***b*** in Table 4.5). When the polymer solution became homogeneous, the hot solution was poured on a glass plate. The film was then exposed to ambient before immersion into water bath at room temperature. The casted films changed their colour from transparent to white after immersion into the non-solvent and separated from the glass plate after sometime. The film was washed under running water and then kept overnight in a water bath. The films were air dried at room temperature for 2 days.

Table 4.5 shows the composition of the different PEBA films prepared by the phase inversion method. Films **“a”** and **“d”** are dense PEBA 2533 and PEBA 4033

respectively and the others are porous films prepared by phase inversion with different compositions.

Table 4.5 – Compositions of the PEBA films by immersion precipitation method.

Films	Polymer matrix	Solvent	Non-solvent	Polymer concentration (wt.%)	Air exposure time before coagulation (s)
a	PEBA 2533	Ethanol	-	10	-
b		Ethanol	Water	10	30
c		NMP	-	10	15 days
d	PEBA 4033	NMP	-	10	-
e				12	5
f				10	5
g				10	30
h			Water	7	30
i				7	60
j				5	60
k				5	90

4.3 Characterization of PDMS and PEBA films

4.3.1 Scanning Electron Microscopy (SEM)

The cross-section morphologies of PDMS and PEBA films were observed by Scanning Electron Microscopy (SEM) using a JEOL JSM-6301F, Oxford INCA Energy 350 equipment. Before being analyzed, the samples were fractured in liquid nitrogen and sputtered with gold/ platinum using a K575X Sputter Coater by Quorum Technologies. This technique was used in order to evaluate if the conductive particles were clustered or not in the synthesized films. On the other hand, the morphology of the films was studied based on SEM microscopy images.

4.3.2 Particle Size Distribution

The particle size distribution of the non-conductive particles was obtained using on a Beckman Coulter LS230 light scattering system. Dispersions of the non-conductive particles were diluted and sonicated for 30 minutes to eliminate agglomeration.

4.3.3 Measurement of Electrical Resistance

The electrical resistance of the prepared films was measured using the method described in Chapter III. Briefly, the electrical resistance of the ECPCs were measured using a multimeter (Fluke 11) in an in-house made mechanical press. The effective area of the electrode was 1 cm^2. Two layers of polymeric electrodes were casted in each side of the ECPC film and then the system was sandwiched between the copper/FlexPCB.

4.4 Results and discussion

4.4.1 Incorporation of non-conductive particles in the dense polymer matrices

Dense films of PDMS and PEBA (2533 and 4033) incorporating of carbon black particles and assembled with polymeric electrodes did not show any pressure sensitivity (Chapter III). The incorporation of non-conductive particles in the polymer matrix would prevent the formation of very close conductive pathways achieving pressure sensitivity. This approach was reported for the first time by Hussain et al. [5]. In their work, non-conductive particles (Al_2O_3) were added to improve the gradual fall of resistivity with applied pressure. In this Chapter, different non-conductive particles with different particle size distributions were tested such as: Al_2O_3, titanium dioxides (Ti-Pure ® R-706 (TiO_2) and Aeroxide® TiO_2 P25), $CaCO_3$, glucose, YSZ and $BaSO_4$. The particle size distributions are shown in Figure 4.1. YSZ showed the smallest particle size (~130 nm) and the narrowest distribution.

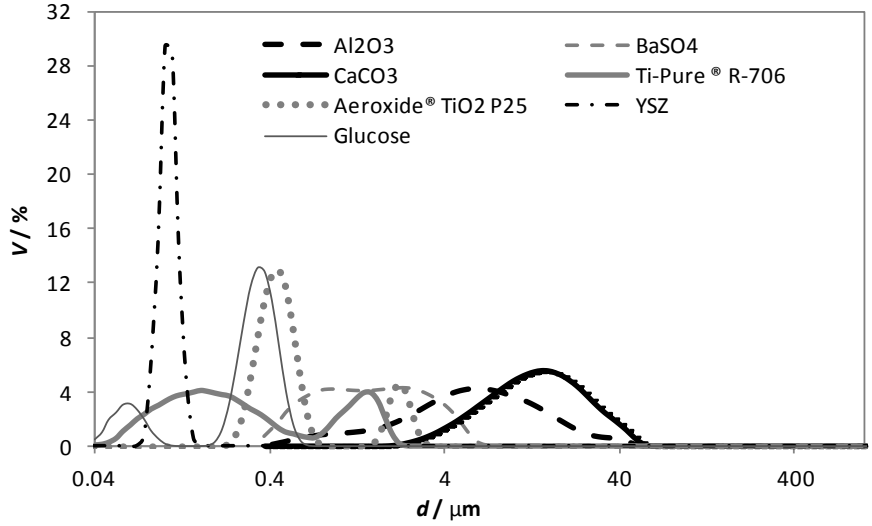

Figure 4.1 - Particle size distributions measured for different non-conductive particles.

Different methods were used for obtaining an optimal dispersion of the particles (conductive and non-conductive) in the polymer matrix: such as mechanical stirring, ultrasonic bath and ball milling. All the dense ECPCs prepared have demonstrated poor pressure sensitivity similar to the sensitivity obtained with the dense ECPCs without non-conductive particles; the inclusion of the non-conductive particles only increased the electrical resistance (Figure 4.2).

Figure 4.2 shows the electrical resistance of a PMDS ECPC with incorporation of 6.6 vol.% carbon black and non-conductive particles of TiO_2; polymeric electrodes described in Chapter III were used. From approximately 2 $N \cdot cm^{-2}$ up to 45 $N \cdot cm^{-2}$, the dense films of PDMS neither present pressure sensitivity nor reproducibility (performance of samples 1 and 2).

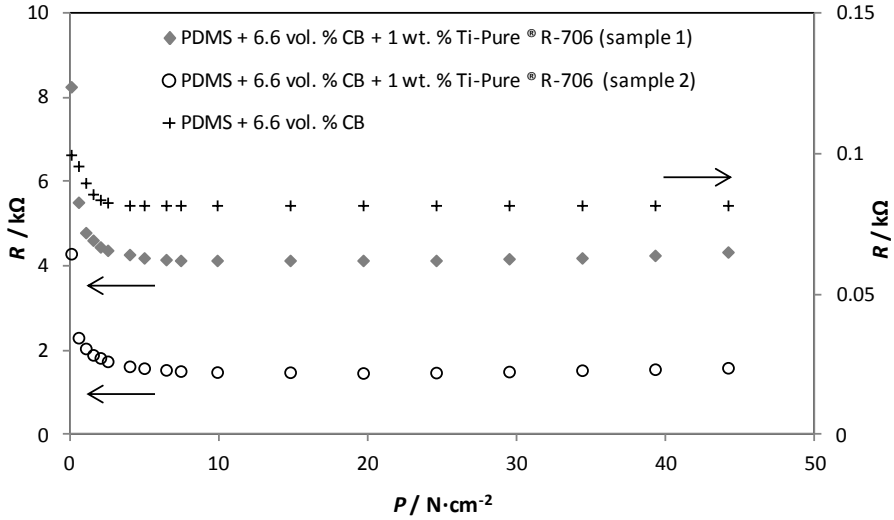

Figure 4.2 - Electrical resistance of PMDS film incorporating carbon black and TiO_2 assembled with polymeric electrodes.

Hussain et al. [5] reported a silicone rubber film with a carbon content of 35 vol.% that showed a very good resistivity response to pressure. In our case, the variation of resistivity with pressure is much lower. Figure 4.3 and Figure 4.4 show SEM images of PDMS films loaded carbon black and TiO_2 (a) and PEBA 2533 loaded with carbon black and TiO_2 (b) to understand the lack of reproducibility. A higher magnification of Figure 4.3 and Figure 4.4 (a_2 and especially b_2) further shows agglomeration of carbon black particles (see Figure 4.2 sample 1 and 2).

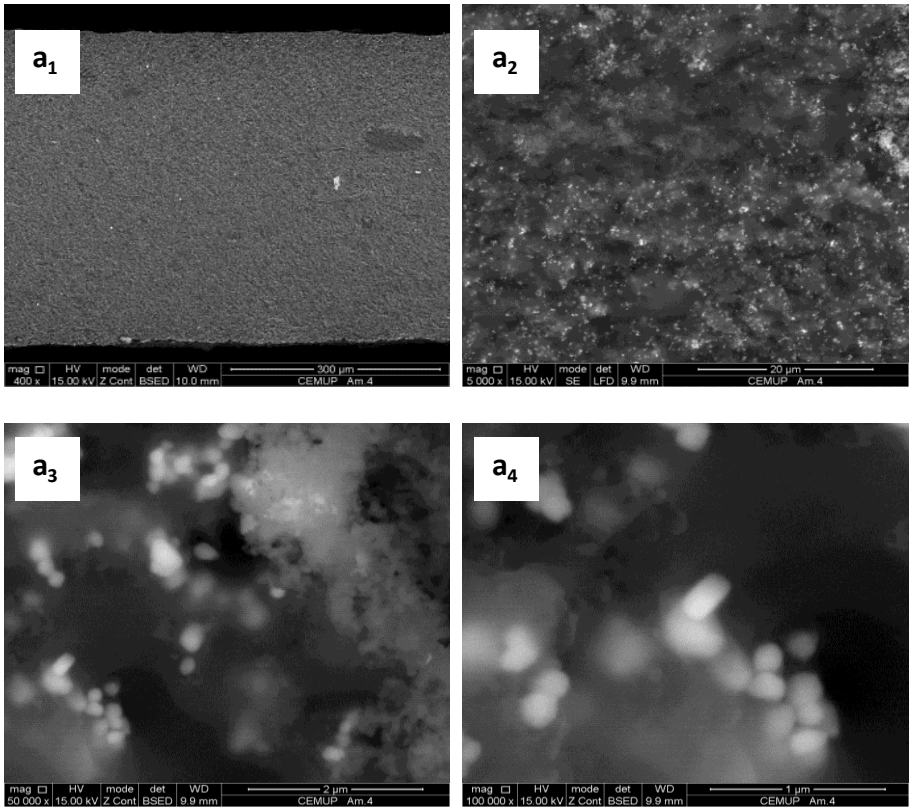

Figure 4.3 - Cross-section SEM images of PDMS films incorporating carbon black and TiO_2: **a_1** - magnification 400x, **a_2 –** magnification 5000x, **a_3** – magnification 50 000x and **a_4** - magnification 100 000x.

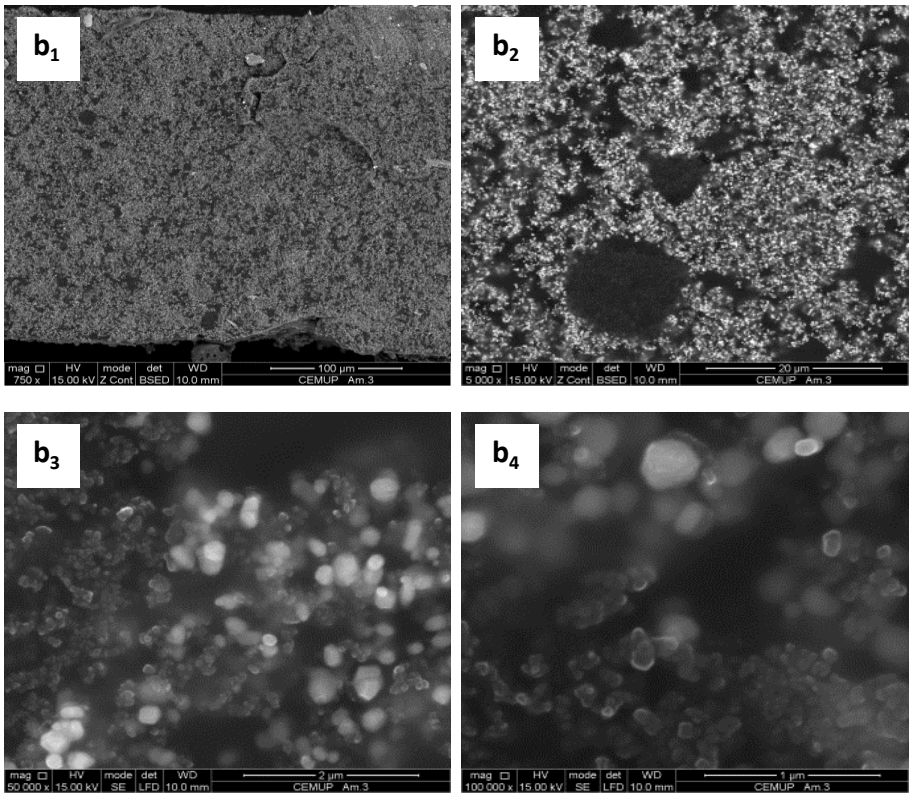

Figure 4.4 - Cross-section SEM images of PEBA 2533 films incorporating carbon black and TiO_2: b_1 - magnification 750x, b_2 – magnification 5000x, b_3 – magnification 50 000x and b_4 - magnification 100 000x.

4.4.2 Porous PDMS films

According to Danesh et al.[15], King et al. [14] and Ravati et al. [13], the effect of porosity on the sensor film is directly related to the response of the sensor to the pressure. Porous PDMS films were prepared by different methods, such as foaming and emulsion methods, as well as various operating conditions and compositions were assessed for each method.

Different compositions of Pluronic P-123 (porogene agent) were used for preparation of porous PDMS films by the foaming method (Table 4.2). This method

showed to be very complex because after introducing Pluronic P-123 into the polymer matrix, the film loses the mechanical properties; for example, incorporating 10 wt.% of P-123 causes noticeable differences in the PDMS crosslinking properties. Because of that, after extraction of the porogene agent additional crosslinker / catalyst was added to assist curing the polymer matrix. The morphology of the film obtained using 10 wt.% of P-123 can be observed on Figure 4.5b where relatively large pores are observed.

Porous PDMS films were also prepared with different compositions in ammonium carbonate and at different pre-polymer curing temperatures (Table 4.3). Ammonium carbonate is used as a gas foaming agent [22, 24]; the polymer matrix loaded with ammonium carbonate was heated to induce the matrix solidification and the formation of gaseous ammonia and carbon dioxide upon heating and consequently the pores. The obtained optimal temperature of pre-cure was 25 °C; at higher temperatures (50 °C, 65 °C and 80 °C) the ammonium carbonate started decomposing before the solidification of the polymer matrix and thus forming no porosity. The morphology of the film prepared by using 5 % of ammonium carbonate can be observed on Figure 4.5c; it can be seen that the porosity obtained is small and not uniformly distributed.

The emulsion method was used to prepare porous PDMS films. Different concentration of porogene agent, type of surfactant, amount of surfactant and amount of energy used to form droplets (power of Ultrasound UIP1000hd Hielscher - 1000 watts, 20 kHz) were tested (Table 4.4). Successfully prepared emulsions were white and homogeneous. The best emulsions were obtained with the incorporation of a butanol aqueous solution (method *f*); this emulsion was stable at room temperature with no phase separation. Figure 4.5 (d, e and f) shows that a higher amount of pores were formed when using this emulsion method. Juchniewich et al. [26] reported that

the most important factors for porosity control in the emulsion method are the amount of energy used to form the droplets and the type of surfactant. The porous PDMS film (f) prepared with a butanol aqueous solution presents the highest porosity both on the surface and in the cross-section. However, there are differences between the surface morphology and the cross-section. Larger and more abundant pores are observed on the top surface then in the film body (Figure 4.6 - surface and cross-section of the PDMS film (f) at higher magnification). These differences might be related to some loss of emulsion stability during PDMS curing.

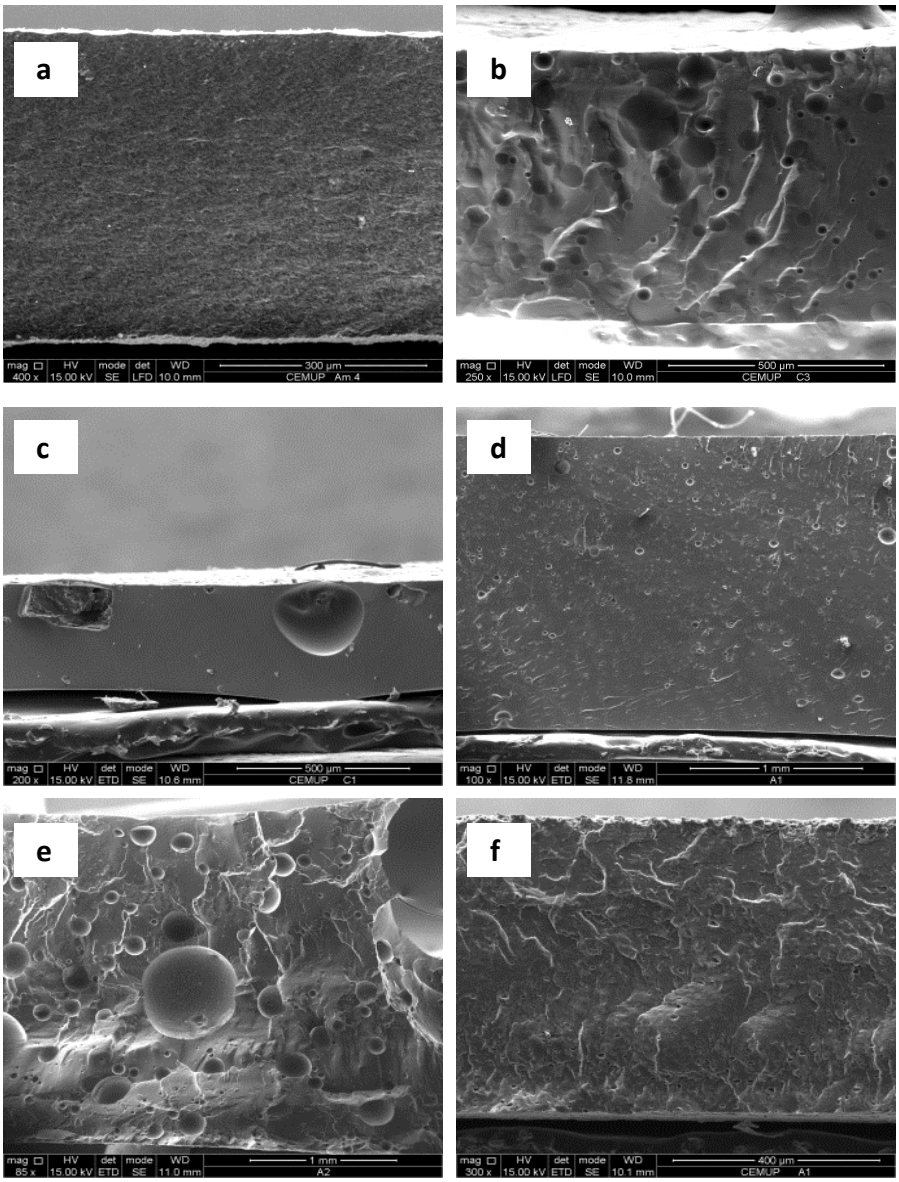

Figure 4.5 - SEM images of cross-section of the films: (a) Pristine PDMS, (b) PDMS + 10 wt.% Pluronic P_{123} , (c) PDMS + 5 wt.% $(NH_4)_2CO_3$ (25 °C), (d) PDMS + 5 wt.% H_2O (4 wt. % P_{123}) , (e) PDMS + 5 wt.% H_2O (4 wt.% SDS), (f) PDMS + 5 wt.% H_2O + 4 wt.% butanol.

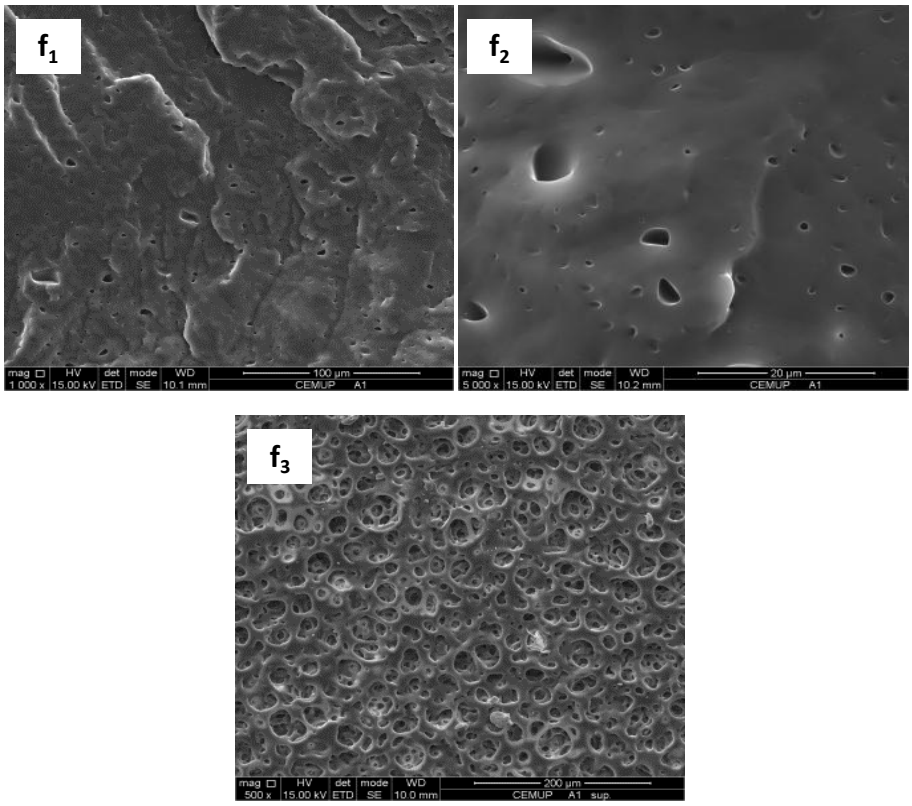

Figure 4.6 - SEM images of top surface and cross-section of the films: **f_1** - PDMS/H_2O+ butanol cross-section in high magnification (1000x), **f_2** - PDMS/H_2O+butanol cross-section in high magnification (5000x) and **f_3** - PDMS/H_2O + butanol top surface.

4.4.3 Porous PEBA films

The feasibility of making porous PEBA films was also evaluated by the phase inversion method (immersion precipitation) [31-38]. According with this method, the polymer solution originates two phases: a polymer rich phase that forms the matrix of the film and a polymer poor phase that forms the porosity of the film. If the precipitation process is fast, the pores tend to be small and the films are asymmetric.

If the precipitation is slow, the pores tend to agglomerate while the casting solution is fluid and the final pores are large [39].

Different compositions and operating conditions were considered when using the phase inversion method for preparing porous PEBA films (Table 4.5). Microscopic observation was carried out by SEM that directly provides the visual information of the cross-sectional morphology of the films. SEM images of the dense and porous PEBA 2533 and PEBA 4033 films are shown in Figure 4.7 and Figure 4.8, respectively. The influence of the preparation conditions (type and concentration of solvent, type of non-solvent and air exposure time before coagulation) on film formation was evaluated. Figure 4.7 (a) and Figure 4.8 (d) shows the cross-section of dense PEBA 2533 and PEBA 4033, respectively. Porous PEBA 4033 films (e), (g) and (h) exhibit a nodule structure with a dense top layer - asymmetric morphology. Porous PEBA 2533 (c) and PEBA 4033 (f), (i) and (k) films present the highest porosity, pore interconnection and symmetric morphology. The polymer concentration of the casting solution and the choice of the solvent/ non-solvent system determined which morphology was obtained. A high affinity of NMP for water, see Chapter I, leads to the formation of a nodule-like structure. The delayed demixing promotes simultaneous nucleation and radial growth of the polymer crystallites in all directions, producing symmetric films [38-39]. Similar film morphologies were observed found by Gugliuzza et al. [40] for the system polyvinylidene fluoride/NMP (solvent) / water (non-solvent).

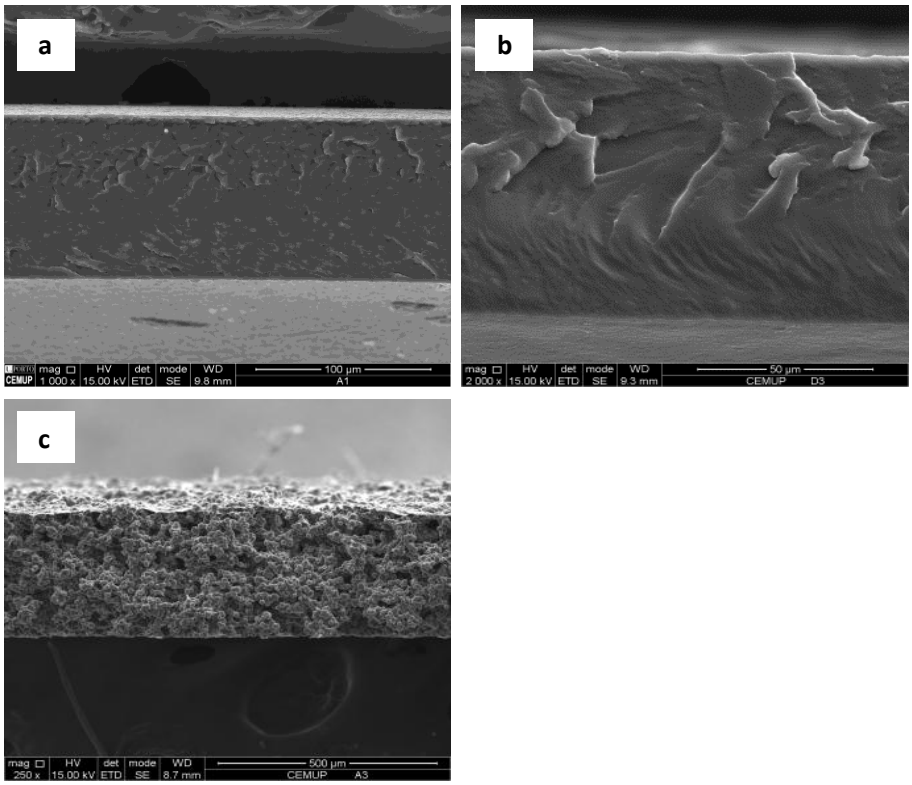

Figure 4.7 - Cross-section SEM images of different PEBA 2533 films (see **Table 4.5**).

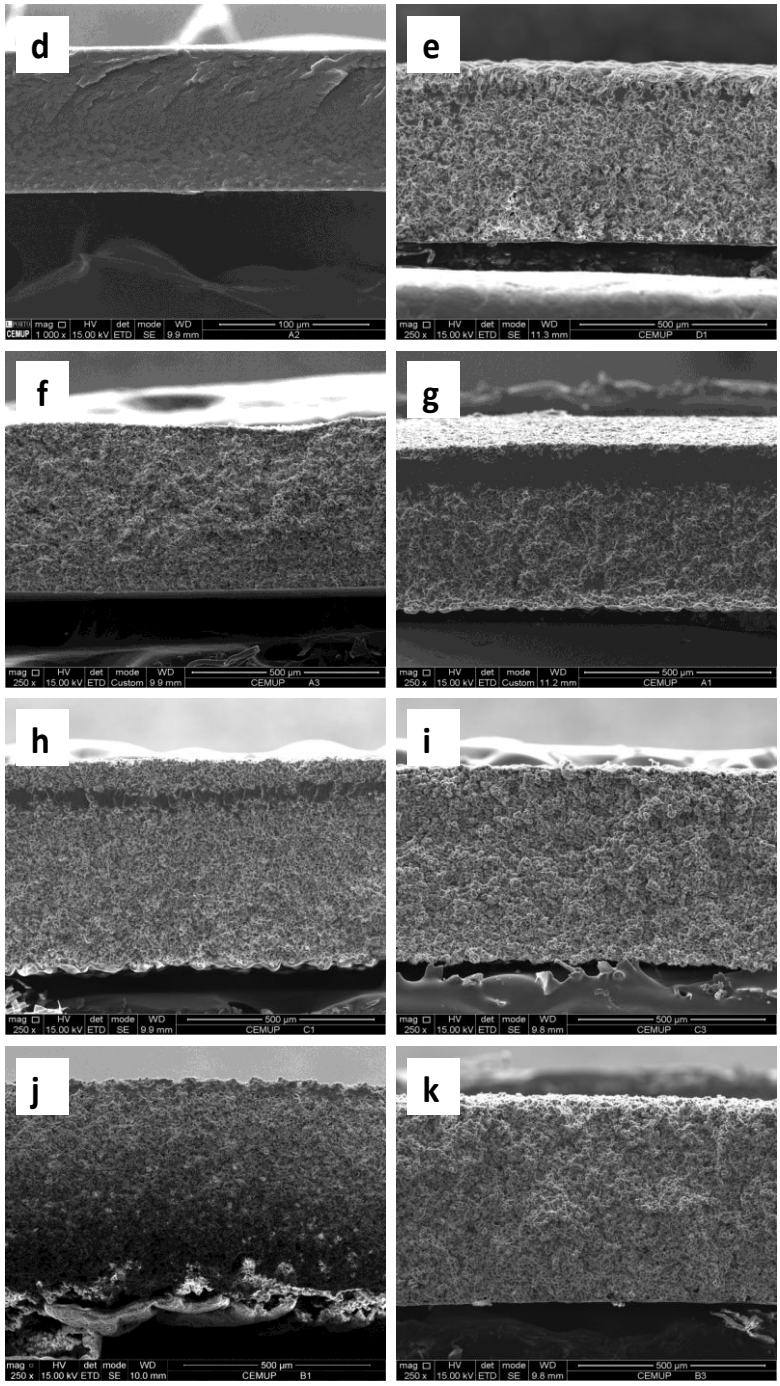

Figure 4.8 - Cross-section SEM images of different PEBA 4033 films (see **Table 4.5**).

Next Chapter will address the incorporation of conductive particles in the porous polymeric matrices developed. The obtained ECPCs to be further tested as pressure sensors.

4.5 Conclusions

Dense PDMS and PEBA (2533 and 4033) based ECPCs incorporating carbon black and non-conductive particles assembled with polymeric electrodes showed very poor pressure sensitivity similar to the sensitivity obtained with the dense films without non-conductive particles. Porous PDMS and PEBA composite films for assembling ECPCs were prepared. The foaming and emulsion methods were studied to prepare porous PDMS films while the phase inversion method was used to prepare porous PEBA films. The emulsion method, using a butanol aqueous solution as emulsifier, allowed the preparation of porous PDMS films but more pores are observed on the top surface morphology due to the poor stability of the emulsion during PDMS curing. On the other hand, the phase inversion method allowed the preparation of porous PEBA films with a nodule structure, high porous and symmetric morphology very promising for preparing porous ECPCs.

4.6 References

1. Knite, M., Teteris, V., Kiploka, A., Kaupuzs, J., *Polyisoprene-carbon black nanocomposites as tensile strain and pressure sensor materials.* Sensors and Actuators A: Physical, 2004. **110**(1-3): p. 142-149.
2. Harsányi, G., *Polymeric sensing films: new horizons in sensorics?* Materials Chemistry and Physics, 1996. **43**(3): p. 199-203.
3. Knite, M., Teteris, V., Polyakov, B., Erts, D., *Electric and elastic properties of conductive polymeric nanocomposites on macro- and nanoscales.* Materials Science and Engineering: C, 2002. **19**(1-2): p. 15-19.

4. Lei, H., Pitt, W.G., McGrath, L.K., Ho, C.K., *Modeling carbon black/polymer composite sensors.* Sensors and Actuators B: Chemical, 2007. **125**(2): p. 396-407.

5. Hussain, M., Choa, Y.-H., Niihara, K., *Fabrication process and electrical behavior of novel pressure-sensitive composites.* Composites Part A: Applied Science and Manufacturing, 2001. **32**(12): p. 1689-1696.

6. Lei, H., Pitt, W. G., McGrath, L.K., Ho, C.K., *Resistivity measurements of carbon-polymer composites in chemical sensors: impact of carbon concentration and geometry.* Sensors and Actuators B: Chemical, 2004. **101**(1-2): p. 122-132.

7. Lussey, D., Laughlin, P., Bloor, D., Hilsum, C., *Polymer composition with electrically-conductive filler*, U.K. Patent GB 2465077 A, May 12, 2010.

8. Lussey, D., *Conductive Strutures*, WO 00/79546 A1, December, 2000.

9. Podoloff, R., Benjamin, M., *Flexible, tactile sensor for measuring pressure distributions and for gaskets*, WO 91/09289, June 27, 1991.

10. Krivopal, B., *Pressure sensitive ink means, and methods of use*, WO 97/25379, July 17, 1997.

11. Lima, J.H., Papakostas, T., *High Temperature Pressure Sensitive Devices And Methods Thereof,* WO 2004102144 A2, November 25, 2004.

12. Lussey, D., Jones, D., Leftly, S., *Flexible Switching Devices*, WO 01/88935 A1, November 22, 2011.

13. Ravati, S., Favis, B.D., *3D porous polymeric conductive material prepared using LbL deposition.* Polymer, 2011. **52**(3): p. 718-731.

14. King, M.G., Baragwanath, A.J., Rosamond, M.C., Wood, D., Gallant, A.J., *Porous PDMS force sensitive resistors.* Procedia Chemistry, 2009. **1**(1): p. 568-571.

15. Danesh, E., Ghaffarian, S.R., Molla-Abbasi, P., *Non-solvent induced phase separation as a method for making high-performance chemiresistors based on conductive polymer nanocomposites.* Sensors and Actuators B: Chemical, 2011. **155**(2): p. 562-567.

16. Li, M., Zhang, W., Wang, C., Wang, H., *In situ formation of 2D conductive porous material with ultra low percolation threshold.* Materials Letters, 2012. **82**(0): p. 109-111.

17. Brady, S., Diamond, D., Lau, K.-T., *Inherently conducting polymer modified polyurethane smart foam for pressure sensing.* Sensors and Actuators A: Physical, 2005. **119**(2): p. 398-404.

18. Tanaka, D., Tanco, M., Okazaki, J., Wakui, Y., Mizukami, F., Suzuki, T., *Preparation of "pore-fill" type Pd–YSZ–γ-Al2O3 composite membrane supported on α-Al2O3 tube for hydrogen separation.* Journal of Membrane Science, 2008. **320**(1–2): p. 436-441.

19. Panek, D., Konieczny, K., *Preparation and applying the membranes with carbon black to pervaporation of toluene from the diluted aqueous solutions.* Separation and Purification Technology, 2007. **57**(3): p. 507-512.

20. Brandão, L., Madeira, L.M., Mendes, A.M., *Mass transport on composite dense PDMS membranes with palladium nanoclusters.* Journal of Membrane Science, 2007. **288**(1-2): p. 112-122.

21. Luheng, W., Tianhuai, D., Peng, W., *Effects of conductive phase content on critical pressure of carbon black filled silicone rubber composite.* Sensors and Actuators A: Physical, 2007. **135**(2): p. 587-592.

22. Hentze, H.P., Antonietti, M., *Porous polymers and resins for biotechnological and biomedical applications.* Reviews in Molecular Biotechnology, 2002. **90**(1): p. 27-53.

23. Muehling, J.K., Arnold, Heather R., House Jr, J. E., *Effects of particle size on the decomposition of ammonium carbonate.* Thermochimica Acta, 1995. **255**(0): p. 347-353.

24. Wang, Y.-Q., Tao, J., Zhang, J.-L., Wang, T., *Effects of addition of NH4HCO3 on pore characteristics and compressive properties of porous Ti-10%Mg composites.* Transactions of Nonferrous Metals Society of China, 2011. **21**(5): p. 1074-1079.

25. Juyue Chen, R.Z.a.W.W. (2012) *Fabricating microporous PDMS using a water-in-PDMS emulsion*.

26. Juchniewicz, M., Stadnik, D., Biesiada, K., Olszyna, A., Chudy, M., Brzózka, Z., Dybko, A., *Porous crosslinked PDMS-microchannels coatings.* Sensors and Actuators B: Chemical, 2007. **126**(1): p. 68-72.

27. Jiraratananon, R., Sampranpiboon, P., Uttapap, D., Huang, R.Y.M., *Pervaporation separation and mass transport of ethylbutanoate solution by polyether block amide (PEBA) membranes.* Journal of Membrane Science, 2002. **210**(2): p. 389-409.

28. Sridhar, S., Suryamurali, R., Smitha, B., Aminabhavi, T.M., *Development of crosslinked poly(ether-block-amide) membrane for CO2/CH4 separation.* Colloids and Surfaces A: Physicochemical and Engineering Aspects, 2007. **297**(1-3): p. 267-274.

29. Bengtson, G., Oehring, M., Fritsch, D., *Improved dense catalytically active polymer membranes of different configuration to separate and react organics simultaneously by pervaporation.* Chemical Engineering and Processing, 2004. **43**(9): p. 1159-1170.

30. Bengtson, G., Scheel, H., Theis, J., Fritsch, D., *Catalytic membrane reactor to simultaneously concentrate and react organics.* Chemical Engineering Journal, 2002. **85**(2-3): p. 303-311.

31. Mulder, M., *Basic Principles of Membrane Technology*. 2 nd ed. 2000: Klumer Academic Publishers.

32. Zhao, Y.-H., Qian, Y.-L., Zhu, B.-K., Xu, Y.-Y., *Modification of porous poly(vinylidene fluoride) membrane using amphiphilic polymers with different structures in phase inversion process.* Journal of Membrane Science, 2008. **310**(1–2): p. 567-576.

33. Ma, Y., Shi, F., Ma, J., Wu, M., Zhang, J., Gao, C., *Effect of PEG additive on the morphology and performance of polysulfone ultrafiltration membranes.* Desalination, 2011. **272**(1–3): p. 51-58.

34. Kim, J.-H., Lee, K.-H., *Effect of PEG additive on membrane formation by phase inversion.* Journal of Membrane Science, 1998. **138**(2): p. 153-163.

35. Jansen, J.C., Buonomenna, M.G., Figoli, A., Drioli, E., *Ultra-thin asymmetric gas separation membranes of modified PEEK prepared by the dry–wet phase inversion technique.* Desalination, 2006. **193**(1–3): p. 58-65.

36. Idris, A., Norashikin M.Z., Noordin, M.Y., *Synthesis, characterization and performance of asymmetric polyethersulfone (PES) ultrafiltration membranes with polyethylene glycol of different molecular weights as additives.* Desalination, 2007. **207**(1–3): p. 324-339.

37. Chakrabarty, B., Ghoshal, A.K., Purkait, M.K., *Effect of molecular weight of PEG on membrane morphology and transport properties.* Journal of Membrane Science, 2008. **309**(1–2): p. 209-221.

38. Van de Witte, P., Dijkstra, P.J., Van den Berg, J.W.A., Feijen, J., *Phase separation processes in polymer solutions in relation to membrane formation.* Journal of Membrane Science, 1996. **117**(1–2): p. 1-31.

39. Baker, R.W., Cussler, E.L., Eykamp, W., Koros, W.J., Riley, R.L., Strathmann, H., *Membrane Separation Systems : Recent Developments and Future Directions*. 1991, United States: Noyes Data Corporation.

40. Gugliuzza, A., Drioli,E., *New performance of hydrophobic fluorinated porous membranes exhibiting particulate-like morphology.* Desalination, 2009. **240**(1–3): p. 14-20.

CHAPTER V

5 Development of porous polymers-based pressure sensors[1]

Abstract

Electrically Conductive Polymer Composites (ECPCs) based on porous polymeric matrices of PDMS and PEBA containing carbon black and others conductive type particles, such as silver and spherical and lamellar zinc were assembled. The emulsion and immersion precipitation methods were used for obtaining the porous morphology. Porous PEBA ECPCs incorporating carbon black were only successfully obtained when a hydrophobic non-solvent (hexane/acetone) was used in the immersion precipitation method and at low carbon black contents; at high carbon black concentration a dense ECPC was obtained due to the highly hydrophobic environment created. A porous PEBA films morphology was also achieved when using water as the non-solvent but only when hydrophilic particles were used. Porous PDMS ECPCs based on carbon black were not possible to obtain by the emulsion method. A piezoresistive response was observed for the porous ECPCs assembled with polymeric electrodes tested containing silver and lamellar zinc although with poor mechanical properties due to the high concentration of metals incorporated. On the other hand, the porous spherical zinc and carbon black/PEBA ECPCs with polymeric electrodes did not show pressure sensitivity.

[1] Adapted from: Gonçalves, V., Brandão, L., Mendes, A., Development of porous polymer-based pressure sensors, *Submitted*.

5.1 Introduction

Recent advances in polymer science and film preparation have made polymer films useful, practical and economical in a wide range of sensor designs and applications [1]. The most often used conductive particles materials are metals, carbon black and semiconducting metal-oxides [2-4]. Conductive porous polymers can be used as pressure sensors on electronic devices [5].

Recently, some studies reported the development of conductive porous polymer composites prepared by different methods [6-10]. Ravati et al. [6] studied a porous ECPC depositing polyaniline (Pani) on a matrix blend composed of poly(methyl methacrylate) (PMMA), high-density polyethylene (HDPE) and polystyrene (PS). The extraction of PS allowed a fully interconnected porous structure and the deposition of Pani in the internal porous surface was made via a layer-by-layer technique. A percolation threshold lower than 0.19 wt.% was observed, and the porous ECPC was sensitive to pressure providing that the void volume percentage and the applied load was sufficiently high. Danesh et al. [7] developed a porous ECPC using poly (methyl methacrylate) (PMMA) as polymer matrix, ethyl acetate (EA) as solvent, 2-methyl-2, 4 -pentanediol (MPD) as non-solvent (less volatile) and carbon black as conductive particles. After complete evaporation of solvent, the film was immersed in aqueous methanol solution to remove the non-solvent. The non-solvent induced the phase separation to create porosity. These authors compared the electrical conductivity of dense and porous ECPCS and concluded that in all carbon black concentrations the conductivity was higher in porous ECPCs than in the dense ones. On the other hand, increasing non-solvent content, the resistivity of the porous ECPCs increased because porosity increased leading to the rupture of conductive paths. Li et al. [8] described a porous ECPC based on polypropylene (PP),polystyrene (PS) and carbon black (CB). The percolation threshold obtained for the dense PP/PS/CBs ECPC was between 5 wt.%

and 10 wt.% while for porous PP/CBs ECPC was between 0.5 wt.% and 1 wt.%. King et al. [9] reported a porous PDMS ECPC prepared by the foaming method with carbon black and sugar particles. The dissolution of the sugar was used to form a porous path. The sensor obtained showed an electrical resistance change from 20 kΩ to 100 Ω. Brady et al. [10] studied an ECPC composed of polyurethane foam with polypyrrole (PPy) as conductive polymer. Firstly, when the conductive foam was compressed, the interstitial spaces within the foam decreased gradually with a very slow increase in the contacting area between PPy coated surfaces. Upon compression more contact area between PPy chains was created, and, a linear response was observed. These authors concluded that the repeatability of the foam sensor was poor and drift was observed due to humidity effects. Hysteresis was also observed due to the poor mechanical properties of the foam.

Previously, different methods were studied for preparing porous PDMS and PEBA films. The present work addresses the development of porous PDMS and PEBA ECPCs prepared by the emulsion and immersion precipitation methods, respectively. Carbon black and other type of conductive particles were used. The influence of the type of conductive particles and the combination of solvent/ non-solvent on the porous morphology was studied; the effect of the conductive particles on the piezoresistive effect was also evaluated.

5.2 Experimental

5.2.1 Materials

Sylgard® 184 Silicone Elastomer was supplied by Dow Corning Corporation and PEBAX polymer was supplied by Atofina Chemicals. Carbon black powder (Vulcan® XC72R) was purchased from Cabot Corporation. Ethanol, hexane and hexane/acetone (95 wt.% / 5 wt.%) were used as non-solvents and it was purchased from Sigma

Aldrich. Lamellar and spherical zinc was supplied by Umicore®. Silver nanopowder, n-methyl-2-pyrrolidone (NMP) and 2, 4 - toluyene diisocyanate were purchased from Sigma Aldrich. Distiled water was used as non-solvent.

5.2.2 Preparation of porous PDMS ECPCs by the emulsion method

A butanol aqueous solution was added to the PDMS pre-polymer (Sylgard 184) using a homogenizer (Ultrasound UIP1000hd Hielscher - 1000 watts, 20 kHz). After that, carbon black was added to the PDMS pre-polymer solution and stirred during 45 minutes; after achieving a homogeneous mixture the curing agent in the proportion 10:1 was added (mass based). The mixture was heated at 80 °C and 100 % relative humidity during two hours for curing the pre-polymer and then placed at 120 °C to evaporate the trapped water and form a porous PDMS film [11-12].

Table 5.1 shows the series of PDMS based ECPCs prepared with different carbon black concentrations.

Table 5.1 – Composition of PDMS films incorporating carbon black particles**.**

Polymer matrix	Carbon black (vol.% based on the polymer)	Butanol (wt.% based on the water)	Water (wt.% based on the polymer)
PDMS	0.5 6 8	4	30

5.2.3 Preparation of porous PEBA 4033 ECPCs by the immersion precipitation method

PEBA 2533 and 4033 were dissolved in NMP to form a polymer solution that was added to a previously prepared NMP suspension of conductive particles. The polymer solution was stirred vigorously at 110 °C under reflux and kept at 90 °C. When the polymer solution became homogeneous, the hot solution was poured on a glass plate. The film was then exposed to ambient before immersion into the non-solvent at room temperature. The film was washed under running water and then kept overnight in a water bath. The films let to dry at room temperature for 2 days [13-14].

Table 5.2 shows the composition of the PEBA films used to assemble ECPC devices.

Table 5.2 – Porous PEBA based ECPCs tested.

Polymer matrix	Solvent	Non-solvent	Polymer concentration (wt.%)	Type of conductive particles	Air exposure time before coagulation (s)
PEBA 2533	NMP	water	10	5.5 vol.% carbon black	15 days
PEBA 4033			10		5
			7		60
			5		90
		ethanol	7	5.5 vol.% carbon black	60
		hexane / acetone	7	5.5 vol.% carbon black	60
			7	7.5 vol.% carbon black	60
		water	7	40 vol.% silver	60
			7	50 vol.% spherical zinc	60
			7	44 vol.% lamellar zinc	60

5.2.4 Preparation of crosslinking of porous PEBA 4033 ECPCs

PEBA 4033 with 44 vol.% of lamellar zinc was immersed in a 2 % (v/v) solution of TDI in hexane for 30 minutes. After that, the film was removed from the bath and washed with distilled water for an hour. The film was then dried in oven at 60 °C followed by vacuum drying for a period of 24 hours to remove the residual solvent present [15].

5.3 Characterization of PDMS and PEBA based ECPCs

5.3.1 Scanning Electron Microscopy (SEM)

The cross-section morphologies of PDMS and PEBA films were observed by Scanning Electron Microscopy (SEM) as described in previous Chapter.

5.3.2 Measurement of Electrical Resistance

The electrical resistance of the prepared ECPCs fabricated with the porous PDMS and PEBA 4033 films were measured using the method described in the previous Chapter.

5.4 Results and discussion

5.4.1 Incorporation of carbon black in PDMS ECPCs

Carbon black was incorporated in the PDMS formulation to prepare porous PDMS films used to fabricate ECPCs. The effect of carbon black on the morphology of the films is illustrated in Figure 5.1. Despite pristine porous PDMS films could be produced by the employed emulsion method, the incorporation of carbon black promoted the formation of a dense composite film. The incorporation of only 0.5 vol.% of carbon black made the produced film to be dense (Figure 5.1a). Probably, the introduction of carbon black (hydrophobic particles) made the polymeric system even

more hydrophobic and water was expelled during the emulsion process (unstable emulsion) and thus the formation of pores does not occur.

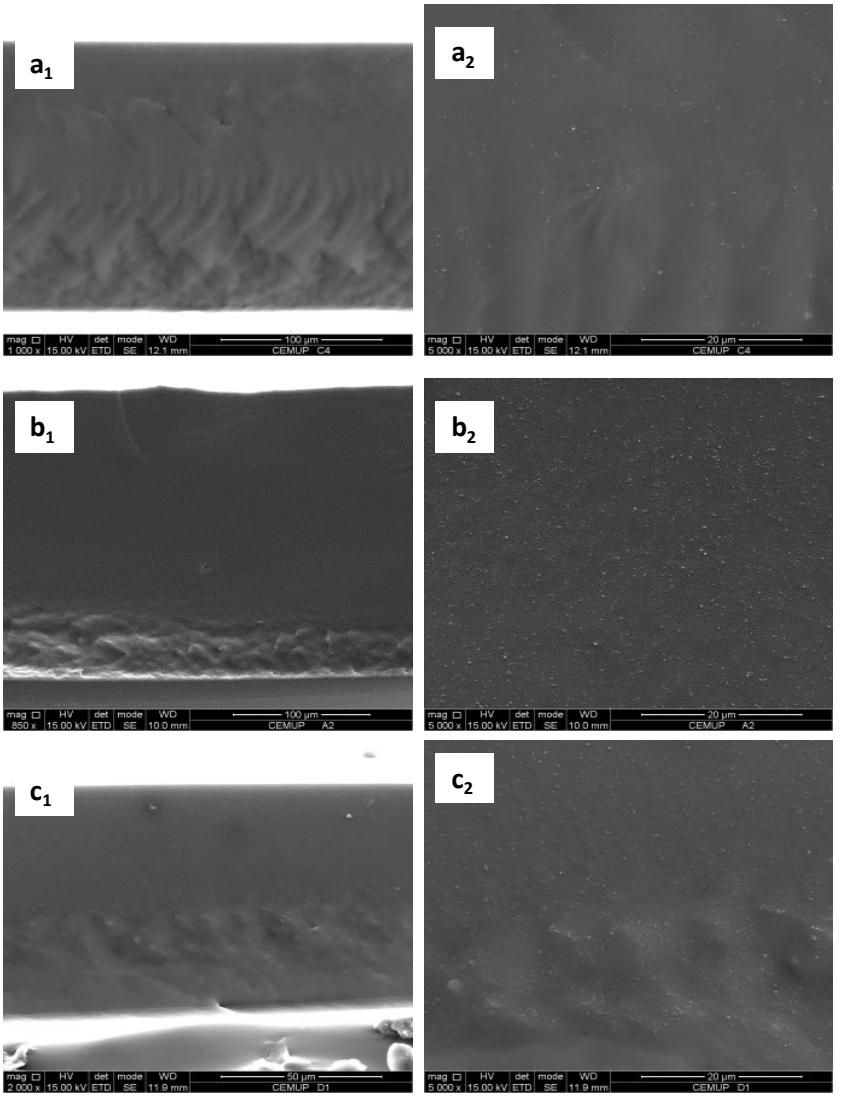

Figure 5.1 - Cross-section SEM images of different PDMS films: (a) PDMS with 0.5 vol.% of carbon black, (b) PDMS with 6 vol.% of carbon black and (c) PDMS with 8 vol.% of carbon black.

5.4.2 Incorporation of carbon black in PEBA 2533 and PEBA 4033 ECPCs

PEBA 2533 and PEBA 4033 ECPCs prepared by the immersion precipitation method and water as the non-solvent and incorporating carbon black also became dense. During the process of phase inversion, water did not exchange with the solvent probably because the system was also highly hydrophobic. Figure 5.2 shows four cases (a, b, c and d) where it was observed that the polymer matrix (PEBA 2533 (a) and PEBA 4033(b, c and d)) became dense after the introduction of carbon black particles. A higher magnification (5000x) of Figure 5.2(b_2, c_2 and d_2) further shows agglomeration of carbon black particles.

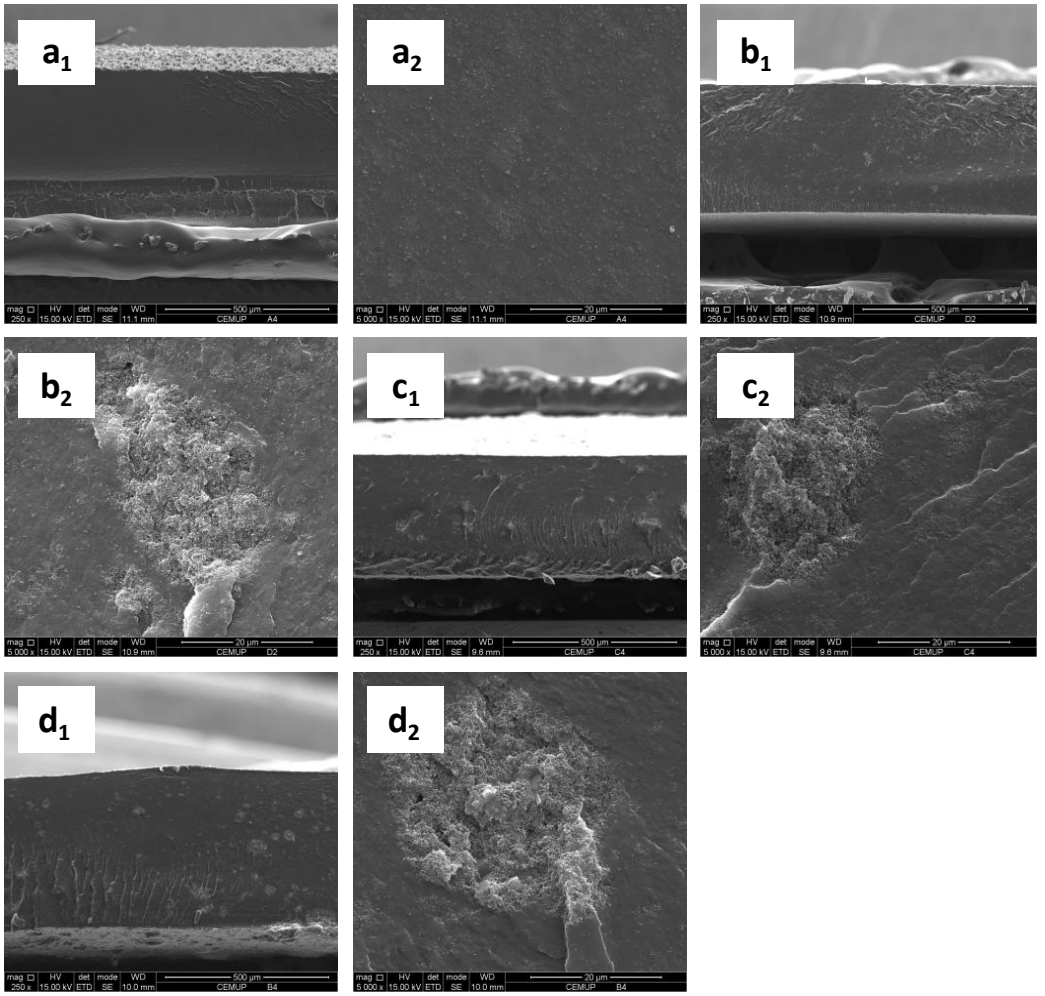

Figure 5.2 - Cross-section SEM images of PEBA films: (a) PEBA 2533 with 5.5 vol.% of carbon black (10 wt.% of polymer concentration), (b) PEBA 4033 with 5.5 vol.% of carbon black (10 wt.% of polymer concentration), (c) PEBA 4033 with 5.5 vol.% of carbon black (7 wt.% of polymer concentration) and (d) PEBA 4033 with 5.5 vol.% of carbon black (5 wt.% of polymer concentration).

5.4.3 Combination of non-solvent/solvent pair in PEBA ECPCs

Different combinations of NMP and non-solvents were tested to study the influence of those solvent/ non-solvent pairs on the porous morphology of PEBA films.

For the choose of the solvent/non-solvent pair, one should have in mind that the solvent has to be miscible in the non-solvent and the non-solvent should be incompatible with the polymer matrix [16]. In this study, several combinations were tested (NMP/ethanol, NMP/hexane and NMP/hexane/acetone); however, the most hydrophobic non-solvent hexane/acetone (95 wt.% / 5 wt.%) showed to be the most promising; NMP is not miscible in hexane but adding a small amount of acetone it becomes miscible. PEBA 4033 ECPCs incorporating carbon black also became dense when using ethanol as non-solvent since ethanol is not sufficiently hydrophobic. Incorporating 5.5 vol.% of carbon black in the PEBA formulation and using hexane/acetone as the non-solvent, a porous film was obtained (Figure 5.3). Upon increasing carbon black concentration to 7.5 vol.%, the morphology of the polymer film changed to dense again due to the highly hydrophobic environment created with the additional carbon black.

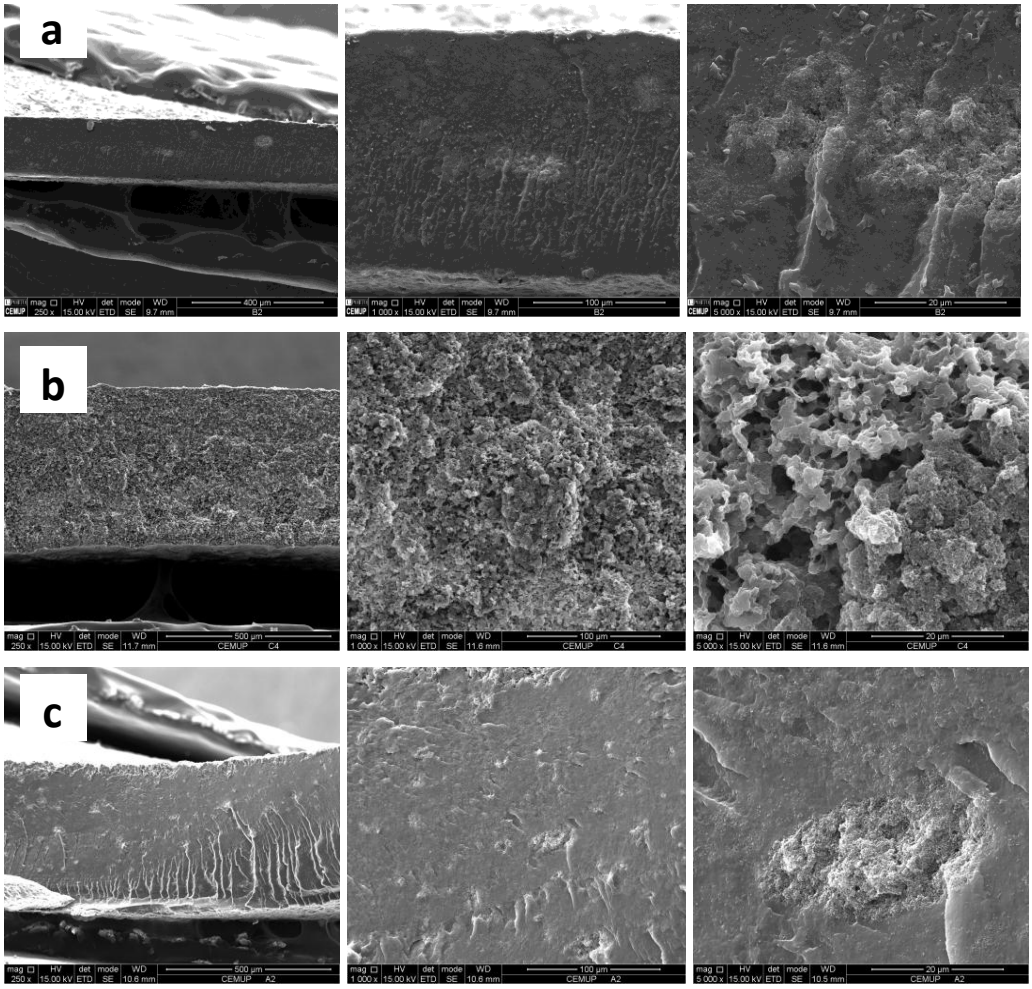

Figure 5.3 - Cross-section SEM images of PEBA 4033 films: (a) PEBA 4033 with 5.5 vol.% of carbon black (non-solvent: ethanol) (b) PEBA 4033 with 5.5 vol.% of carbon black (non-solvent: hexane/acetone) and (c) PEBA 4033 with 7.5 vol.% of carbon black (non-solvent: hexane/acetone).

5.4.4 Incorporation of metallic particles in PEBA 4033 ECPCs

The incorporation of metallic particles on the formation of porous PEBA films was also assessed. It is expected that the introduction of a more hydrophilic component on the PEBA formulation would allow the formation of pores when using water as the non-solvent. Figure 5.4 shows porous PEBA 4033 films incorporating silver nanoparticles (*a*), spherical zinc (*b*) and lamellar zinc (*c*) using water as the non-solvent in the immersion method. The addition of metallic particles in the polymer matrix did not change the porous morphology of the films. In the first case (*a*), there is a poor distribution of the particles due to the high density of the metallic particles when compared to the density of the polymer matrix. In the case of spherical zinc (*b*), the particles seem to be embedded in the polymeric matrix such that they do not touch each other when the film is compressed, originating then non - piezoresistive films. Finally, with the incorporation of lamellar zinc (*c*) the morphology of the film is quite interesting because it presents a cellular structure type “honeycomb”. Despite the high density of zinc when compared to the polymer matrix (PEBA 4033), this seems to be reasonably distributed.

The introduction of a more hydrophilic component (conductive particles) on the hydrophobic polymer matrix (PEBA 4033) allowed the formation of pores by the immersion precipitation using water as the non-solvent.

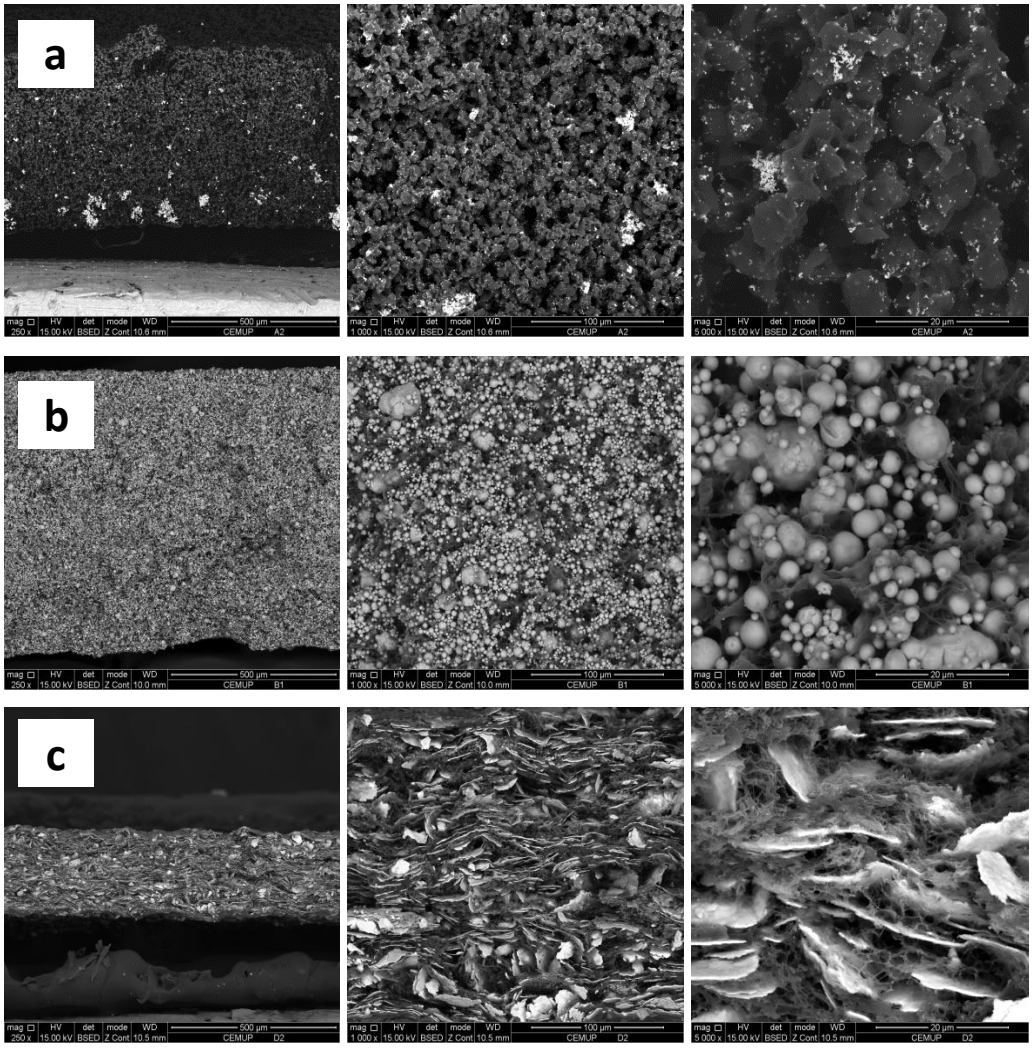

Figure 5.4 - Cross-section SEM images of PEBA 4033 films: (a) PEBA 4033 with 40 vol.% of silver particles, (b) PEBA 4033 with 50 vol.% of spherical zinc and (c) PEBA 4033 with 44 vol.% of lamellar zinc.

5.4.5 Piezoresistive response on porous PEBA 4033 ECPCs

The electrical resistance as a function of applied pressure of porous PEBA 4033 film was studied assembled with polymeric electrodes. The ECPC made of porous PEBA loaded with carbon black (<5.5 vol.%) and prepared with hexane/acetone as the non-solvent presented an electrical resistance to high. According to Danesh et al. [7] and Li et al. [8] the electrical conductivity is higher in porous polymer composite films than in dense, not as observed in the present work. Also, and as mentioned before, the spherical zinc PEBA ECPC also did not show piezoresistive response, probably because of the big size of the metallic particles. On the other hand, Figure 5.5 shows the electrical resistance of porous PEBA 4033 loaded 40 vol.% of silver nanoparticles as function of the pressure applied in a log-log plot. A piezoresisitive response can be observed up to ~ 15 $N \cdot cm^{-2}$ of applied pressure where the electrical resistance changed from 118 kΩ to 30 kΩ. From approximately 15 $N \cdot cm^{-2}$up to 45 $N \cdot cm^{-2}$, the film does not show pressure response.

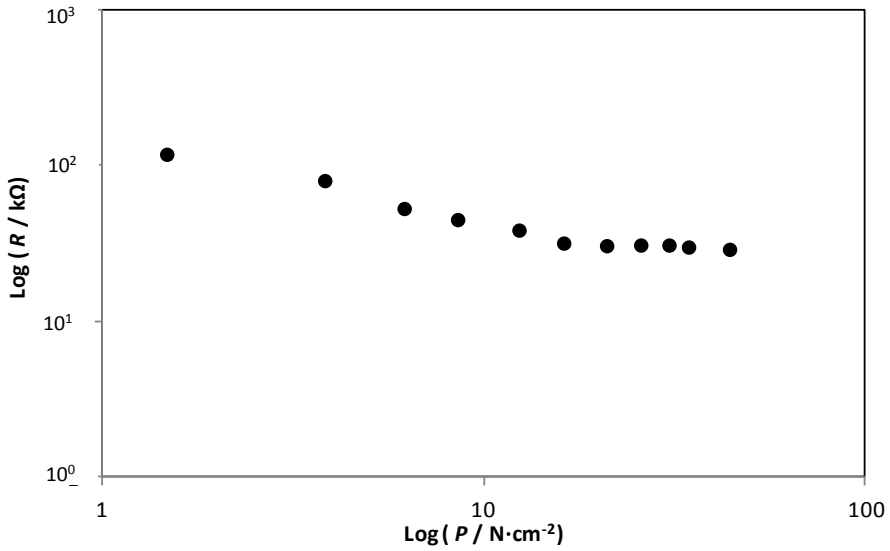

Figure 5.5 - Electrical resistance as a function of the applied pressure of PEBA 4033 film incorporating 40 vol.% of silver nanoparticles assembled with polymeric electrodes.

Figure 5.6 shows the electrical resistance of PEBA 4033 with 44 vol.% of lamellar zinc as a function of the applied pressure applied in a log-log plot for two different sensor samples. A piezoresisitive response was observed up to ~ 35 $N \cdot cm^{-2}$ of applied pressure where the electrical resistance changed from approximately 2000 kΩ to 200 kΩ; the samples are quite reproducible.

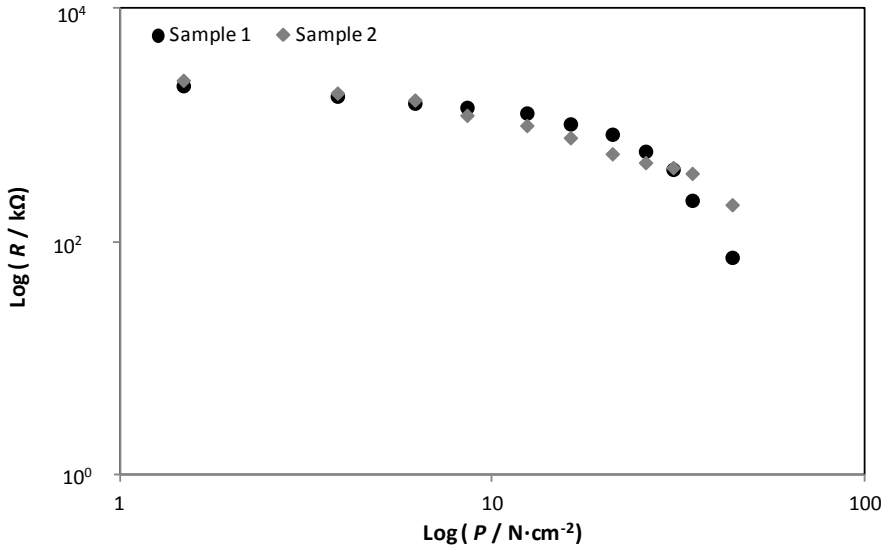

Figure 5.6 – Electrical resistance as a function of the applied pressure of PEBA 4033 film incorporating 44 vol.% of lamellar zinc assembled with polymeric electrodes.

Porous PEBA 4033 loaded 44 vol.% of lamellar zinc exhibited a more linear response than the porous PEBA 4033 loaded 40 vol.% of silver nanoparticles in a log-log plot. The amount of conductive particles incorporated in the polymer matrix is so high (higher than 40 vol.%) that in both cases the composite film became brittle with poor mechanical properties.

5.4.6 Crosslinking of porous PEBA 4033 incorporating 44 vol.% of lamellar zinc

To improve mechanical properties, a film of porous PEBA 4033 ECPC loaded 44 vol. % of lamellar zinc was crosslinked. Crosslinking of PEBA 4033 produces urethane linkages between the terminal hydroxyl groups of the polymer and the isocyanate groups of TDI [15]. The mechanical properties effectively improved by crosslinking

(evaluated upon handling the sample). The porous crosslinked PEBA 4033 film loaded 44 vol.% of lamellar zinc and assembled with the polymeric electrodes, Figure 5.7, exhibited a higher electrical resistance compared with the film without crosslinking. Moreover, it showed an approximately linear response (in a log-log plot) as a function of the applied pressure.

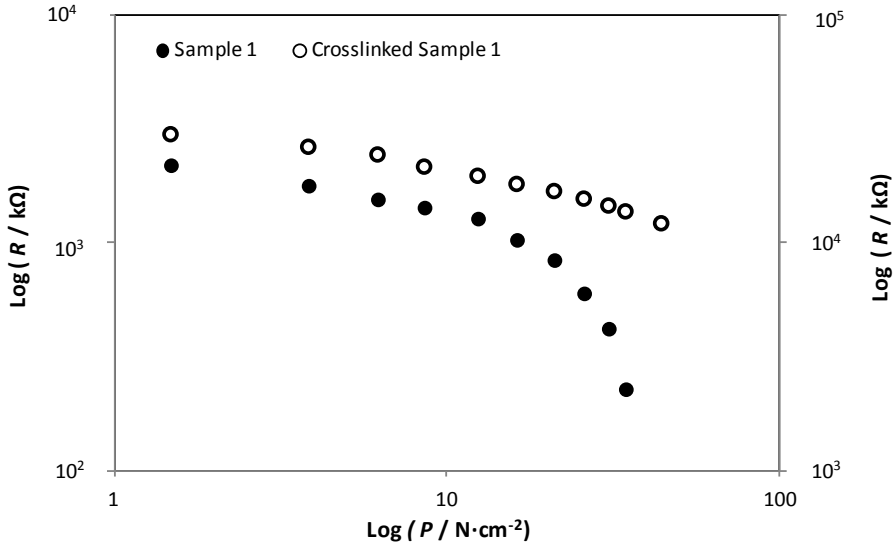

Figure 5.7 – Electrical resistance as a function of the applied pressure of unmodified and crosslinked PEBA 4033 loaded 44 vol.% of lamellar zinc films assembled with polymeric electrodes.

5.5 Conclusions

ECPCs made of porous PEBA 4033 films incorporating carbon black and assembled with polymeric electrodes were only successfully obtained when a hexane/acetone as non-solvent was used, but at high carbon black concentration the hydrophobicity of non-solvent was not enough to avoid the formation of a dense

ECPC due to the highly hydrophobic environment created. ECPCs made of porous PDMS films incorporating carbon black were not obtained.

On the other hand, with the incorporation of hydrophilic metallic particles in the polymer matrix, a porous PEBA morphology was achieved when using water as the non-solvent. A piezoresistive response was successfully achieved for some of the porous ECPCs assembled with polymeric electrodes tested: 1 – the electrical resistance of the PEBA 4033 loaded 40 vol.% of silver nanoparticles ECPC changed from 180 kΩ to 30 kΩ by applying pressure up to 15 $N \cdot cm^{-2}$, 2- For the PEBA 4033 loaded 44 vol.% of lamellar zinc ECPC the electrical resistance changed from approximately 2000 kΩ to 200 kΩ by applying pressure up to 35 $N \cdot cm^{-2}$, 3- the crosslinked PEBA 4033 loaded 44 vol.% of lamellar zinc ECPC exhibited a higher electrical resistance compared with the same ECPC without crosslinking. The electrical resistance of crosslinked porous PEBA 4033 loaded 44 vol.% of lamellar zinc ECPC changed approximately linearly with the pressure applied in a log -log plot. However, poor mechanical properties were observed due to the high concentration of zinc incorporated in the polymer matrix.

5.6 References

1. Harsányi, G., *Polymeric sensing films: new horizons in sensorics?* Materials Chemistry and Physics, 1996. **43**(3): p. 199-203.
2. Albert, K.J., Lewis, N.S., Schaner, C.L., Sotzing, G.A., Stitzel, S.E., Vaid, T.P., *Cross-Reactive chemical sensor arrays.* Chem. Rev, 2000. **100**: p. 2595-2626.
3. Freund, M.S., Lewis, N.S., *A chemically diverse conduction polymer-based "electronic nose".* 1995. **92**: p. 2652-2656.
4. Lonergan, M.C., Severin, E.J., Doleman, B.J., Beaber, S.A., Grubbs, R.H., Lewis, N.S., *Array-based vapor sensing using chemically sensitive, carbon black-polymer resistors.* Chem. Mater., 1996. **8**: p. 2298-2312.

5. Hentze, H.P., Antonietti, M., *Porous polymers and resins for biotechnological and biomedical applications.* Reviews in Molecular Biotechnology, 2002. **90**(1): p. 27-53.

6. Ravati, S., Favis, B.D., *3D porous polymeric conductive material prepared using LbL deposition.* Polymer, 2011. **52**(3): p. 718-731.

7. Danesh, E., Ghaffarian, S.R., Molla-Abbasi, P., *Non-solvent induced phase separation as a method for making high-performance chemiresistors based on conductive polymer nanocomposites.* Sensors and Actuators B: Chemical, 2011. **155**(2): p. 562-567.

8. Li, M., Zhang, W., Wang, C., Wang, H., *In situ formation of 2D conductive porous material with ultra low percolation threshold.* Materials Letters, 2012. **82**(0): p. 109-111.

9. King, M.G., Baragwanath, A.J., Rosamond, M.C., Wood, D., Gallant, A.J., *Porous PDMS force sensitive resistors.* Procedia Chemistry, 2009. **1**(1): p. 568-571.

10. Brady, S., Diamond, D., Lau, K.-T., *Inherently conducting polymer modified polyurethane smart foam for pressure sensing.* Sensors and Actuators A: Physical, 2005. **119**(2): p. 398-404.

11. Juchniewicz, M., Stadnik, D., Biesiada, K., Olszyna, A., Chudy, M., Brzózka, Z., Dybko, A., *Porous crosslinked PDMS-microchannels coatings.* Sensors and Actuators B: Chemical, 2007. **126**(1): p. 68-72.

12. Wang, J.C.R.Z.W. (2012) *Fabricating microporous PDMS using a water-in-PDMS emulsion*.

13. Chakrabarty, B., Ghoshal, A.K., Purkait, M.K., *Effect of molecular weight of PEG on membrane morphology and transport properties.* Journal of Membrane Science, 2008. **309**(1–2): p. 209-221.

14. Jansen, J.C., Buonomenna, M.G., Figoli, A., Drioli, E., *Ultra-thin asymmetric gas separation membranes of modified PEEK prepared by the dry–wet phase inversion technique.* Desalination, 2006. **193**(1–3): p. 58-65.

15. Sridhar, S., Suryamurali, R., Smitha, B., Aminabhavi, T.M., *Development of crosslinked poly(ether-block-amide) membrane for CO2/CH4 separation.* Colloids and Surfaces A: Physicochemical and Engineering Aspects, 2007. **297**(1-3): p. 267-274.

16. Mulder, M., *Basic Principles of Membrane Technology*. 2 nd ed. 2000: Klumer Academic Publishers.

CHAPTER VI

6 Development of porous polymer pressure sensors incorporating graphene platelets[1]

Abstract

Electrically Conductive Polymer Composites (ECPCs) based on porous polymeric matrices of PEBA 4033 incorporating different types of graphene platelets were prepared and tested. PEBA 4033 polymer was mixed with 5 different graphene platelets: a) grade H5 (length of 5 μm, average thickness of 15 nm and surface area between 50 and 80 $m^2 \cdot g^{-1}$); b) grade MX (where X is the length: 5 μm, 15 μm or 25 μm, average thickness of 6-8 nm and surface area between 120 and 150 $m^2 \cdot g^{-1}$) and c) grade C–750 (length of 1-2 μm, average thickness of 2 nm and average surface area of 750 $m^2 \cdot g^{-1}$). Porous morphology was obtained for the ECPCs prepared with the graphene platelets grade MX and H5 while for the grade C–750, only a dense ECPCs was obtained. The porous ECPC loaded with 15 vol.% of graphene M5 exhibited a linear piezoresistive response in a log-log plot. However, some limitations were detected for this ECPC namely hysteresis and drift due to the poor mechanical properties. The porous ECPC loaded with 15 vol.% M5 was further crosslinked, which improved its mechanical properties but the piezoresistive effect became negligible. The incorporation of carbon black in this ECPC formulation, was shown to be much more efficient than crosslinking to improve mechanical properties, but the piezoresistive response became poor.

[1] Adapted from: Gonçalves, V., Brandão, L., Mendes, A., Development of porous polymer pressure sensors incorporating graphene platelets, Polymer Testing, 37 (2014) 129-137.

6.1 Introduction

In recent years, there has been an increasing interest in the use of carbon based materials in many applications as sensors and composites materials [1-2]. The discovery of graphene, the elementary structure of graphite, made a revolutionary change in scientific and technological applications and has earned Kostya S. Novoselov and Andre K. Geim the Physics Nobel Prize in 2010. Graphene is a single layer of sp^2 bonded carbon atoms patterned in a hexagonal lattice that has unique properties such as high electrical conductivity and mechanical strength that can be used in electrically conductive polymers composites (ECPCs) [2-4]. Graphene is classified by the number of stacked layers: single layer, few-layer (2-10 layers) and multi-layer (thin graphite); the number of layers needed for the properties of graphene to fully match those of bulk graphite is over 100 [4]. Recently, some studies reported the preparation of the polymer-graphene/expanded graphite composites [3, 5-9]. Some authors studied different methods of preparation of polymer matrix incorporating graphene platelets and their effects on the mechanical and electrical properties. They concluded that the effect of graphene dispersion influence the electrical response of ECPCs [3, 5-10]. Chandrasekaran et al. [3], for example, employed two mixing methods, three-roll milling and sonication combined with high speed shear mixing and they concluded that the three-roll milling method improved electrical conductivity 5 orders of magnitude at 0.3 wt.%. On the other hand, polymer composites incorporating graphene platelets showed a low percolation threshold [3, 9] and promote an improvement in the mechanical properties that increase the storage modulus (*E'*) and improve the stiffness of the material [3, 7-8, 10]. However, the diameter of graphene platelets influences mechanical properties. Kalaitzidou et al. [7], for example, fabricated polypropylene containing exfoliated graphite platelets , xGnP, (graphene sheets 10 nm thickness) by melt mixing and injection molding. The

addition of xGnP – 1 (~1 μm diameter) promote a greater improvement in the mechanical properties than adding carbon black. However, the addition of xGnP - 15 (~15 μm diameter) led to poor mechanical properties due to the difficulty of dispersing, it and resulted in a non-homogeneous composites.

In the previous Chapter, it was concluded that lamellar zinc loaded into porous PEBA 4033 originated a ECPC sample exhibiting very promising piezoresistive effect properties though with poor mechanical properties due to the high concentration of lamellar zinc (44 vol.%). Graphene platelets have similar shape of lamellar zinc though significantly smaller density (d_{zinc} ~ 7 g·cm^{-3} [11], $d_{graphene}$ ~ 2 g·cm^{-3} [12]). The present work targets for the first time the development and characterization of porous ECPCs prepared loaded with graphene platelets of different geometries (length, surface area and thickness). The piezoresistive response and mechanical properties were also evaluated.

6.2 Experimental

6.2.1 Materials

PEBAX polymer was supplied by Atofina Chemicals. Ethanol, hexane, 2, 4 - toluyene diisocyanate (TDI), n-methyl-2-pyrrolidone (NMP) and acetone were purchased from Sigma Aldrich. Distilled water was also used as non-solvent. Carbon black powder (Vulcan® XC72R) was purchased from Cabot Corporation. Graphene platelets (GNP) grade C-750, M5, M15, M25 and H5, were purchased from XG Sciences. These materials have following characteristics: M type-maximum length of 5 μm, 15 μm and 25 μm, respectively M5, M15 and M25, average thickness of 6-8 nm and surface area between 120 m^2·g^{-1} and 150 m^2·g^{-1}; H5-maximum length 5 μm, average thickness of 15 nm and surface area between 50 m^2·g^{-1} and 80 m^2·g^{-1} and C-

750 maximum length 1-2 µm, average thickness of 2 nm and average surface area of 750 $m^2 \cdot g^{-1}$.

6.2.2 Preparation of porous PEBA 4033 ECPCs by immersion precipitation method

Different weight fractions of GNPs were dispersed in NMP by sonication for 15 minutes. PEBA 4033 was dissolved in NMP to form a polymer solution that was added to a previously prepared NMP suspension of conductive particles. When the polymer solution became homogeneous, it was poured on to a glass plate. The procedure used is described elsewhere (Chapter V). ECPCs were prepared by the immersion precipitation method (Chapter V). Briefly, the film was then exposed to room temperature before immersion into the non-solvent at room temperature. After that, the film was washed under running water and then kept overnight in a water bath. Finally, the film let to dry at room temperature for 2 days.

Figure 6.1 shows the PEBA 4033 films obtained after using the immersion precipitation method. The initially cast PEBA 4033 films changed their colour from a transparent liquid film to a white porous film (high light dispersion originated by the occlusion of air bubbles) after immersion in the non-solvent. Shrinkage of the film was also observed that caused it to be easily separated from the glass plate after 5 minutes (left image). With incorporation of graphene, the change of colour due to the build-up of the pores was not easily detected by visual inspection. However, it was observed that PEBA 4033 formulations containing graphene changed their colour from dark grey (casted film) to a lighter grey upon build-up of pores (right image).

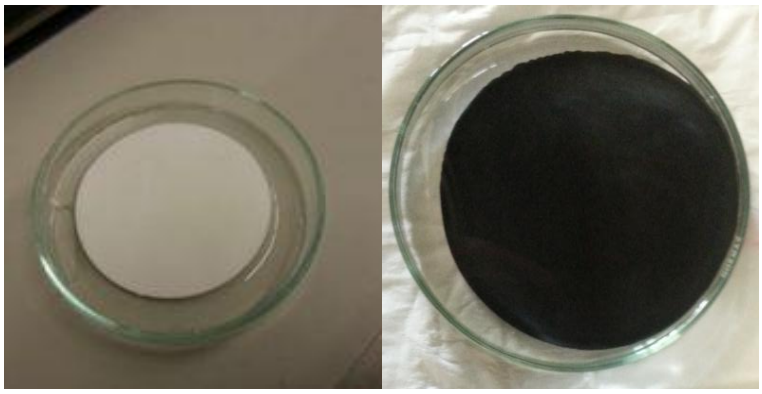

Figure 6.1 - PEBA 4033 films obtained after the immersion precipitation method (left image: porous plain PEBA 4033 film, right image: porous PEBA 4033 film incorporating graphene platelets).

Table 6.1 represents the PEBA 4033 films prepared by the immersion precipitation method with different types of graphene platelets.

Table 6.1 – Porous PEBA 4033 ECPCs incorporating graphene platelets.

Films	Non-solvent	Type of graphene	Concentration of graphene (vol.%)	Concentration of carbon black (vol.%)
a	water	M5	5.5	
b	ethanol	M5	5.5	
c	hexane/acetone	M5	5.5	
d		C-750	15	
e		H5	15	
f		M5	15	
g		M15	15	
h		M25	15	
i		M5	18	
j			13	2
k		M5	10	5
l			8	2

6.2.3 Crosslinking of porous PEBA 4033 ECPCs

The crosslinking procedure is described elsewhere (Chapter V). Briefly, ECPCs based on PEBA 4033 loaded with graphene platelets was immersed in a 2 % (v/v) solution of TDI in hexane for 30 minutes. The ECPC was removed from the bath and

washed with distilled water for an hour. Finally, the ECPC was then dried in oven at 60 °C followed by vacuum drying for 24 hours.

6.3 Characterization of PEBA 4033 ECPCs

6.3.1 Scanning Electron Microscopy (SEM)

The cross-section morphologies of ECPCs based on PEBA 4033 were observed by Scanning Electron Microscopy (SEM) using a JEOL JSM-6301F, Oxford INCA Energy 350 equipment. Samples were fractured in liquid nitrogen and sputtered with gold/platinum using a K575X Sputter Coater by Quorum Technologies.

6.3.2 Measurement of Electrical Resistance

The electrical resistance of the prepared ECPCs based on PEBA 4033 was measured using a multimeter (Fluke 11) in an in-house made mechanical press. The effective area of the electrode was 1 cm^2. The electrical contact between the ECPC film and the multimeter was obtained using a copper layer applied over a polymeric film (FlexPCB). Two layers of a polymeric film with similar composition to ECPCs but having on electrical conductivity two orders of magnitude were applied in each side of the ECPC film to be characterized. The procedure used is described elsewhere (Chapter III).

6.3.3 Dynamic Mechanical Analysis (DMA)

DMA experiments were performed using a DMA 242 E from Netzsch in film compression mode at frequency of 1 Hz and 10 Hz. Nitrogen gas was used at a flowing rate of 80 ml/min. Samples were tested at temperatures ranging from -20 °C to 100 °C with a heating rate of 2 °C/min.

6.4 Results and discussion

6.4.1 Incorporation of graphene platelets in PEBA 4033 ECPCs with different combinations of non-solvent/solvent pair

Some combinations of non-solvent/solvent (NMP) were tested in order to achieve the best procedure for obtaining porous ECPCs based on PEBA 4033 and incorporating M5 graphene platelets. Previous Chapter indicated that when using carbon black as conductive particles, ECPCs of non-porous morphology was usually obtained.

Figure 6.2 shows the effect of the non-solvent on the morphology of PEBA 4033 incorporating 5.5 vol.% of M5. When using water, the ECPC obtained is dense due to the hydrophilic nature of the non-solvent. The same was observed in the previous Chapter, where after incorporating 5.5 vol.% of carbon black in the PEBA 4033 matrix and using water as the non-solvent, a dense film was obtained. On the other hand, the hexane/acetone mixture (95 wt.% / 5 wt.%) and ethanol were the most promising non-solvent for preparing ECPCs based on graphene conductive particles. This observation is different from the previous Chapter: when using ethanol as non-solvent, a porous structure was not observed while when using hexane/acetone a porous morphology was observed for the ECPCs prepared. We found that, the porous morphology was observed even after increasing graphene concentration to 15 vol.%, see below, (Figure 6.4).

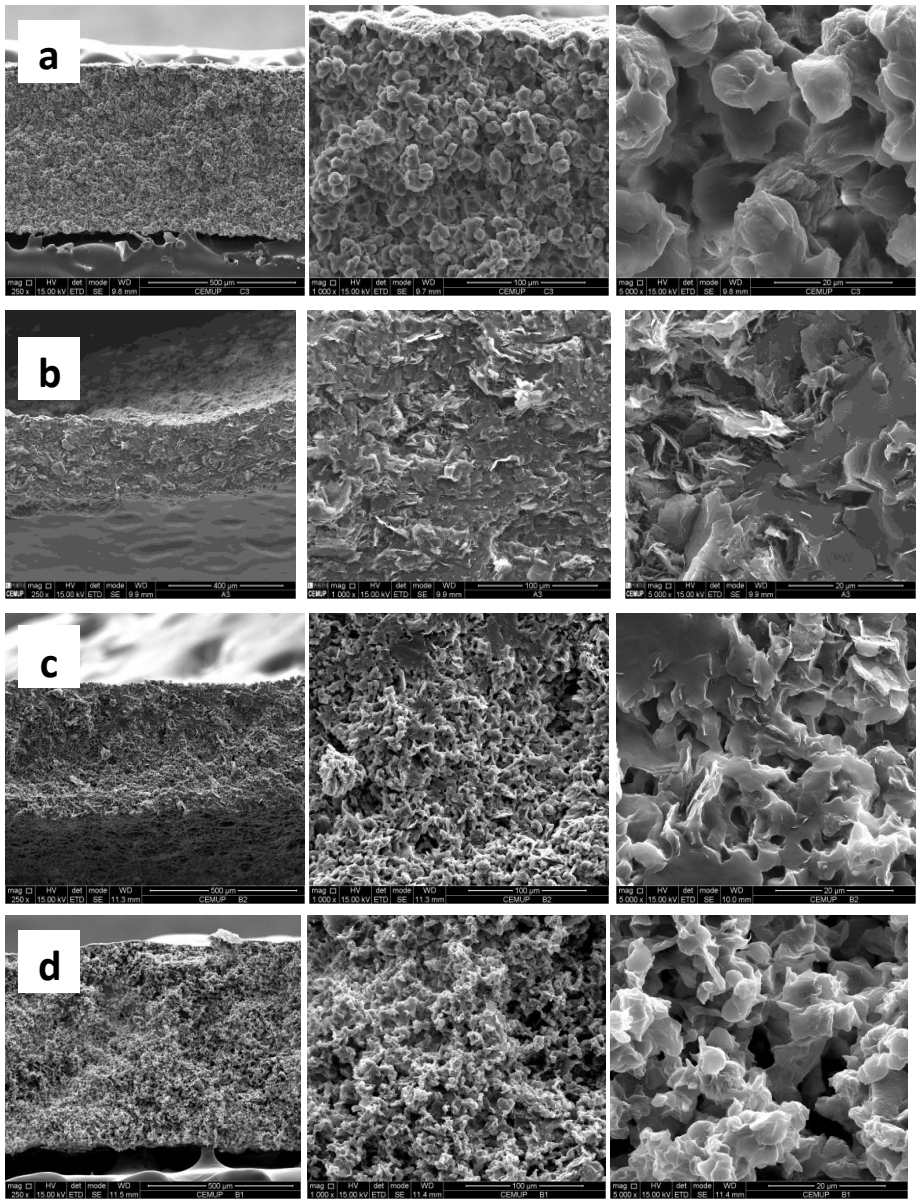

Figure 6.2 - Cross-section SEM images of the PEBA 4033 film (a) and the ECPCs (b-d) with 5.5 vol.% M5 at different magnifications and different non-solvents: film (a) - non-solvent: water, film (b) - non-solvent: water, film (c) - non-solvent: ethanol and film (d) - non-solvent: hexane/acetone.

6.4.2 Incorporation of different types of the graphene platelets in ECPCs

The different types of graphene were employed to prepare ECPCs based on PEBA 4033 and using hexane/acetone as non-solvent. As mentioned before, with incorporation of 5.5 vol.% M5, the ECPCs obtained were porous. Increasing graphene M5 concentration to 15 vol.%, the ECPC morphology kept it porosity (Figure 6.3 and Figure 6.4). A porous morphology was also observed for graphene types M15, M25 and H5 at a concentration of 15 vol.%, (Figure 6.3 and Figure 6.4). On the other hand, the ECPCs incorporating 15 vol.% of graphene C–750 showed a dense morphology (Figure 6.3 d) similar to the one obtained when incorporating carbon black (Chapter V). This should be related to the smaller thickness (2 nm) and higher surface area (750 $m^2 \cdot g^{-1}$) of this graphene, which are more similar to carbon black.

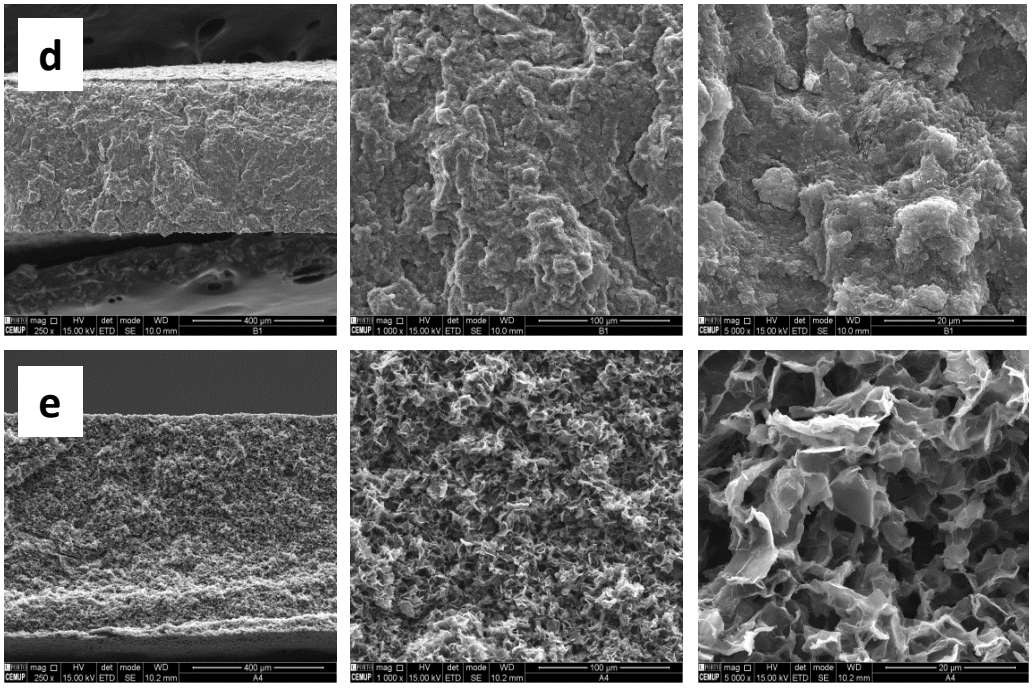

Figure 6.3 - Cross-section SEM images of the ECPCs (films d and e) incorporating 15 vol.% of graphene with different types: film (d) – C–750 and film (e) - H5.

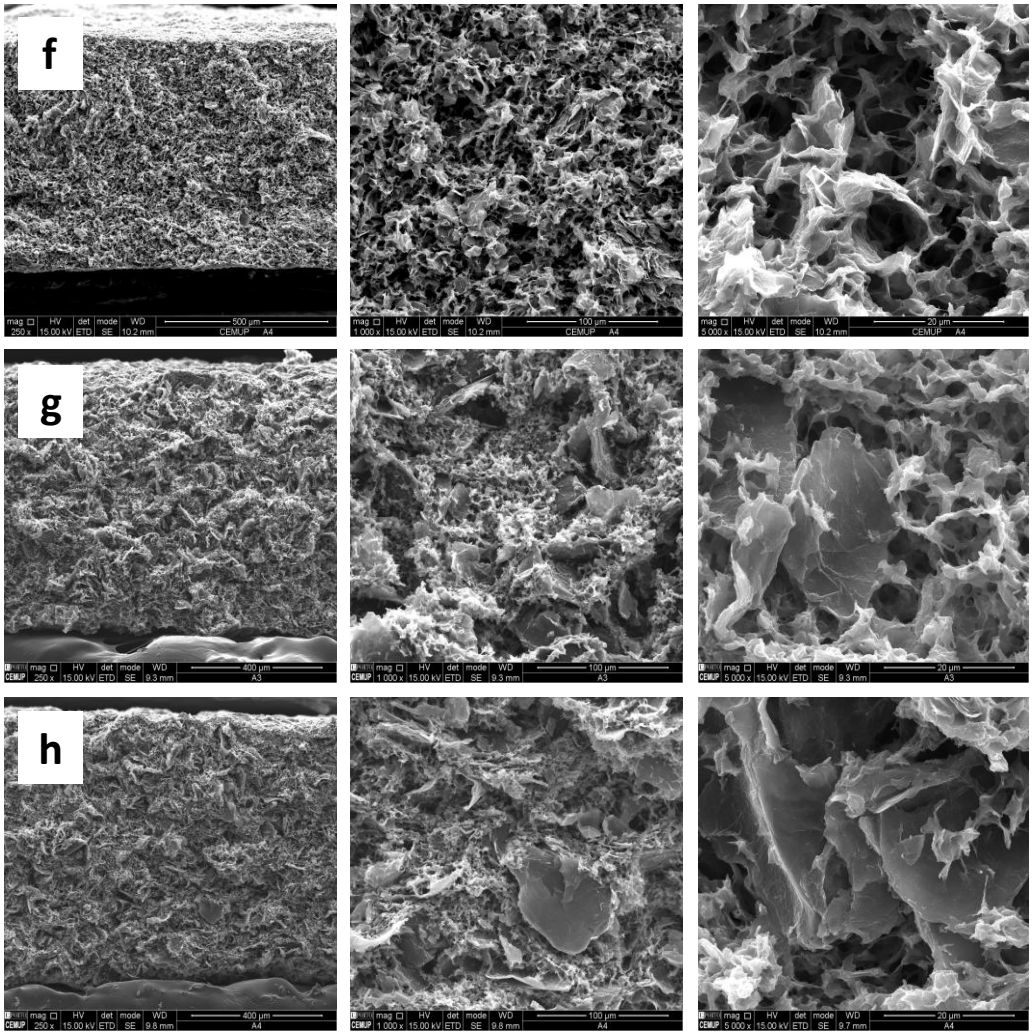

Figure 6.4 - Cross-section SEM images of the ECPCs (films f-h) incorporating 15 vol.% of graphene MX: film (f) – M5,film (g) –M15 and film (h) - M25.

It should be stressed that the morphology of the films obtained with graphene type H and type M (Figure 6.3 and Figure 6.4) is quite interesting showing a regular cellular structure with a large range of interconnecting pores. This type of porous polymeric composite films can be used in applications such as thermal and

mechanical insulators, packaging materials, drug carrier systems, medical devices and solid supports for catalysis [13] and for biosensors, chemical gas sensors, electronic devices and smart fabrics [14-17].

Figure 6.5 shows a higher magnification (20 000 x) of the platelets that seem to be embedded in the polymeric matrix.

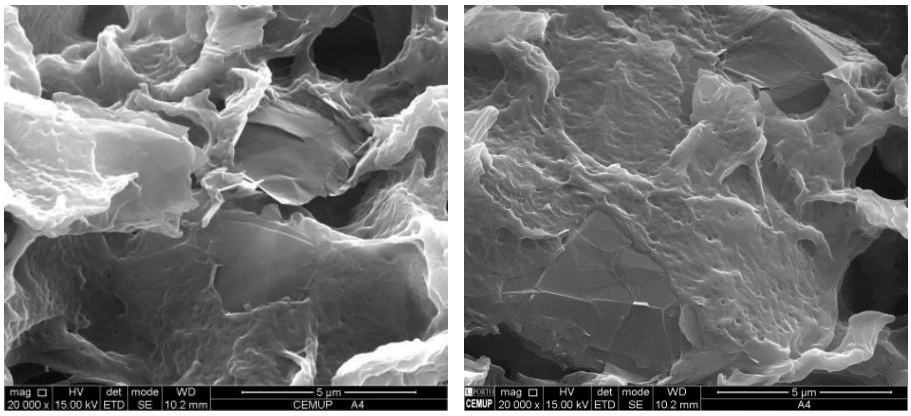

Figure 6.5 – Cross-section in high magnification of ECPCs (film e and f) incorporating 15 vol.% graphene with different types: (left) –M5 and (right) –H5.

6.4.3 Piezoresistive response on the porous ECPCs based on PEBA 4033 loaded with graphene platelets

The piezoresistive behaviour of the prepared porous ECPCs incorporating graphene platelets was evaluated. The electrical resistance of ECPCs incorporating 5.5 vol.% of graphene M5 were too high. A very high electrical resistance was also observed for the ECPCs loaded with the same concentration of carbon black (Chapter V).

Figure 6.6 shows the electrical resistance as a function of the applied pressure for ECPCs loaded with 15 vol.% graphene MX and H5. The H5-ECPC exhibited the

lowest electrical resistance of all the ECPCs tested while the others ECPCs showed similar electrical resistances. Moreover, H5-ECPC did not show any pressure sensitivity. On the other hand, the most promising piezoresistive response was obtained with the ECPC loaded with graphene M5, which exhibited an approximately linear response in a log-log plot.

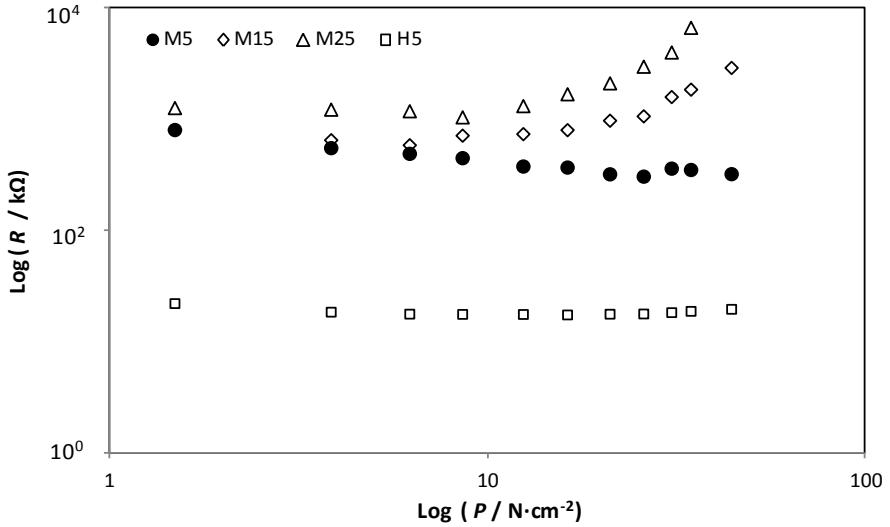

Figure 6.6 - Electrical resistance (log-log plot) as a function of the applied pressure of ECPCs based on PEBA 4033 loaded with 15 vol.% of graphene (type M5, M15, M25 and H5) assembled with polymeric electrodes.

It can also be observed that the electrical resistance changes from 810 kΩ to 340 kΩ (approximately), from no pressure applied to ca. 25 $N \cdot cm^{-2}$, Figure 6.7. From approximately 25 $N \cdot cm^{-2}$ to 45 $N \cdot cm^{-2}$, M5-ECPC does not show pressure sensitivity, while M15-ECPC and M25-ECPCs did not stand pressures above of 6 $N \cdot cm^{-2}$ (suffered mechanical damage). At pressures higher than 6 $N \cdot cm^{-2}$, the destruction of the

conductive paths is higher than their formation and this decrease of conductive pathways number increases electrical resistance [18-20].

6.4.4 Hysteresis and drift of M5-ECPC

Since the most promising piezoresistive response observed was the M5-ECPC, hysteresis and drift were also assessed. Figure 6.7 shows the electrical response as a function of the applied pressure for two load and two unload steps cycles obtained for the M5-ECPC assembled with polymeric electrodes. The sample responded steadily after 5 s under load and 10 s after unload. During the first step, the electrical resistance changed from 810 kΩ to 340 kΩ and after the first unload step, the electrical resistance changed from 340 kΩ to 460 kΩ, indicating a significant hysteresis. In the second load step, begun 30 s after the end of first unload step and after 5 s under load, the electrical resistance changed from 510 kΩ to 180 kΩ, and after 10 s of the second unload steps, the electrical resistance change 180 kΩ to 350 kΩ, showing again hysteresis. The poor mechanical properties of M5-ECPC could be responsible for the electrical hysteresis and drift [14]. The hysteresis of M5-ECPC is related to the plastic deformations occurring during the load step and these irreversible phenomena are related to the ECPC high load of graphene particles [21].

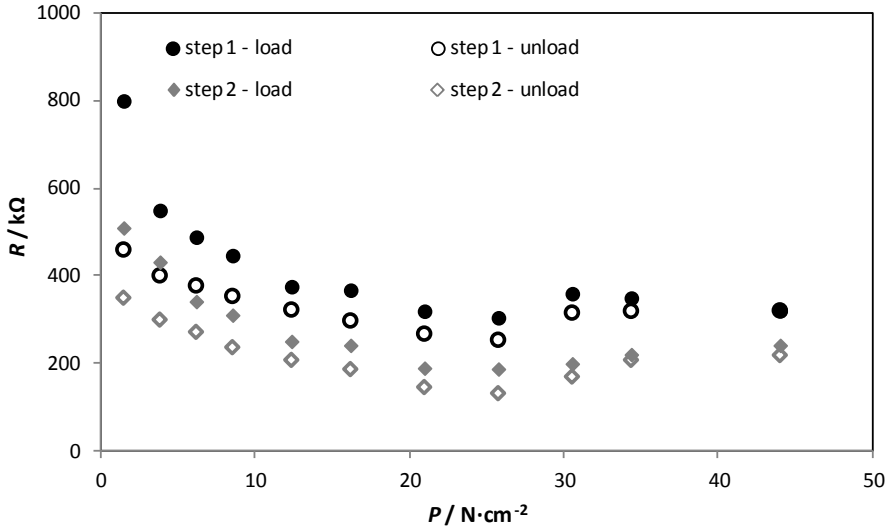

Figure 6.7 - Electrical resistance as a function of the applied pressure (load and unload steps) of ECPC based on PEBA 4033 loaded with 15 vol.% of graphene M5 assembled with polymeric electrodes.

6.4.5 Dynamic Mechanical Properties

The mechanical properties were evaluated by Dynamic Mechanical Analysis (DMA) that measures the cyclic response of a material to stress as a function of the temperature. The storage modulus (*E'*) and phase angle (*δ)* of the prepared ECPC/graphene polymer films and pure dense and porous PEBA 4033 polymer films from -20 °C to 100 °C are shown in Figure 6.8 and Figure 6.9. The storage modulus represents the elastic component of a material and is an indicator of the capability of a material to store energy reversibly. Pure dense PEBA 4033 film exhibits an *E'* higher than porous PEBA 4033 film, 149 MPa versus 13.45 MPa at 25 °C. On the other hand, porous M5-ECPC (incorporating 15 vol.% of graphene M5) showed an *E'* 22.9 % higher compared to the pure porous PEBA 4033 film (13.45 MPa versus 16.53 MPa at 25 °C,

respectively). The same behaviour was observed by Tang et al. [10] who concluded that the storage modulus increased when introducing graphene (1.2 nm thick) in a polymeric film. However, with introduction of the larger graphene platelets (graphene M15), the storage modulus decreased 30.3 % compared with the pure porous PEBA 4033 film (10.32 MPa versus 16.53 MPa at 25 °C). The good dispersion of graphene M5 in PEBA 4033, also related to the small size of the graphene M5 platelets (ca. 5 µm length and 6-8 nm thick), could be the reason why the composite film display better mechanical properties [3, 7-8, 10]. In case of porous M15-ECPC, it was more difficult to disperse the graphene particles.

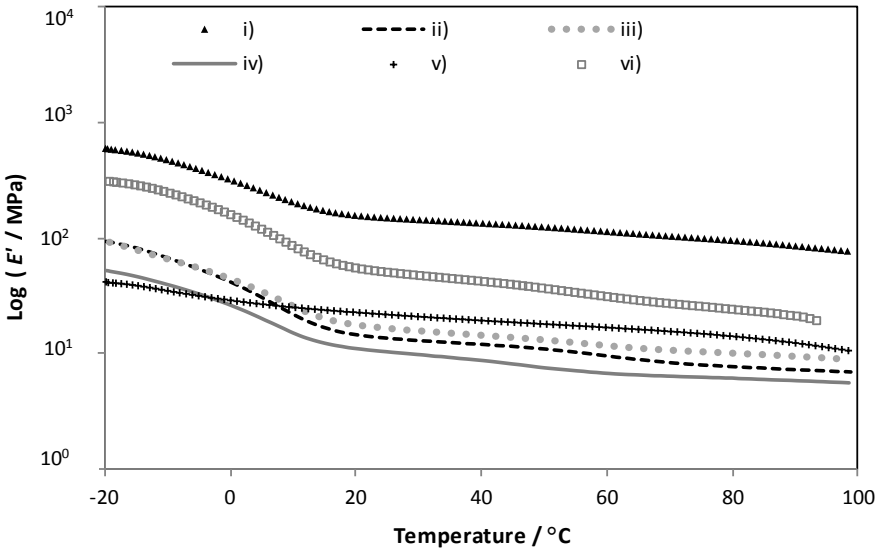

Figure 6.8 - *E'* (log scale) as a function of temperature for: i) pure dense PEBA 4033 film, ii) pure porous PEBA 4033 film, iii) porous M5-ECPC, iv) porous M15-ECPC, v) crosslinked porous M5-ECPC and vi) porous M5/carbon black-ECPC.

To further improve the mechanical properties, ECPCs were crosslinked or carbon black was added to the PEBA 4033 polymer matrix. The crosslinked M5-ECPC

showed a storage modulus of 22.0 MPa at 25 °C while the M5/carbon black-ECPC showed a storage modulus of 51.0 MPa (an increase 63.6 % versus an increase of 379 %, compared with the pure porous PEBA 4033 film, respectively).

Tan δ is the ratio between the amount of energy dissipated by viscous mechanisms and the energy stored in the elastic component, providing information about the viscoelastic properties of the material [8]. The maximum tan δ as a function of temperature is related to the glass-transition temperature (*Tg).* Table 6.2 shows the glass-transition temperature of the prepared polymers films. In the case of crosslinking porous M5-ECPC the peak of tan δ was not clear indicating that the glass-transition temperature was obtained at a lower temperature (maximum tan δ was shifted to left) or the crosslinked reduced the mobility of polymer chains and decreased the height of the tan δ peak [3]. On the other hand, the introduction of carbon black on porous M5-ECPC raised the glass-transition temperature ca. 10 °C.

Table 6.2 – Mechanical properties of the prepared polymer films.

Films	Maximum tan δ	*Tg* (°C)
i)	0.100	-0.6
ii)	0.090	-3.6
iii)	0.144	-5.6
iv)	0.118	-3.1
v)	-	-
vi)	0.124	10

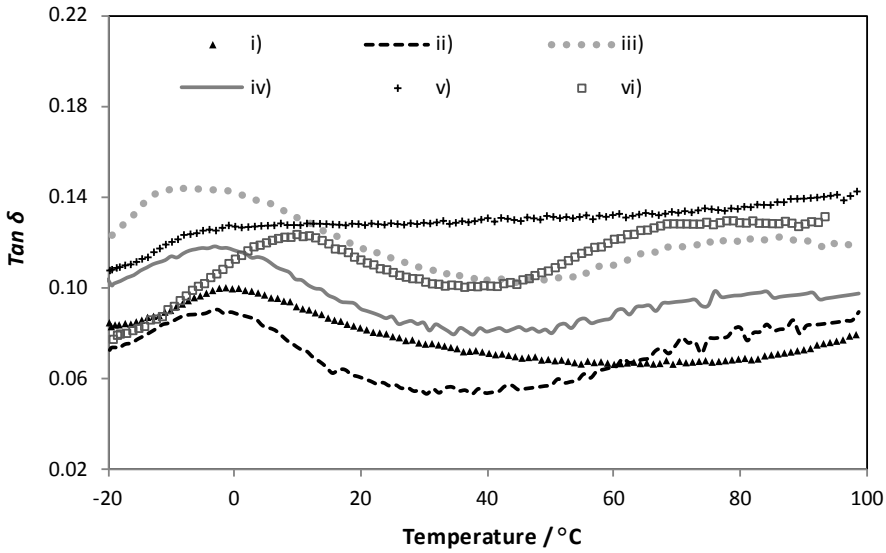

Figure 6.9 - Tan δ as a function of temperature for: i) pure dense PEBA 4033 film, ii) pure porous PEBA 4033 film, iii) porous M5-ECPC, iv) porous M15-ECPC, v) crosslinked porous M5-ECPC and vi) porous M5/carbon black ECPC.

6.4.6 Crosslinking of the porous M5-ECPC

Porous M5-ECPC was crosslinked in order to reduce the hysteresis and drift by increasing mechanical properties. The crosslinked M5-ECPC assembled with the polymeric electrodes exhibited a higher electrical resistance when compared to the M5-ECPC without crosslinking (Figure 6.10). This behaviour was also observed with the lamellar zinc-ECPC film (Chapter 4). In fact, there is a systematic increase in electrical resistance when the sample is crosslinked. Indeed, after crosslinking none of the ECPCs based on PEBA 4033 loaded with graphene M5 (loads of 15 vol.% and 18 vol.%) showed a piezoresistive response.

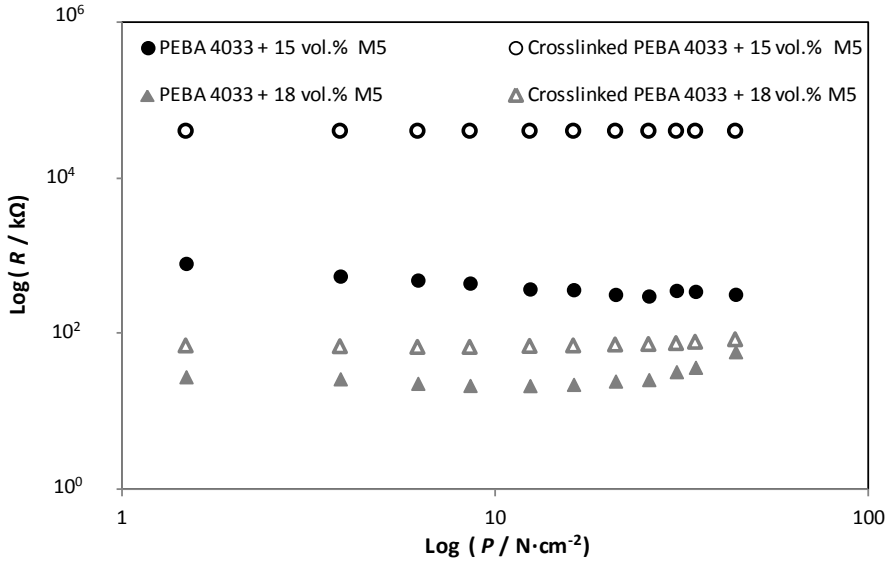

Figure 6.10 - Electrical resistance (log-log plot) as a function of the applied pressure of unmodified and crosslinked M5-ECPC assembled with polymeric electrodes.

6.4.7 Introduction of carbon black in porous M5-ECPCs

Apart from crosslinking, carbon black proved also to improve the mechanical properties of ECPCs (Chapter 3). Figure 6.11 shows the electrical resistance of M5-ECPC and a M5/carbon black-ECPC as a function of the applied pressure. With introducing 2 vol.% of carbon black, the electrical resistance and porosity decreased. Figure 6.12 shows SEM images of M5/carbon black-ECPC film where a decrease of the porosity can be seen. A higher porosity seems to be related to a smaller electrical conductivity and to keep the electrical conductivity within the required bounds the introduction of carbon black should be followed by the decrease of graphene load. However, the best piezoresistive response was obtained for the ECPC incorporating 15 vol.% of graphene M5 and without carbon black, despite the potential improvement of the mechanical properties that this additive could bring.

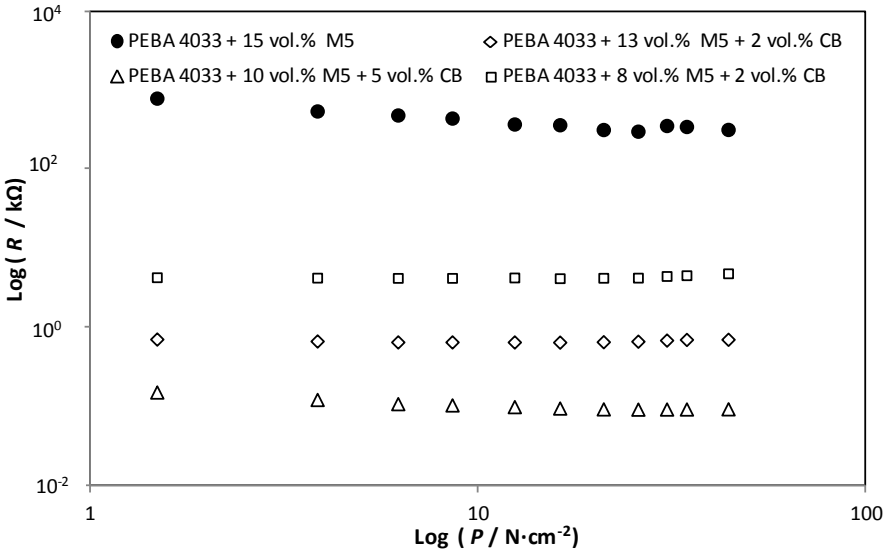

Figure 6.11 - Electrical resistance (log-log plot) as a function of the applied pressure of M5/carbon black-ECPCs assembled with polymeric electrodes.

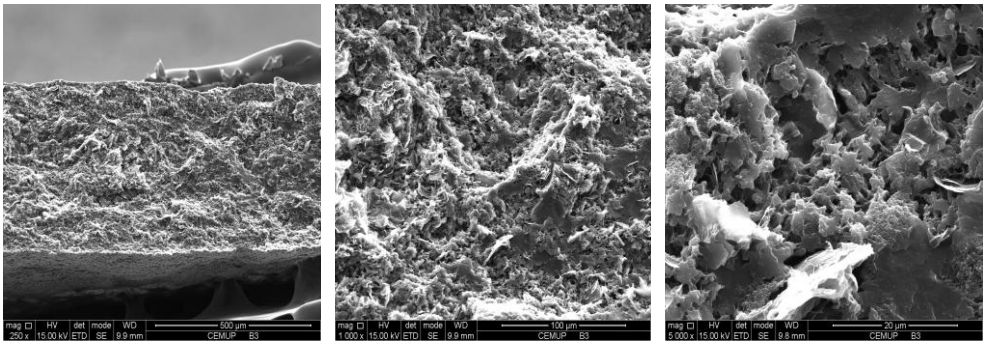

Figure 6.12 - Cross-section SEM images of M5/carbon black-ECPC.

6.5 Conclusions

Porous ECPCs based on PEBA 4033 and incorporating different types of graphene (C, M and H) platelets were prepared. The immersion precipitation method allowed the preparation of porous composite films with a nodule structure and symmetric morphology when a mixture of hexane/acetone was used as the non-solvent. ECPCs based on PEBA 4033 loaded with 15 vol.% of graphene M5 exhibited a piezoresistive response more linear in a log-log plot than the other prepared ECPCs. Porous M5-ECPC (incorporating 15 vol.% of graphene M5) showed however some hysteresis and drift due to poor mechanical properties. Crosslinked PEBA 4033 and the incorporation of carbon black were considered to improve the mechanical properties but significantly worse piezoresistive responses were observed.

6.6 References

1. Pinto, A.M., Gonçalves, I.C., Magalhães, F.D., *Graphene-based materials biocompatibility: A review.* Colloids and Surfaces B: Biointerfaces, 2013. **111**(1 November 2013): p. 188-202.
2. Batzill, M., *The surface science of graphene: Metal interfaces, CVD synthesis, nanoribbons, chemical modifications, and defects.* Surface Science Reports, 2012. **67**(3–4): p. 83-115.
3. Chandrasekaran, S., Seidel, C., Schulte, K., *Preparation and characterization of graphite nano-platelet (GNP)/epoxy nano-composite: Mechanical, electrical and thermal properties.* European Polymer Journal, 2013. 49 (12): p. 3878-3888.
4. Artiles, M.S., Rout, C. S., Fisher, T. S., *Graphene-based hybrid materials and devices for biosensing.* Advanced Drug Delivery Reviews, 2011. **63**(14–15): p. 1352-1360.
5. Pinto, A.M., Martins, J., Moreira, J. A., Mendes, A. M., Magalhães, F. D., *Dispersion of graphene nanoplatelets in poly(vinyl acetate) latex and effect on adhesive bond strength.* Polymer International, 2013. **62**(6): p. 928-935.

6. Yasmin, A., Luo, J.- J., Daniel, I. M., *Processing of expanded graphite reinforced polymer nanocomposites.* Composites Science and Technology, 2006. **66**(9): p. 1182-1189.

7. Kalaitzidou, K., Fukushima, H., Drzal, L. T., *Mechanical properties and morphological characterization of exfoliated graphite–polypropylene nanocomposites.* Composites Part A: Applied Science and Manufacturing, 2007. **38**(7): p. 1675-1682.

8. Zheng, W., Wong, S.-C., *Electrical conductivity and dielectric properties of PMMA/expanded graphite composites.* Composites Science and Technology, 2003. **63**(2): p. 225-235.

9. Liang, J., Wang, Y., Huang, Y., Ma, Y., Liu, Z., Cai, J., Zhang, C., Gao, H., Chen, Y., *Electromagnetic interference shielding of graphene/epoxy composites.* Carbon, 2009. **47**(3): p. 922-925.

10. Tang, Z., Kang, H.,Wei, Q., Guo, B., Zhang, L., Jia, D., *Incorporation of graphene into polyester/carbon nanofibers composites for better multi-stimuli responsive shape memory performances.* Carbon, 2013. **64**(November 2013): p. 487-498.

11. Vincentz, *Shaped for performance.* European Coatings Journal, 2007(09/2007).

12. Sciences, X. *XG Sciences The Material Difference*. 2013 [cited 2013 july]; Available from: http://xgsciences.com/products/graphene-nanoplatelets/.

13. Hentze, H.P., Antonietti, M., *Porous polymers and resins for biotechnological and biomedical applications.* Reviews in Molecular Biotechnology, 2002. **90**(1): p. 27-53.

14. Brady, S., Diamond, D., Lau, K.-T., *Inherently conducting polymer modified polyurethane smart foam for pressure sensing.* Sensors and Actuators A: Physical, 2005. **119**(2): p. 398-404.

15. Ravati, S., Favis, B.D., *3D porous polymeric conductive material prepared using LbL deposition.* Polymer, 2011. **52**(3): p. 718-731.

16. Li, M., Zhang, W., Wang, C., Wang, H., *In situ formation of 2D conductive porous material with ultra low percolation threshold.* Materials Letters, 2012. **82**(1 September 2012): p. 109-111.

17. Danesh, E., Ghaffarian, S.R., Molla-Abbasi, P., *Non-solvent induced phase separation as a method for making high-performance chemiresistors based on conductive polymer nanocomposites.* Sensors and Actuators B: Chemical, 2011. **155**(2): p. 562-567.

18. Luheng, W., Tianhuai, D., Peng, W., *Influence of carbon black concentration on piezoresistivity for carbon-black-filled silicone rubber composite.* Carbon, 2009. **47**(14): p. 3151-3157.

19. Lu, J., Chen, X., Lu, W., Chen, G., *The piezoresistive behaviors of polyethylene/foliated graphite nanocomposites.* European Polymer Journal, 2006. **42**(5): p. 1015-1021.

20. Sadasivuni, K.K., Ponnamma, D., Thomas, S., Grohens, Y., *Evolution from graphite to graphene elastomer composites.* Progress in Polymer Science,2014. 39 (4) (April 2014): p. 749-780.

21. Barra, G. *Parte 1: Fundamentos de Reologia de Materiais Poliméricos*. [cited 2012 may]; Available from: http://emc5744.barra.prof.ufsc.br/Reologia%20parte%201.pdf.

CHAPTER VII

7 Interface contact pressure sensors based on ECPCs

Abstract

Electrically Conductive Polymer Composites (ECPCs) assembled with polymeric electrodes were prepared and tested. The ECPCs prepared were based on dense or porous PEBA 4033 matrix incorporating graphene platelets and carbon black. Highly conductive polymeric electrodes based on dense PEBA 2533 matrix incorporating 25 vol.% of carbon black were used. The influence on the piezoresistive response of the type of bonding between the electrodes and the ECPC, either casted or glued at the edges, was assessed. The ECPCs pressure sensors assembled with the polymeric electrodes glued at the edges to the ECPC exhibited a linear piezoresistive response in a log-log plot while the polymeric electrodes casted on the ECPC exhibited a nearly flat profile. Results indicated that the pressure response of the interface pressure sensor is due a change in the interface contact with the ECPC while the casted polymeric electrodes induced a negligible piezoresistive effect. Moreover, the interface dense ECPCs exhibited both low hysteresis and drift.

7.1 Introduction

The aim of the present work is the development of Electrically Conductive Polymer Composites (ECPCs) assembled with polymeric electrodes casted on the ECPC to form a pressure sensor. However, all the pressure sensors prepared by the author (Chapter III) and based on dense polymer matrices incorporating conductive particles assembled with polymeric electrodes casted on the ECPC presented no piezoresistive response. Despite, several studies can also be found in literature regarding the development of dense polymeric pressure sensors showing piezoresistive response [1-7] but none of them explain clearly out how the electrodes are attached to the ECPC. The type of electrodes used to measure the piezoresistive response largely influences the electrical response of the ECPCs. As concluded elsewhere (Chapter III), different types of electrodes originated different electrical responses to the pressure. The electrical resistance of the ECPCs change with the type of the electrodes mainly due to the roughness present on the ECPC surface where among the materials tested only polymeric electrodes casted on the ECPC provides an effective electrical contact. When polymeric electrodes casted on the ECPC are not used, the pressure response depends mostly on the contact between the electrodes and the ECPC (Chapter III); as pressure builds up the electrodes gain better contact with the ECPC and the electrical conductivity increases up to the saturation.

Hussain et al. [2] reported a pressure sensor based on silicone rubber loaded with carbon black particles. This sensor presented a good piezoresistive response but the type of electrodes used for measuring the electrical response is not clear. These authors only reported that the resistivity measurements were carried out by a digital force sensor. Probably, the contacts with the ECPC were achieved with aluminium or steel plates as electrodes that usually offer a poor surface contact with the ECPC. Luheng et al. [3] studied the influence of carbon black concentration on the

piezoresistivity of a silicone rubber composite. The experimental set-up used for measuring the piezoresistive response was a digital force gauge with an elevator platform where the sample was placed between two electrodes. These authors only reported that the area of electrode plate is a slightly smaller than the sample but it is not clear the type of the electrodes used. Usually, a rigid metal plate is used as electrode when there is not a more detailed description of them.

The literature also reports the development of porous polymeric pressure sensors [8-13]. The porosity of the ECPC is directly related to the performance of the pressure sensor, e.g., when the ECPC porosity increases, sensitivity to pressure increases [10-11]. This happens because upon applying pressure, the conductive particles come into contact but the pores become the limiting link in the percolation threshold [13]. Following, the authors prepared pressure sensors based on porous polymer matrix incorporating conductive particles assembled with the polymeric electrodes casted on the ECPC. But again very poor pressure sensitivity was obtained. King el al. [13] investigated a porous carbon black/polydimethylsiloxane (PDMS) composite and used sugar to create a highly porous and compressible material. These authors report that the sponge/foam showed a good piezoresistive response. However, these authors reported that the sample is held between 2 conducting contacts and compressed by means of a triaxial testing rig moving upwards, compressing the sponge against a rigid metal bar. The electrical response showed a poor contact between the electrical contacts (rigid metal bar) and ECPC due to a poor surface contact. Brady et al. [8] studied a inherently conducting polymer modified with a polyurethane smart foam for being used as pressure sensor. The type of electrodes used to connect the two opposite ends of the foam was a conductive self-adhering foil of copper. This sensor showed a good piezoresistive response displaying some limitations as hysteresis and drift effect due to the poor mechanical properties.

Again, the contact between the ECPC and the electrodes might be controlling the pressure sensor response.

Piezoresistive pressure sensors measure the change in electrical resistance of the ECPC element when a force is applied while the interface pressure sensors are based on the electrical resistance between two electrical conductive layers. The interface sensors compared with piezoresistive sensors are more sensitive to pressure, show a low dependence on temperature and humidity and a more robust performance [14-15].

There are different types of commercial pressure sensors. XSensor®[14], Novel® [16] and Pressure Profile Systems® [17] are interface sensors that are made of two parallel electrical conductive layers separated by a dielectric element. FlexiForce® and Peratech® are also interface pressure sensors where the response depends on the contact between the electrodes and the ECPC element. For instance, a typical FlexiForce® pressure sensor consists of two parallel electrical conductive layers separated by a dielectric element, which may be air or a compressible elastomer, applied to the flexible polyester substrate with a silver layer. The pressure on the sensor causes deformation, reducing the distance between the two conductive layers (increasing the contact area) and consequently the electrical conductivity increases [18-20]. In the case of Peratech® sensors, the configuration consists of two parallel layers of carbon electrodes separated by a dielectric, which may be air or an elastomer, applied to the substrate [21-24].

Despite long mentioned in the literature, the authors did not find evidences of significant piezoresistive response of any type of ECPC element – dense polymer matrix or porous polymer matrix with different conductive particles or with conductive particles and non-conductive particles. Moreover, all commercial pressure sensors seem to be based on two conductive layers sandwiching a dielectric element

and not on a sensitive ECPC element. The material of the electrodes and the bonding type between the electrodes and the ECPC element are essential to the pressure response and must be carefully and clearly addressed in any further work.

The present work targets the development and characterization of the ECPCs assembled with polymeric electrodes. The influence of the way the electrodes are bonded to the ECPC, casted or glued by the edges, on the electrical resistance measurements (piezoresistive response) is addressed and hysteresis and drift response is evaluated. A commercial pressure sensor was compared with the ECPCs prepared.

7.2 Experimental

7.2.1 Materials

PEBAX polymer was supplied by Atofina Chemicals. Hexane/acetone (95 wt.% / 5 wt.%), n-methyl-2-pyrrolidone (NMP) and ethanol were purchased from Sigma Aldrich. Graphene platelets (GNP) grade M5 was purchased from XG Sciences. Graphene M5 has following characteristics given by the producer: M5 - maximum length of 5 µm, M5, average thickness of 6-8 nm and surface area between 120 $m^2 \cdot g^{-1}$ and 150 $m^2 \cdot g^{-1}$. Carbon black powder (Vulcan® XC72R) was purchased from Cabot Corporation.

7.2.2 Preparation of ECPCs based on polymer PEBA 4033

Porous and dense ECPCs were prepared by the casting method based on polymer PEBA 4033 where the preparation method is described elsewhere (Chapter V). Briefly, porous ECPC were prepared by the casting method of a polymer solution incorporating conductive particles. After casting, the porous ECPCs were obtained by the immersion precipitation method. Three porous ECPCs were prepared: PorousG15 loaded with 15 vol.% of graphene M5, PorousG8CB2 and PorousG10CB5, loaded

respectively with 8 vol.% of graphene M5 and 2 vol.% of carbon black and with 10 vol.% of graphene M5 and 5 vol.% of carbon black. Carbon black was added to improve the mechanical properties of the porous ECPCs (cf. Chapter V). A dense ECPC was also prepared by the casting polymer solution incorporating conductive particles. The ECPC prepared, named DenseCB6.5, was loaded with just carbon black with a concentration of 6.5 vol.%. A commercial pressure sensor (CPS) produced by company IEE was tested to compare with the ECPCs prepared.

7.2.3 Preparation of the dense polymeric electrodes

The procedure used for preparing dense polymeric electrodes is described elsewhere (Chapter III). Briefly, the polymer solution incorporating 25 vol.% of carbon black (CB) was prepared by the casting method and applied at room temperature.

7.3 Characterization of ECPCs

7.3.1 Measurement of Electrical Resistance

The procedure used for measuring the electrical resistance is described elsewhere (Chapter III). Briefly, the electrical resistance of the ECPCs were measured using a multimeter (Fluke 11) in an in-house made mechanical press. The effective area of the electrode was 1 cm^2. Two layers of polymeric electrodes were casted in each side of the ECPC film and then the system was sandwiched between the copper/FlexPCB (Figure 7.1, left image). In another configuration (Figure 7.1,right image), two layers of polymeric electrodes were glued by the edges in each surface of the ECPC film with white glue Axton®, with a ca. 1 mm diameter glue cord.

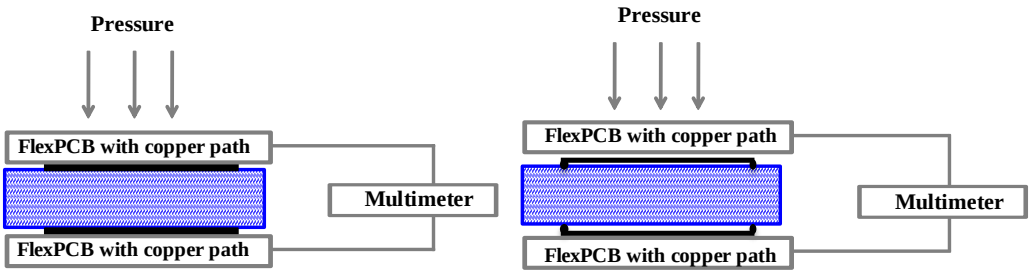

Figure 7.1 - Experimental set-up for measuring of the electrical resistance of the ECPCs (left –electrodes casted, right – electrodes glued at the edges).

7.4 Results and discussion

7.4.1 Piezoresistive response of the ECPCs assembled with the polymeric electrodes glued at the edges

The ECPCs were assembled with polymeric electrodes: a) casted on both surfaces, as described elsewhere and b) glued at the edges on both surfaces. The best pieozoresistive response was obtained with the ECPC incorporating 15 vol.% of graphene M5 (PorousG15 sensor); casted polymeric electrodes were used to have negligible combined interface response. However, this ECPC showed hysteresis and drift due to poor mechanical properties (Chapter V). Figure 7.2 shows the electrical resistance response of the three pressure sensors assembled with glued polymeric electrodes (PorousG8CB2, PorousG10CB5 and DenseCB6.5) and pressure sensor PorousG15 assembled with casted polymeric electrodes. The ECPCs assembled with polymeric electrodes glued at the edges to the ECPC exhibited a greater electrical response than the ECPC assembled with casted polymeric electrodes (Figure 7.2). In this case, the pressure response combines piezoresistive and interface responses, where the interface response seems to be more important. The material of the electrodes and the bonding type between the electrodes and the ECPC element are essential to the pressure response. The author was not able to prepare any stable

piezoresistive sensor despite the great efforts employed (Chapter III, Chapter IV, Chapter V and Chapter VI), though the quite stable and sensitive interface pressure sensors prepared.

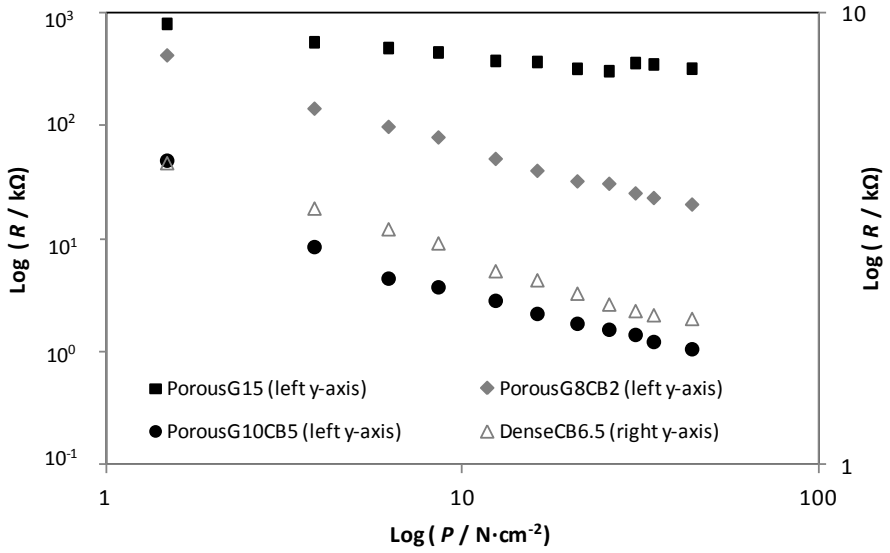

Figure 7.2 – Electrical resistance as a function of the applied pressure of ECPCs assembled with polymeric electrodes: a) castes on both surfaces: PorousG15 and b) glued at the edges on the both surfaces: PorousG8CB2, PorousG10CB5 and DenseCB6.5.

7.4.2 Reproducibility of ECPCs assembled with the polymeric electrodes glued at the edges

Figure 7.3 shows the electrical resistance of a ECPC based on porous PEBA 4033 loaded with 8 vol.% of graphene M5 and 2 vol.% of carbon black (PorousG8CB2) as a function of the applied pressure in a log-log plot for two different sensor samples. A piezoresisitive response was observed up to approximately 35 $N \cdot cm^{-2}$ of applied

pressure where the electrical resistance changed from approximately 500 kΩ to 50 kΩ; the samples are reasonably reproducible. In order to increase the reproducibility it is necessary to apply always the same area of glue by the edges.

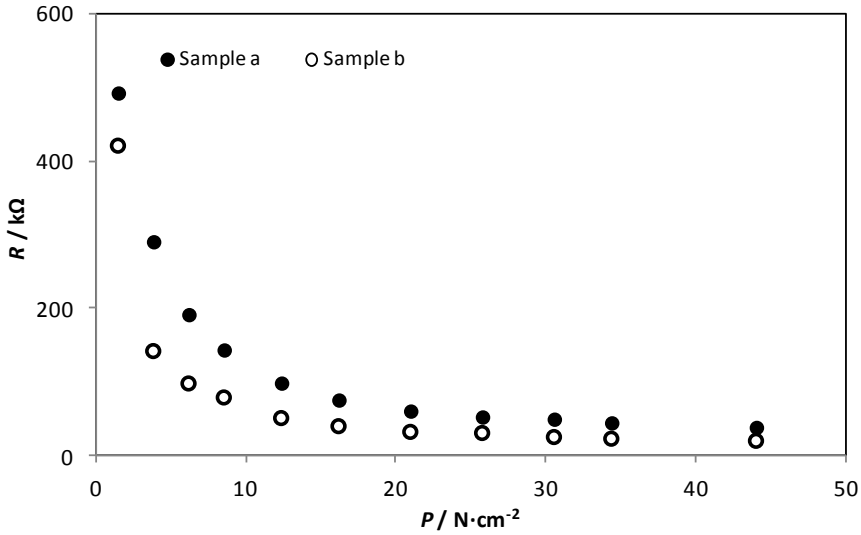

Figure 7.3 - Electrical resistance as a function of the applied pressure of PorousG8CB2 assembled with glued polymeric electrodes for two samples.

7.4.3 Hysteresis and drift of ECPCs

Figure 7.4, Figure 7.5 and Figure 7.6 show the electrical response as a function of the applied pressure for three load steps and two unload steps obtained for different ECPCs: PorousG10CB5 and PorousG8CB2 sensors glued to the polymeric electrodes (Figure 7.4 and Figure 7.5) and DenseCB6.5 sensor glued to the polymeric electrodes (Figure 7.6). All samples responded steadily after 5 s under load and 10 s after unload. The second load step begun 30 s after the end of first unload step. Finally, the third load step begun 30 s after the end of second unload step.

As concluded by the author (Chapter V), the electrical resistance of thePorousG15 assembled with casted polymeric electrodes in the log-log plot changes approximately linearly with the applied pressure up to approximately 35 N·cm^{-2}. A significant hysteresis and drift effect was observed. The poor results in terms of drift and hysteresis are probably related to the fragile mechanical properties of the porous graphene-ECPC element.

Figure 7.4 shows the ECPCs based on PEBA 4033 loaded with 10 vol.% of graphene M5 and 5 vol.% of carbon black (PorousG10CB5) glued to the polymeric electrodes. These ECPCs presented largely improved mechanical properties when carbon black is incorporated (see Chapter V).

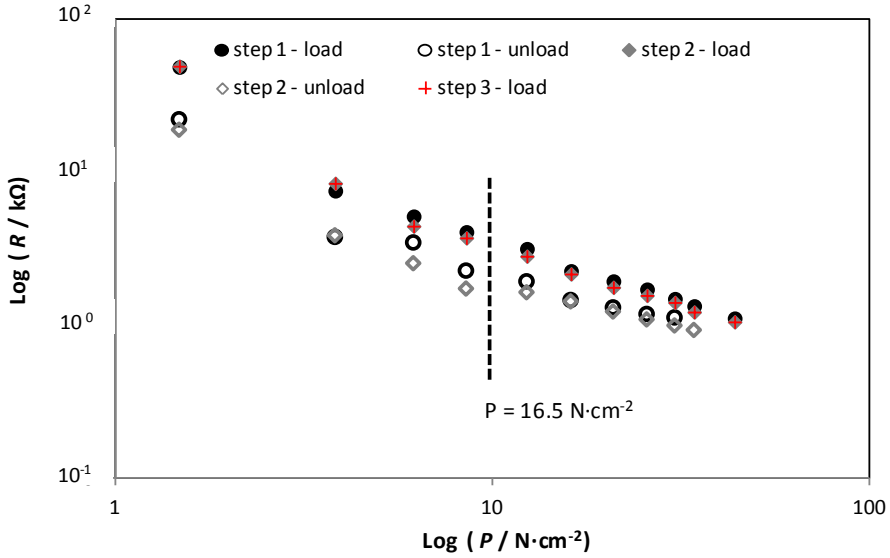

Figure 7.4 - Electrical resistance as a function of the applied pressure (load and unload steps) of PorousG10CB5 assembled with glued polymeric electrodes.

During the first loading step, the electrical resistance changes as a function of the applied pressure and after the first unload step a low hysteresis is observed. In the second step, the electrical resistance showed a low drift effect (the electrical resistance decreased 2 % at 16.5 N·cm^{-2}), and after 10 s of the second unload step, the electrical resistance showed a very low hysteresis (the electrical resistance decreased 18 % at 16.5 N·cm^{-2} on the second load step).

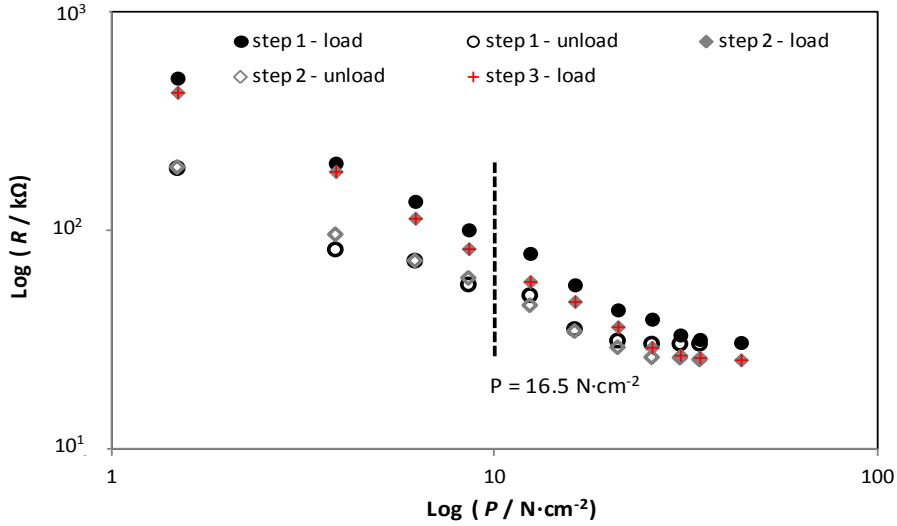

Figure 7.5 - Electrical resistance as a function of the applied pressure (load and unload steps) of PorousG8CB2 with glued polymeric electrodes.

On the other hand, the ECPC based on PEBA 4033 loaded with 8 vol.% of graphene M5 and 2 vol.% of carbon black (PorousG8CB2) with glued polymeric electrodes showed a similar hysteresis (the electrical resistance decreased 34 % at 16.5 N·cm^{-2} on the second load step) than the ECPC incorporating 10 vol.% of graphene M5 and 2 vol.% of carbon balck (PorousG10CB5) but less than the ECPC with casted polymeric electrodes (PorousG15).

DenseCB6.5 pressure sensor assembled with glued polymeric electrodes showed the lowest hysteresis (the electrical resistance decreased 6 % at 16.5 $N \cdot cm^{-2}$ on the second load step) and drift (the electrical resistance decreased 1 % at 16.5 $N \cdot cm^{-2}$ on the second load step) response among the tested sensors - Figure 7.6. This behaviour was assigned to the good mechanical properties of the dense ECPC element.

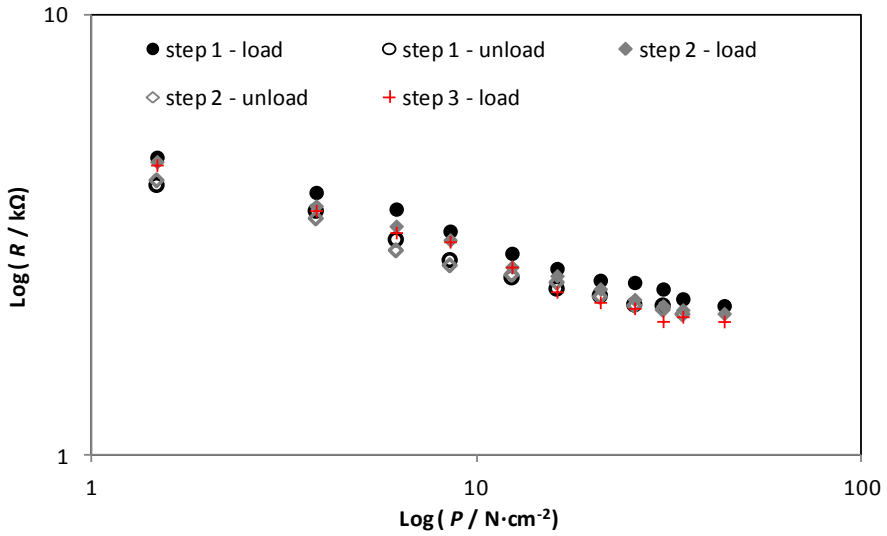

Figure 7.6 - Electrical resistance as a function of the applied pressure (load and unload steps) of DenseCB6.5 assembled with glued polymeric electrodes.

In the case of interface pressure sensors, the electrical resistance changes with the quality of the electrodes due to the roughness present on the ECPC surface (Chapter III). For example, when using a copper foil as electrodes, an approximately linear (in log-log plot) piezoresistive response is obtained (Chapter III) but a change in contact area would produce a response of the sensor that changes with time (interface responsive element), originated for example by the walk shear strength.

Because of that, interface pressure sensors usually suffer from low robustness due to the robustness of the electrodes. The difference between interface pressure sensors developed in Chapter III and in this Chapter is the robustness of the electrodes, in this Chapter the electrodes are made of the same material of the ECPCs that can be more resisting towards shear forces.

7.4.4 DenseCB6.5 pressure sensor vs Commercial pressure sensor

Figure 7.7 shows the electrical response as a function of the applied pressure for three load steps and two unload steps obtained for DenseCB6.5, which was assembled with glued polymeric electrodes, and for commercial pressure sensor (CPS) (produced by IEE, Luxembourg). These sensors were left for 3 days under pressure of 50 $N \cdot cm^{-2}$ and tested again to assess their hysteresis and drift behaviour. Figure 7.7 shows that CPS sensor has the highest pressure sensitivity before and after 3 days under pressure. On the other hand, CPS sensor shows neither significant drift nor hysteresis - it has a very good stability. The DenseCB6.5 sensor presents constant hysteresis behaviour, similar to that of CPS sensor; however, it has a larger drift than CPS sensor - see Figure 7.8.

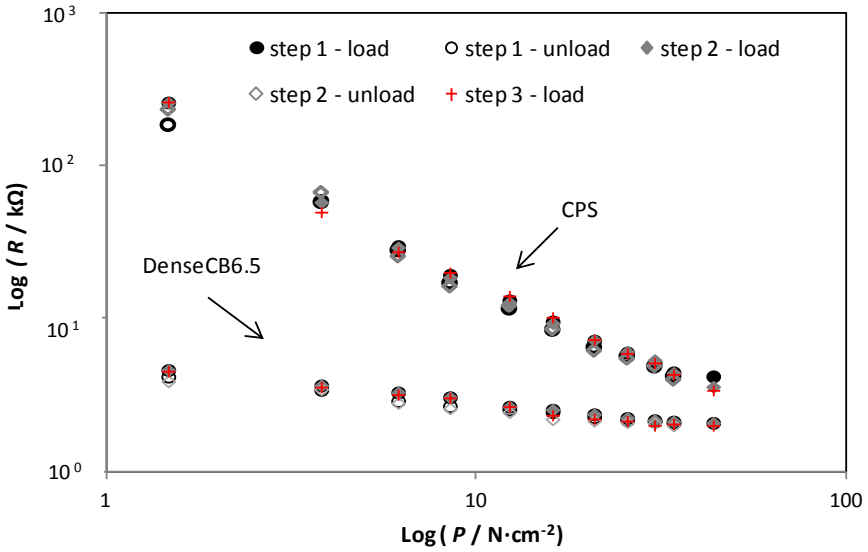

Figure 7.7 - Electrical resistance as a function of the applied pressure (load and unload steps) of CPS sensor and DenseCB6.5 sensor assembled with glued polymeric electrodes before and after 3 days under pressure.

As future work, it would be optimized the preparation of interface pressure sensors based on an assembly of two polymeric electrodes glued at the edges to the ECPC element, where relevant factors will be optimized. These factors are namely the morphology and concentration of the conductive particles, the stiffness of the polymeric matrix and the bonding type between the ECPC element and electrodes. Electrochemical impedance spectroscopy (EIS) should be used to assess the interface contribution of claimed piezoresistive pressure sensor, definitively contributing to clarify the working principal of a given pressure sensor.

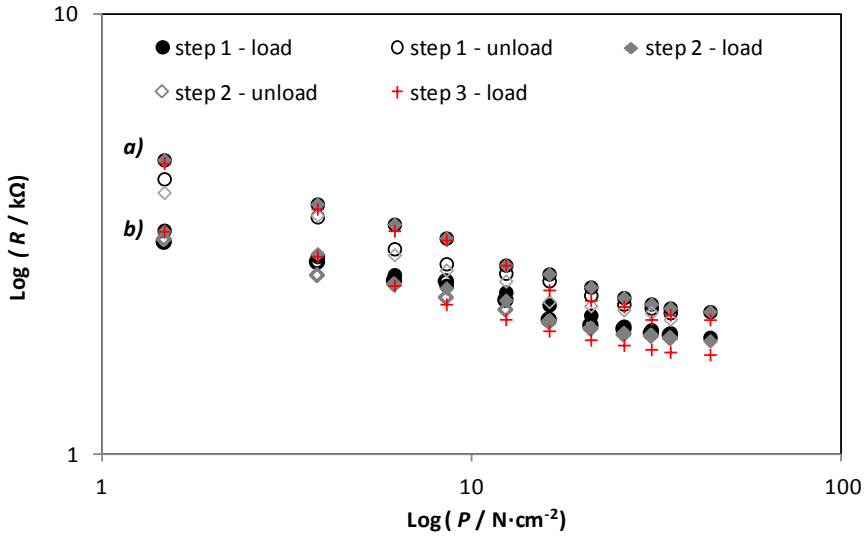

Figure 7.8 - Electrical resistance as a function of the applied pressure (load and unload steps) of DenseCB6.5 sensor assembled with glued polymeric electrodes before (***a)***) and after (***b)***) 3 days under pressure.

7.5 Conclusions

ECPCs assembled with polymeric electrodes casted or glued at the edges to the ECPC were characterized. The effect of these polymeric electrodes on the piezoresistive response was tested with different ECPCs. The ECPCs assembled with glued polymeric electrodes exhibited a strong pressure response compared to the ECPCs assembled with casted polymeric electrodes. The polymeric electrodes glued at the edges to the ECPC influences the electrical resistance response due to a change in the interface contact between the ECPC and electrodes favouring a pressure response (interface response). Moreover, DenseCB6.5 sensor assembled with glued polymeric electrodes showed the lowest hysteresis and drift response. However, CPS commercial sensor displayed the highest pressure sensitivity and the greatest

stability. In the future it would be important to optimize the preparation of interface pressure sensors based on composite polymer films.

7.6 References

1. Knite, M., Teteris, V., Kiploka, A., Kaupuzs, J., *Polyisoprene-carbon black nanocomposites as tensile strain and pressure sensor materials.* Sensors and Actuators A: Physical, 2004. **110**(1-3): p. 142-149.
2. Hussain, M., Choa, Y.-H., Niihara, K., *Fabrication process and electrical behavior of novel pressure-sensitive composites.* Composites Part A: Applied Science and Manufacturing, 2001. **32**(12): p. 1689-1696.
3. Luheng, W., Tianhuai, D., Peng, W., *Influence of carbon black concentration on piezoresistivity for carbon-black-filled silicone rubber composite.* Carbon, 2009. **47**(14): p. 3151-3157.
4. Bendo, L., Soldi, V., Domenech, S.C., *Compósitos elastoméricos condutores a base de terpolímero de etileno-co-propileno-5-etilideno-2-norborneno e negro de fumo modificado com polímeros condutores intrínsecos utilizados na construção de um protótipo de sensor de dígito-pressão*, in *Departamento de Química*. 2006, Universidade Federal de Santa Catarina: Florianópolis. p. 57.
5. Knite, M., Teteris, V., Polyakov, B., Erts, D., *Electric and elastic properties of conductive polymeric nanocomposites on macro- and nanoscales.* Materials Science and Engineering: C, 2002. **19**(1-2): p. 15-19.
6. Zavickis J., K.M., Ozols K., Malefan G., *Development of percolative electroconductive structure in piezoresistive polyisoprene-nanostructured carbon composite during vulcanization.* Materials Science and Engineering: C, 2011. **31**(2): p. 472-476.
7. Zavickis, J.K., Maris; Podins, Gatis; Linarts, Artis; Orlovs, Raimonds, *Polyisoprene-nanostructured carbon composite - A soft alternative for pressure sensor application.* Sensors and Actuators A: Physical. **In Press, Corrected Proof**.
8. Brady, S., Diamond, D., Lau, K.-T., *Inherently conducting polymer modified polyurethane smart foam for pressure sensing.* Sensors and Actuators A: Physical, 2005. **119**(2): p. 398-404.
9. Hentze, H.P., Antonietti, M., *Porous polymers and resins for biotechnological and biomedical applications.* Reviews in Molecular Biotechnology, 2002. **90**(1): p. 27-53.

10. Ravati, S., Favis, B.D., *3D porous polymeric conductive material prepared using LbL deposition.* Polymer, 2011. **52**(3): p. 718-731.

11. Danesh, E., Ghaffarian, S.R., Molla-Abbasi, P., *Non-solvent induced phase separation as a method for making high-performance chemiresistors based on conductive polymer nanocomposites.* Sensors and Actuators B: Chemical, 2011. **155**(2): p. 562-567.

12. Brady, S., Lau, K.T., Megill, W., Wallace, G.G., Diamond, D., *The Development and Characterisation of Conducting Polymeric-based Sensing Devices.* Synthetic Metals, 2005. **154**(1-3): p. 25-28.

13. King, M.G., Baragwanath, A.J., Rosamond, M.C., Wood, D., Gallant, A.J., *Porous PDMS force sensitive resistors.* Procedia Chemistry, 2009. **1**(1): p. 568-571.

14. *www.xsensor.com*. [cited 2014 March].

15. Pritchard, E., Mahfouz, M., Evans III, B., Eliza, S., Haider, M., *Flexible capacitive sensors for high resolution pressure measurement*, in *IEEE SENSORS 2008 Conference*. 2008. p. 1484-1487.

16. *www.novel.de*. [cited 2014 March].

17. *http://www.pressureprofile.com/*. [cited 2014 March].

18. *http://www.tekscan.com/*. [cited 2013 january].

19. Podoloff, R., Benjamin, M., *Flexible, tactile sensor for measuring pressure distributions and for gaskets*, WO 91/09289, June 27, 1991.

20. Krivopal, B., *Pressure sensitive ink means, and methods of use*, WO 97/25379, July 17, 1997.

21. *http://www.peratech.com/qtc-material-inspirations.html*. [cited 2013 january].

22. Lussey, D., Jones, D., Leftly, S., *Flexible Switching Devices*, WO 01/88935 A1, November 22, 2011.

23. Lussey, D., Laughlin, P., Bloor, D., Hilsum, C., *Polymer Composition,* U.K. Patent GB 2465077 A, May 12, 2010.

24. Lussey, D., *Conductive Strutures*, WO 00/ 79546 A1, December 28,2000.

CHAPTER VIII

8 Conclusions and Future Work

The present thesis addressed the development of a robust and low cost pressure sensor based on conducting polymer films. This sensor should be lightweight, highly flexible, cheap and elastic and should be very resistant to compression. The electrodes should preferentially be made of the same material to avoid stress and delamination of the contact area. The electrodes should have a very good adhesion to the sensor. So, this pressure sensitive sensor was envisioned as a pressure sensitive layer sandwiched between two electrical conductive layers.

Electrically Conductive Polymer Composites (ECPCs) based on dense polymer matrices of polydimethylsiloxane (PDMS) and polyetherblockamide (PEBA) incorporating conductive particles were prepared and studied. The factors concerning the ECPC preparation were studied: filler material and morphology and preparation conditions such as solvent, application method and drying temperature. Carbon black was shown to be a promising filler to incorporate in PEBA based ECPCs due to the low cost, close density compared with the polymer matrix, high conductivity and small particle size. The influence of the electrodes on the piezoresistive response was tested to different ECPCs. The type of electrodes largely influenced the electrical response of the pressure sensor produced. The electrical resistance response of the ECPCs changes with the type of the electrodes mainly due to the roughness present on the ECPC surface. Among the materials tested only polymeric electrodes casted on the ECPC provided an effective electrical contact. Although, pressure sensors based on a dense polymer matrix incorporating carbon black assembled with casted polymeric electrodes presented no piezoresistive response.

Porous conducting polymer composite films were considered since the porosity of the ECPC is directly related to the performance of the pressure sensor. Porous

PDMS films were prepared by the foaming and emulsion methods while PEBA films were prepared by the phase inversion method. The emulsion method using water and butanol as emulsifiers allowed the preparation of porous PDMS films with a high amount of pores. However, larger and more abundant pores are observed on the top surface morphology in comparison to the cross-section. The phase inversion method allowed the preparation of porous PEBA films with a nodular structure, highly porous and with a symmetric morphology, being very promising for preparing porous polymer matrix. PDMS and PEBA based ECPCs incorporating carbon black and other types of conductive particles, such as silver and spherical and lamellar zinc were assembled. ECPCs made of porous PDMS films incorporating carbon black were not obtained. ECPCs made of porous PEBA 4033 films incorporating carbon black were only successfully obtained when a hexane/acetone as non-solvent was used, but at low carbon black concentration (<5.5 vol.%). The incorporation of hydrophilic metallic particles in the polymer matrix allowed obtaining a porous PEBA morphology when water was used as the non-solvent. A piezoresistive response was observed for the porous ECPCs incorporating silver and lamellar zinc and casted polymeric electrodes but poor mechanical properties were obtained due to the high concentration of metals incorporated.

Since particle morphology of graphene platelets is similar to that of lamellar zinc but with a significantly smaller density, the study of the incorporation of different types of graphene platelets (grade C - 750, MX and H5) on a porous PEBA film was evaluated. The porous PEBA 4033 film incorporating 15 vol.% of graphene M5 exhibited a piezoresistive response more linear in a log-log plot than the other grades of graphene platelets and exhibited the best mechanical properties. These results confirmed the potential of a porous PEBA 4033 film incorporating graphene as pressure sensor but some limitations were observed as hysteresis and drift in the response after compression. To improve mechanical properties, crosslinked PEBA

4033 and the incorporation of carbon black were considered but the piezoresistive response worsened.

On the other hand, the influence of the polymeric electrodes on the piezoresistive response was tested after being casted or glued to different ECPCs. ECPCs assembled with glued polymeric electrodes exhibited a higher piezoresistive response in a log-log plot than the ECPCs assembled with casted polymeric electrodes. The polymeric electrodes glued at the edges to the ECPC influences the electrical resistance response due to a change in the interface contact with the ECPC favouring a pieozoresistive response. Moreover, dense ECPCs assembled with glued polymeric electrodes showed to be reasonably reproducible and exhibited a low hysteresis and drift.

As future work and taking into account the results of this thesis, it would be important to study and optimize the preparation of interface pressure sensors, ECPCs and polymeric electrodes glued at the edges, such as: electrodes and the type of the ECPC used (morphology of the conductive particles, stiffness of the polymeric matrix, etc) and type of glue to apply between the ECPC and electrodes. The material of the electrodes and the bonding type between the electrodes and the ECPC element are essential to the pressure response and must be carefully and clearly addressed. It is also important to study the aging of the pressure sensor, e.g., long-term studies should be addressed.

On the other hand, it is suggested the use of impedance spectroscopy (EIS) to study the response of the sensors. The most common and standard procedure in impedance measurements consists of applying a small sinusoidal voltage perturbation and monitoring the resulting current response of the system at the corresponding frequency. EIS is a technique widely used for characterising the electrical behaviour of

systems. EIS can be used to determine the charge transport resistance and capacitance at the interfaces, besides given the electrical behaviour on the bulk parts of the sensor. This will allow relating the response of the sensor with more fundamental properties and assessing the interface contribution of claimed piezoresistive pressure sensor, definitively contributing to clarify the working principal of a given pressure sensor.